EVALUATION AND ENHANCEMENT OF SOLAR PV HOSTING CAPACITY FOR MANAGEMENT OF VOLTAGE RISE IN LV NETWORKS

Weerasingha Liyanage Dilhani Madhusha Chathurangi

178014B (UOM)

5676563 (UOW)

Thesis submitted in partial fulfillment of the requirements for the degree of Doctor of Philosophy of Engineering in Electrical Engineering
under the Joint PhD program

Department of Electrical Engineering
University of Moratuwa
Sri Lanka
and
School of Electrical, Computer and Telecommunications Engineering
University of Wollongong
Australia

June 2022

Declaration

I declare that this is my own work and this thesis does not incorporate without acknowledgment any material previously submitted for a Degree or Diploma in any other University or institute of higher learning and to the best of my knowledge and belief it does not contain any material previously published or written by another person except where the acknowledgment is made in the text.

Also, I hereby grant to University of Moratuwa, Sri Lanka and University of Wollongong, Australia the non-exclusive right to reproduce and distribute my thesis, in whole or in part in print, electronic or other medium. I retain the right to use this content in whole or part in future works (such as articles or books).

Signature :

UOM Verified Signature

Date : 22 June 2022

W.L.D.M. Chathurangi

The above candidate has carried out research for the PhD thesis under our supervision.

Signature of the supervisor(s):

UOM Verified Signature

Date : 23June 2022

Dr. J.V.U.P. Jayatunga

UOM Verified Signature

Date : 25 Jun 2022

Dr. Tilak Siyambalapitiya

UOM Verified Signature

Date : 27 June 2022

Prof. Sarath Perera (UOW)

UOM Verified Signature

Date : 28 June 2022

Assoc. Prof. Ashish P. Agalgaonkar (UOW)

Abstract

Proliferation of solar photovoltaics (PV) in low-voltage (LV) distribution networks is inciting technical challenges in network design and operation with regard to the quality of power. Violations of operational performance limits are increasingly evident at higher solar PV penetration levels, in particular, local voltage rise has become the major issue of concern in LV distribution networks. As the solar PV industry continues to grow, emerging challenges need to be addressed by adopting best policies and practices at a utility level. Thus, to comply with stipulated network operational limits, distribution network operators (DNOs) are compelled to develop comprehensive techniques to determine acceptable levels of solar PV hosting capacity (HC) and explore HC enhancement options.

Complexity of modelling distribution networks is a barrier for DNOs to decide levels of maximum solar PV penetration using stochastic approaches. Thus, there is a necessity to develop a systematic approach to assess solar PV HC, considering factors such as geographic layout of networks and their electrical characteristics.

This thesis extends the knowledge of managing of solar PV integration in LV networks by developing systematic approaches to evaluate solar PV HC subjected to over voltage curtailment. In this regard, a novel feeder based solar PV HC evaluation approach was developed to address the diverse network characteristics of multi feeder systems in LV distribution networks. To assess the voltage violations and critical factors affecting the solar PV HC, a comprehensive analysis of potential power quality issues was conducted on a practical LV distribution network in Sri Lanka.

The approach proposed in this thesis establishes a safe limit for solar PV HC for a given distribution feeder based on the locational and operational aspects of the solar PV units deployed on a LV network. The safe limit for HC was developed employing a number of sensitivity analyses considering factors influencing solar PV HC. Further, the proposed feeder based solar PV HC approach was extended to develop a generic method to quantify solar PV HC under different operating con-

ditions of PV inverters. Thus, it can be used as an approximate guide or a rule of thumb to evaluate solar PV HC at a given point on an LV feeder without using complex stochastic techniques.

With the increasing demand for solar PV systems, development of both solar PV HC assessment and enhancement techniques is essential in managing network voltage. DNOs have recognised the need for smart PV inverter technologies to maintain acceptable voltage levels in distribution networks. Smart PV inverters possess fast and flexible active and reactive power control functions such as; Volt-VAr and Volt-Watt control modes which can be used to manage over-voltage conditions that often limit the solar PV HC. At present, most of solar PV connection standards provide a set of rules and guidelines to mitigate voltage violations by enabling Volt-VAr and Volt-Watt control modes of the inverters. In particular, it is imperative to analyse the impact of such solar PV connection standards on HC assessment and its potential to enhance solar PV HC. Thus, a detailed analysis of smart solar PV inverter capabilities and a comparative evaluation of solar PV HC enhancement facilitated by different connection standards are presented in this thesis.

Electricity utilities around the world seek to develop strategies to increase solar PV integration while maintaining acceptable network performance. Hence, more generalised and straightforward tools are required to rapidly assess solar PV HC without complex and extensive network modelling and simulations. Extending the deterministic outcomes, a nomogram based solar PV HC assessment approach is proposed in this thesis to determine HC values specific to any location of a given conductor. Further, solar PV connection criteria is proposed which permits the electric utilities to approve new solar PV connections which facilitates reasonable modelling insights to assess HC. The proposed nomogram based solar PV HC assessment approach and solar PV connection criteria cover technical and regulatory aspects to manage PV integration in LV distribution networks.

For the continued development of solar PV as a distributed generation, accuracy of PV connection approval process is crucial to correctly and easily allow PV

connections that will not cause issues. Therefore, grid codes, distribution codes or guidelines on interconnection of solar PV require to be refined or re-written in relation to solar PV HC assessment/enhancement and approval criteria for new PV connections in LV distribution networks. The solar PV HC assessment/enhancement and solar PV connection criteria proposed in this thesis shall be a contribution to further improvement of the available guidelines/standards on solar PV installation in LV networks.

All network modeling and simulations presented in this thesis were carried out in DIgSILENT PowerFactory platform.

Acknowledgments

I wish to express my sincere appreciation to all who helped me in numerous ways throughout my PhD candidature at the University of Moratuwa (UOM), Sri Lanka and University of Wollongong (UOW), Australia to make my research a success.

I would like to pay my greatest gratitude and appreciation to my principal supervisors, Professor Sarath Perera of University of Wollongong, Australia and Dr Upuli Jayatunga of University of Moratuwa, Sri Lanka for the excellent guidance throughout my postgraduate study period in many ways. You have always been more than supervisors to me. Your dedication, patience, knowledge and experience inspired me to grow up academically and personally over last few years.

Besides my principal supervisors, I would like to convey my sincere thanks to my co-supervisors, Associate Professor Ashish P. Agalgaonkar of University of Wollongong, Australia and Dr Tilak Siyambalapitiya, Managing Director, Resource Management Associates (Pvt.) Limited, Sri Lanka for their great support. I really admire all of your encouragement, insightful comments and guidance given to complete my research.

I wish to convey my appreciation to University of Moratuwa, especially the Vice Chancellor, the Dean of the faculty of Engineering and Head of the Department of Electrical Engineering for the support given to me to pursue my postgraduate studies at University of Wollongong.

My PhD research project was supported by SRC grant SRC/LT/2017/16, University of Moratuwa during the stay at University of Moratuwa and University of Postgraduate Award (UPA), University of Wollongong during the stay at University of Wollongong. Without the financial support received from these organisations, my dream to complete a PhD degree may not have been realised. Also, I wish to thank the support given by Resource Management Associates (Pvt.) Limited, Sri Lanka and Lanka Electricity Company Ltd., Sri Lanka for providing necessary data and field measurements for my PhD research work.

Very special thanks go to Dr Amila Wickramasinghe and Eng. Mahesh Rath-

nayake for their valuable input to my research given during my candidature at University of Moratuwa. Thanks also go to my friends Pathum, Dilini, Thisandu, Lasanthika, Samadhi, Omesha, Piyaka and Namal for their support during good times as well as in hard times through out the way.

Last but not least, I would like to thank my parents, husband and the rest of my family for their unconditional love and continuous support. My PhD dream became a reality through your sacrifices and commitment.

List of Principal Symbols and Abbreviations

PV	photovoltaic
HC	hosting capacity
LV	low voltage
MV	medium voltage
HV	high voltage
POC	point of connection
MCS	monte-carlo simulation
DNO	distribution network operator
GW	gigawatt
kW	kilowatt
MW	megawatt
kVAr	kilovar
kWh	kilo watt hour
ABC	aerial bundle cable
AAC	all aluminum conductor
SAM	system advisor model
AC	alternating current
DC	direct current
am	ante meridiem
pm	post meridiem
UVF	voltage unbalance factor (%)
V_n	neutral voltage
DNSP	distribution network service provider
HC_{min}	minimum hosting capacity
HC_{max}	maximum hosting capacity

DG	distributed generation
p.u.	per unit
R	resistance
X	inductance
Z	impedance
P_{LOAD}	active power of the load
S_{LOAD}	apparent power of the load in p.u.
S_{inv}	rating of the PV inverter
$Q_{Volt/VAr}$	required reactive power of VAr priority Volt-VAr control
Q_{avail}	available reactive power of Watt priority Volt-VAr control
OLTC	on-load tap changer
BESS	battery energy storage system
P_{DG}	total solar PV capacity
P_{tr}	MV/LV transformer rating
$P_{thermal\_line}$	thermal limit of the feeders,
$HC_{Feeder,Min}$	minimum hosting capacity of a given feeder
$HC_{Feeder,Max}$	maximum hosting capacity of a given feeder
HC_{min_LV}	minimum hosting capacity of a given distribution network
HC_{max_LV}	maximum hosting capacity of a given distribution network
HC_{Fn_End}	maximum connectable solar PV capacity at the feeder end of n^{th} feeder
HC_{Fn_Front}	maximum connectable solar PV capacity at the feeder front of n^{th} feeder
HC^*	solar PV hosting capacity obtained from the nomogram
P_{PV}	active power of PV system
Q_{PV}	reactive power of PV system
P_L	active power of the load
Q_L	reactive power of the load
P	active power
Q	reactive power
V_{PV}	voltage at the point of connection
V_S	voltage at the supply end
I_S	net current

I_L	load current
I_{PV}	net PV current
I_{p1}	active current component of net current when solar PV system operating at unity power factor
I_{q1}	reactive current component of net current when solar PV system operating at unity power factor
I_{p2}	active current component of net current when solar PV system operating at lagging power factor
I_{q2}	reactive current component of net current when solar PV system operating at lagging power factor
I_{p3}	active current component of net current when solar PV system operating at leading power factor
I_{q3}	reactive current component of net current when solar PV system operating at leading power factor
I_{pl}	active current component of load current
I_{ql}	reactive current component of load current
V_{PV1}	voltage at the point of connection when solar PV system operating at unity power factor
V_{PV2}	voltage at the point of connection when solar PV system operating at lagging power factor
V_{PV3}	voltage at the point of connection when solar PV system operating at leading power factor
I_{PVp}	active current component of PV system
I_{PVq}	reactive current component of PV system
DV_l	total voltage drop at the feeder end
l	feeder length
V_b	nominal line-line voltage
P_S	real power component of the total load
Q_S	reactive power component of the total load
d	distance to the POC from the distribution transformer
P_d	active power flow at a distance d from the distribution transformer

Q_d	reactive power flow at a distance d from the distribution transformer
$d^{'}$	zero crossing point of active power
$Q^{'}$	reactive power flow at a distance $d^{'}$ from the distribution transformer
λ	ratio between the distance to POC and feeder length
VD_l^{re}	real component of voltage drop
VD_l^{im}	reactive component of voltage drop
ΔV	total voltage drop made by the load across the feeder
$d^{''}$	zero crossing point of reactive power
pf_{pv}	inverter operating power factor
θ	voltage angle deviation
$HC_{calculated}$	HC obtained from the proposed analytical approach
$HC_{simulated}$	HC obtained from the DIgSILENT PowerFactory simulations
CIGRE	International Council on Large Electric Systems
IEC	International Electrotechnical Commission
IEEE	Institute of Electrical and Electronics Engineers
EPRI	Electric Power Research Institute
MPP	maximum power point
V_{array}	voltage of PV array
I_{array}	current of PV array
$V_{mmp-array}$	voltage in the maximum power point
P_{conv}	active power signal from power measurement device
E	irradiance
V_{dc}	DC output voltage of PV system
I_{cap}	differential current in DC capacitor
C	capacitance
V_{dcin}	output DC voltage from DC bus-bar and capacitor link
V_{dcref}	reference DC voltage
V_{ac}	measured AC voltage at the output of PV inverter
V_{ref}	reference AC voltage
Id_ref	reference active power current
Iq_ref	reference reactive power current

cos_{ref}	d-axis reference angle
sin_{ref}	q-axis reference angle
id	d-axis current
iq	q-axis current
id_{min}	d-axis minimum current
id_{max}	d-axis maximum current
iq_{min}	q-axis minimum current
iq_{max}	q-axis maximum current
db	dead-band
ab	active-band
ib	ideal-band
K_{iq}	reactive current droop gain
K_{id}	active current droop gain
V_0	input voltage
P_{max}	maximum real power output of PV inverter
P_{min}	minimum real power output of PV inverter
I_{rated}	rated current of PV inverter
VVC	volt-var control
VWC	volt-watt control
VUL	upper voltage limit
AS	Australian Standard
NZS	New Zealand Standard
HR14	Hawaii Rule 14
CR21	California Rule 21
LECO	Lanka Electricity Company
STC	standards test condition

Publications Arising from the Thesis

Book Chapters

1. D. Chathurangi, U. Jayatunga, S. Perera and A. Agalgaonkar, "A Generalised Deterministic Approach to Evaluate PV Hosting Capacity of LV Distribution Networks Under Different Operating Conditions," In: Zobaa A., Abdel Aleem S., Ismael S., Ribeiro P. (eds) Hosting Capacity for Smart Power Grids. Springer Cham, 2020.

Journal Papers

1. D. Chathurangi, U. Jayatunga, S. Perera, A. P. Agalgaonkar and T. Siyambalapitiya, "Comparative evaluation of solar PV hosting capacity enhancement using Volt-VAr and Volt-Watt control strategies," Renewable Energy, Vol.177, pp.1063-1075, November 2021.

2. D. Chathurangi, U. Jayatunga, S. Perera, A.P. Agalgaonkar and T. Siyambalapitiya, "A Nomographic Tool to Assess Solar PV Hosting Capacity Constrained by Voltage Rise in Low-Voltage Distribution Networks," International Journal of Electrical Power & Energy Systems, Vol.134, pp. 107409, January 2022.

Conference Papers

1. D. Chathurangi, U. Jayatunga, S. Perera and A. Agalgaonkar, "Evaluation of Maximum Solar PV Penetration: Deterministic Approach for Over Voltage Curtailments," 2019 IEEE PES Innovative Smart Grid Technologies Europe (ISGT-Europe), Bucharest, Romania, pp. 1-5, September 2019.

2. D. Chathurangi, U. Jayatunga, S. Perera, A. Agalgaonkar, T. Siyambalapitiya and A. Wickramasinghe, "Connection of Solar PV to LV Networks: Considerations for Maximum Penetration Level," 2018 Australasian Universities Power Engineering Conference (AUPEC), Auckland, New Zealand, pp. 1-6, November 2018.

3. D. Chathurangi, U. Jayatunga, M. Rathnayake, A. Wickramasinghe, A. Agalgaonkar and S. Perera, "Potential power quality impacts on LV distribution networks with high penetration levels of solar PV," 2018 18th International Conference on Harmonics and Quality of Power (ICHQP), Ljubljana, pp. 1-6, May 2018.

Table of Contents

List of Figures

List of Tables

Chapter 1

Introduction

1.1 Statement of the Problem

The world population is growing, economic systems are developing and global energy consumption is accelerating than ever before, especially in developing countries. The conventional energy sources; mainly supplied by combustion of fossil fuels are inadequate in meeting the rising electricity demand. Therefore, many nations around the world are pushing towards the deployment of renewable energy sources such as solar, wind, hydro and geothermal with expectation to supply a considerable percentage of future world electricity requirements. Renewables 2021 - global status report [1] states more than 256 gigawatts (GW) of new renewable power generating capacity has been installed in 2020, raising the global total to 2,839 GW by the end of 2020, which is estimated to be 29% of global electricity production.

Among the renewable power technologies, solar photovoltaic (PV) systems have received immense attention in the recent years due to a number of well known reasons; depletion of fossil fuel resources, abundance of solar energy, environmental concerns, declining cost and comparatively simple installations [2]. Fig. 1.1 shows the growth of electricity generation from solar PVs over the world from 2010 to 2020. Out of total renewable power capacity of 2,839 GW, the capacity of solar PV installations worldwide had exceeded 760 GW by the end of 2020, as shown in Fig. 1.1. The year 2020 was a landmark for solar PV installations where 139 GW was

installed worldwide for electricity generation which is more than half of the total renewable additions [1].

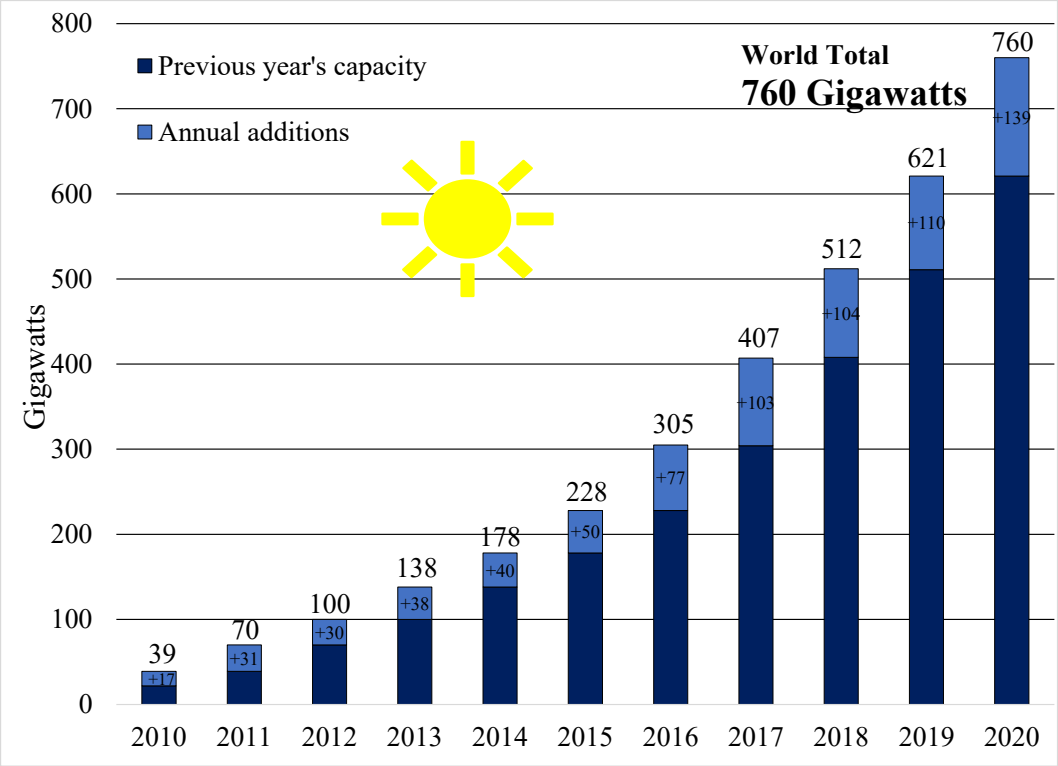

Figure 1.1: Solar PV global capacity and annual additions, 2010-2020

Generally, solar PV systems are connected to the grid as utility scale installations (solar farms scattered in a large open area) preferably at the medium voltage (MV) or higher network with a capacity usually above 1 megawatt (MW) or as rooftop generation plants at low-voltage (LV) level [2]. Recent expansion in rooftop solar PV technology and the potential initiatives from government subsidies have promoted installation of PV systems with capacities ranging from several kilowatts (kW) to 1 MW or even more depending on the size of the area in residential, commercial and industrial applications [2]. In addition, the cost of PV installations has gradually been declining over recent years, so the average size of solar PV installations has been increasing [1].

However, there are several concerns in integrating solar PV systems in LV distribution networks. The challenge with solar PV generation is its nature of intermittency and non-dispatchability, rendering it hard to match supply and demand

which itself is variable. Further, high solar PV penetration levels can have negative impacts on the existing distribution network, which can inflict various protection, stability and power quality issues [3, 4]. With high solar PV penetration levels, reverse power flow will be evident in LV/MV distribution networks resulting in malfunctioning of protection systems [5]. In case of large scale solar PV systems, network voltage and frequency instability will be significant due to nature of solar intermittency [3]. Further, solar PV penetration in distribution networks may lead to a number of technical problems including power quality problems; such as over-voltage limit violations, over-loading of feeders and transformers, voltage unbalance, excessive line losses and high harmonic distortion levels exceeding the stipulated limits [2, 6]. Power quality is the major issue of concern in distribution networks, which covers various operational limits and plays a key role in industrial, commercial and residential power needs [6]. Degree of the occurrence of power quality problems increases with the maximum permissible solar penetration level, especially when the maximum connectable solar PV generation exceeds acceptable limits.

Key negative impacts associated with high solar PV penetration levels may be overcome to a certain extent by network reinforcements such as asset upgrades (conductors and transformers) and advanced monitoring and protection schemes [4]. However, such reinforcements are not economically feasible in general. Given the potential obstacles, it is desirable to develop systematic approaches for new solar PV deployment from network planning perspectives so as to optimally utilise existing assets instead of network augmentation.

The concept of solar PV hosting capacity (HC) has been introduced to represent the maximum amount of solar PV capacity that can be connected to a distribution network or a feeder, without causing any adverse effects on normal system operations [6, 7, 8]. HC for solar PV integration is defined based on an appropriate performance index or indices subjected to well-defined operational criteria or limits [8, 9]. Appropriate power quality indices have been chosen as performance indices; voltage rise, voltage unbalance and thermal over-loading of feeders and transformers

while complying with the operational limits of the network [10, 11, 12]. However, uncertainty in solar PV HC calculations may arise due to many factors such as unknown solar PV locations and ratings, the intermittent nature of power output of PVs and load variations [13]. Therefore, evaluation of solar PV HC of a practical network is not a straightforward exercise since a single value does not fit all networks.

The most common concern of higher solar PV penetration levels in LV networks is reported to be voltage rise and the resulting over-voltage limit violations in LV distribution networks [9, 14]. Thus, over-voltage is a key factor which leads to curtailment of solar PV capacity in LV distribution networks, and it is important to develop certain criteria to facilitate the maximum solar PV HC while maintaining network voltage within stipulated limits.

Solar PV HC assessment in LV distribution networks is facilitated using both deterministic and stochastic/probabilistic methods. Deterministic methods are typically based on traditional power flow analysis, whereas stochastic methods use Monte Carlo simulation (MCS) approaches which accommodate randomness in the solar PV location, size and uncertainties in solar PV power generation and variations in customer load [10]. However, the accuracy of solar PV HC calculated in stochastic methods depends on the number of simulations and complexity of the network model. On the other hand, deterministic methods can only be applied to one location at a time and are incapable of capturing all performance criteria of hosing capacity. Hence, there is a need for more generalised and straightforward methodologies for solar PV HC evaluation alleviating complex and extensive network modelling and simulations.

Distribution network operators (DNOs) are overwhelmed by unprecedented number of new solar PV connection applications with the growing demand for renewable energy generation, thus, they are required to ensure that the connection of new solar PV systems do not violate any associated operational limits. At present, most DNOs follow simple practices and/or rules of thumb in order to assess the solar

PV HC of existing distribution networks. Methods widely used by most of electricity distribution companies for preliminary HC assessment and their rules of thumb for PV connections are mainly based on the percentage of the peak load of the feeder, percentage of transformer rating and thermal limits of the affected feeders [4, 7]. However, adopting a fixed HC percentage for networks or feeders is inefficient as it does not address PV locational impact or individual network characteristics. Overall, both deterministic and stochastic approaches present in literature to assess solar PV HC are not simple practices for DNOs to adopt. Hence, DNOs need generalised systematic approaches for solar PV HC evaluation constrained by overvoltage, which possess a close representation of the overall network configuration including topological and electrical parameters.

With the increasing demand for solar PV deployments, both solar PV HC assessment and enhancement techniques play vital role in managing unacceptable voltage rise in LV distribution networks. Therefore, DNOs recognise the need for smart inverter technologies in order to maintain acceptable voltage levels in distribution networks [15, 16]. Smart PV inverters possess fast and flexible active and reactive power control functions such as; Volt-VAr and Volt-Watt control modes which regulate the voltage at the point of connection (POC) [15, 17, 18]. Moreover, these functions fully utilise capabilities of solar PV inverters in order to comply with operational limits of networks and hence prevent costly network augmentations. However, although smart inverters can be configured to manage the voltage at the POC by controlling the necessary reactive and active power using Volt-VAr and Volt-Watt control modes, distributed nature of solar PV resources and different network characteristics/configurations may limit the HC enhancement as a comprehensive understanding of such advanced coordinated control strategies are not available to date. Further, various provisions/approaches facilitated by different solar connection standards pose challenges in the selection of best practice for HC enhancement with smart inverters. Therefore, it is significantly important to investigate and analyse different practices/rules imposed by widely used solar PV connection standards on

solar PV HC enhancement.

1.2 Research Objectives and Methodologies

The contribution from this thesis concentrates on developing a novel approach to extend the knowledge of solar PV planning, especially in the area of hosting capacity analysis. The main thrust of the work presented in this thesis is to broaden the understanding of solar PV HC assessment mechanism and associated evaluation approaches constrained by over-voltage and hence development of a novel generalised solar PV connection criteria in LV distribution networks. Further, the HC improvement possible through smart inverters is investigated by employing advanced inverter control functions where such improvements are subjected to locational aspects of inverters in distribution systems. Research outcomes provide a comprehensive solar PV hosting capacity assessment mechanism and enhancement approaches which contributes to the development of solar PV connection standards/guidelines.

The major research objectives can be stated as follows:

- Investigation of performance indicators and potential factors which influence the maximum solar PV penetration level in LV distribution networks.
- Development of systematic approaches to determine the solar PV HC in LV networks.
- Development of generalised mathematical models for solar PV HC evaluation.
- Investigation of smart solar PV inverter capabilities and comparative evaluation of solar PV enhancement facilitated by different connection standards.
- Development of solar PV connection criteria as a contribution to utility guidelines.

The preliminary work covers a comprehensive analysis of potential power quality issues on a practical LV distribution network, which has more than 40% of solar

penetration (based on the transformer capacity), as a detailed modelling exercise based on measurements obtained via smart energy meter readings. Critical factors affecting the solar PV HC in the practical LV network are investigated with the verification of simulation results by means of field measurements obtained from smart meters.

Using existing knowledge of the stochastic HC assessment approach, a novel feeder based solar PV HC assessment concept is developed employing a number of sensitivity analyses considering the influencing factors on solar PV HC. The proposed feeder based solar PV HC assessment approach was further established by developing a deterministic approach for HC assessment and is justified by considering the drawbacks of the stochastic approach.

Enhancement of solar PV HC analysis is further investigated by exploring the potential capabilities of smart PV inverters in order to mitigate over-voltage issue. By clearly demonstrating the benefits of adopting a particular smart inverter function; Volt-VAr or Volt-Watt control strategies, solar PV HC enhancement is investigated in the study by reviewing the existing solar connection standards and guidelines which refer to criterion and requirements for active and reactive power control facilitating the mitigation of voltage related issues. A laboratory verification was implemented for the verification of the smart PV inverter model developed in DIgSILENT PowerFactory.

Further, a generalised solar PV connection criteria was developed for approval of new solar PV connections into LV distribution networks. A nomogram based approach is proposed to evaluate the HC at a given point of distribution feeder constrained by over-voltage limits. Nomogram based graphical representation of HC assessment method facilitates reasonable modeling insights to accommodate influencing factors to be considered simultaneously.

Overall, the proposed novel solar PV HC assessment/enhancement approaches and solar PV connection criteria are believed to be a contribution to further improvement of the available standards/guidelines on solar PV installation in LV networks.

1.3 Outline of the Thesis

A brief description on the contents of the remaining chapters is given below:

Chapter 2 is a literature review on the background information on solar PV integration and related aspects of solar PV HC in distribution systems. It includes a general overview of distribution networks with distributed solar PV systems and their impact on distribution networks, concept of solar PV HC, perceptions and enhancement techniques for solar PV HC. The chapter also includes a section on general guidelines on HC assessment and enhancement as per the solar connection standards and guidelines.

Chapter 3 presents a case study on a practical LV distribution network in Sri Lanka with high solar penetration level as a preliminary study. This network is reported as the maximum solar penetrated network in Sri Lanka by 2017 and it was a 40% by the transformer capacity. The network performance including power quality issues under varying solar penetration levels are analysed in this study while voltage rise has been identified as the limiting factor of maximum solar PV connections. Further, voltage rise analysis based on smart meter measurement for the LV network is presented in this chapter further justifying the voltage rise is the major concern over high solar penetration levels in LV distribution networks.

As a continuation of the work presented in Chapter 3, Chapter 4 describes a stochastic approach of HC assessment of the aforementioned LV network using Monte Carlo Simulation method. Further, influencial factors on solar PV HC are analysed in detailed to define novel parameters which describe the safe limit for HC by employing a number of sensitivity analyses. Further, safe limit of HC is used to develop a novel concept of feeder based solar PV HC assessment approach for LV distribution networks.

Chapter 5 presents a novel generalised deterministic approach that can be used to evaluate solar PV HC at a given point on an LV distribution feeder subjected to over-voltage curtailment. The safe limit of solar PV HC that is defined in Chapter 4 is evaluated using the proposed approach. Furthermore, the proposed determin-

istic approach can be used to evaluate the solar PV HC under different operating conditions of solar PV inverter; unity power factor and fixed power factor (leading or lagging) operation.

Chapter 6 examines the use of smart inverter technology to enhance network solar PV HC by employing active and reactive power control functions. Solar connection standards provide a set of guidelines and practices associated with smart inverter functions mainly the Volt-VAr and Volt-Watt control strategies to mitigate voltage related issues in power network while, power control functions provide different set of settings in different standards. Thus, influence of different PV connection standards on solar PV HC are analysed to investigate the most beneficial approach to address the issue of voltage violations subjected to locational aspects of inverters in distribution systems.

Chapter 7 presents the development of a generalised solar PV connection criteria utilising the outcomes of proposed deterministic approach for solar PV HC assessment in LV distribution networks. Accordingly, a nomogram based solar PV HC assessment approach and simplified solar PV connection criteria are developed for different network configurations.

Chapter 8 summarises the major findings of the work presented in the thesis and makes recommendations for future work.

Chapter 2

Literature Review

2.1 Introduction

This chapter presents general aspects of solar PV generation in distribution networks, with a focus on the solar PV HC, followed by a review on the existing concepts and knowledge on active management of HC in LV distribution systems. A general overview on solar PV integration in LV distribution networks which imposes a number of technical and operational issues is given in Section 2.2. Recent investigations on solar PV HC concepts and assessment methodologies are reviewed in Section 2.3 in order to broaden the research context in this thesis. Section 2.4 outlines the transition towards a smarter distribution network, which provides alternatives and cost-efficient options to improve solar PV HC levels. The final section describes current practices and policy frameworks for connection of solar PV systems in LV networks, establishing the background knowledge required for the work presented in Chapter 6.

Overall, this chapter provides a detailed review of the existing developments and relevant research on solar PV HC, which lays a solid foundation for the development of a systematic approach for solar PV HC assessment in LV distribution networks.

2.2 Impact of Solar PV Integration on Distribution Networks

Conventional power systems are designed to supply power unidirectionally from source to the load, over longer distances, via a hierarchical series of functional networks as HV transmission, MV distribution and LV distribution networks. This network layout establishes an optimised connection of a smaller number of higher capacity power generation plants to large number of distributed customer loads while maintaining network redundancy, protection, power quality and minimum power losses [19]. Networks be operated at or above 110 kV are generally considered to be transmission networks, while lower voltages, such as 66 kV and 33 kV, are usually considered to be sub-transmission voltages. Voltages less than 33 kV are usually used for distribution networks. In Sri Lanka and Australia, transmission networks are operated at 132 kV and higher voltages, 66 kV, 33 kV and 11 kV voltage levels are used in MV distribution networks, and 400 V in LV distribution networks [20, 21, 22].

Apart from the voltage levels, transmission and distribution networks have their own characteristics to facilitate each network's operational aspects [19]. Transmission lines are generally meshed or interconnected to furnish multiple connection among sources and loads to enhance the system reliability and for ease of maintenance, with minimum power outages being experienced by consumers. In contrast, majority of LV distribution networks are almost entirely radial [19]. LV distribution networks start at a step down transformer and then divided into a number of radial feeders which in turn result in uni-directional power flow from source to the load. However, recent advancement and technological developments in distributed generation, such as solar PV systems, require LV distribution networks to perform a different role.

Present day, solar PV systems are connected to the grid in different scales which is a result of rapidly declining cost of solar PV installations making the solution

attractive to both consumers and utilities. Generally, two types of solar PV systems are connected to the grid. The first type is utility-scale installations with a capacity usually above 1 MW which require large, open land area [2]. The second type is small scale roof-top solar power generation. Residences can sufficiently supply with small systems of usually up to 20 kW, while larger public, commercial, and industrial buildings may have systems with a capacity as large as 1 MW or even more [2].

The major issue with the grid integrated solar PV is the fluctuation of the output power due to the variations in solar irradiance caused by the movement of clouds, which may continue for minutes or hours [3]. These fluctuations can degrade the performance of the electric networks causing power quality, protection and stability issues [3, 23]. In case of large scale solar PV systems, network voltage and frequency instability will be significant due to nature of solar intermittency [3]. However, with significant penetration levels of solar PV, reverse power flow becomes evident in distribution networks, which causes operational conflicts with protection schemes. Furthermore, high solar power generation can degrade the performance of the distribution networks resulting in a number of power quality issues [4]. In general, power quality covers all deviations from ideal voltage and current in a number of ways, including voltage limit violations, harmonics distortion and voltage unbalance being dominant [4, 9, 12, 14] which will be discussed in detail in Sections 2.2.1, 2.2.2, 2.2.3 and 2.2.4.

2.2.1 Local Voltage Rise

The integration of a large number of solar PV systems is transforming conventional distribution networks into active networks, thus making bi-directional power flow a reality, which in turn causes a significant rise in local voltage levels [24]. Most importantly, under high PV generation and low load conditions, the power injection from solar PVs has a substantial impact at locations towards the end of LV feeders [25].

The voltage rise phenomenon when a grid-connected solar PV system injects

active and reactive power to the grid can be explained using a model of a PV system connected to an LV distribution feeder as shown in Fig. 2.1 [24]. The grid impedance seen at the point of connection (POC) by the PV system is $R+jX$. The voltage at the POC is V_{PV} and the supply end voltage is V_S while PV system injects active and reactive powers, P_{PV} and Q_{PV} respectively. Total load of the distribution feeder is P_L, Q_L and I_S is the resultant current flowing through the distribution line.

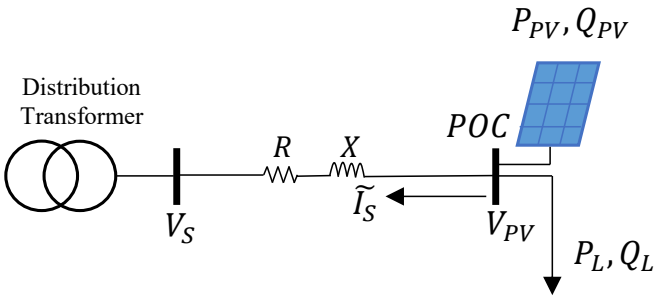

Figure 2.1: Simplified model of a distribution feeder with a solar PV system

As illustrated in Fig. 2.1, if the solar PV output, P_{PV} is much larger than the local load, P_L ($P_{PV} > P_L$), power flows towards the distribution transformer and hence, the voltage at the feeder end may rise over the network stipulated limits. In addition, the voltage impact depends on the total solar PV capacity, type of network and location of solar PV system to be connected [10].

The voltage rise phenomenon at POC can be derived theoretically. The complex power at the POC of the PV system is given by (2.1).

$$\vec{V_{PV}}\vec{I_S^*} = (P_{PV} - P_L) + j(Q_{PV} - Q_L) \tag{2.1}$$

Further,

$$\vec{V_{PV}} - \vec{V_S} = \vec{I_S}(R + jX) \tag{2.2}$$

From (2.1) and (2.2),

$$\vec{V_{PV}} - \vec{V_S} = \left(\frac{(P_{PV} - P_L) + j(Q_{PV} - Q_L)}{V_{PV}} \right)^* (R + jX)$$

$$\vec{V_{PV}} - \vec{V_S} = \left(\frac{(P_{PV} - P_L) - j(Q_{PV} - Q_L)}{V_{PV}} \right) (R + jX) \tag{2.3}$$

If the phase angle deviation of V_S with reference to V_{PV} is assumed to be negligible and considering V_{PV} to be the reference phasor, (2.3) can be simplified as,

$$\Delta V = \frac{(P_{PV} - P_L)R + (Q_{PV} - Q_L)X}{V_{PV}} \tag{2.4}$$

where ΔV is the $|V_{PV}| - |V_S|$. As per the simplified expression (2.4), the steady-state voltage rise, ΔV can be increased by increasing active and reactive power injected to the grid as a result of the additional power flow. On the other hand, ΔV can be decreased by absorbing reactive power from the grid.

Furthermore, the appearance of unacceptably high voltages which could far exceed voltage limits at the PV inverter connection points, often give rise to frequent disconnection of inverters as part of protection against islanding and reduces the contribution of solar PV systems to the total generation [2].

2.2.2 Harmonic Distortion

Harmonic problems are common in distribution networks, mainly originating from nonlinear loads, transformers and increased use of power electronic equipment. In general, solar PV systems incorporate PV panels, maximum power point tracking (MPPT) controller, a boost converter, a DC/AC inverter and an interfacing LC filter, which are significant harmonic polluters [26]. Harmonic generation from inverters will be divergent, which depends on the type of control strategy, size of solar PV systems and on the existing grid harmonic level [26]. Low order current harmonics (frequency components up to 2 kHz) are significant due to the inability of switching control system of PV inverter to produce a perfectly sinusoidal current which is caused by control strategies or background distortion present at the POC

or during partial loading conditions [6]. Further, solar PV systems can inject high frequency current harmonics (in the range of 2 kHz to 150 kHz) at switching frequency or associated side bands [6]. The total harmonic emission of PV inverters consists of two parts, namely primary emission and secondary emission [6] which is variable and difficult to separate. With larger PV installations, the grid side filter circuits can cause significant resonance at low frequencies, showing high impact on the network impedance where the resonance frequency decreases with increasing number of PV inverters [6]. Also, harmonic currents of individual inverters can add up arithmetically up to higher harmonic order in multiple PV inverter systems [6] and the harmonic interaction between nonlinear loads at the vicinity can lead to generation of non-characteristic harmonics.

Furthermore, the impact of harmonic current produced by solar PV systems mainly depends on the impedance of the grid. Hence, solar PV connections to LV distribution networks can lead to an increase of the harmonic distortion of the network due to low short circuit capacity or high network supply impedance. Excessive harmonic currents flowing through the grid can lead to increasing line losses, transformer overheating and premature ageing of transformers [27].

2.2.3 Voltage Unbalance

Another significant power quality issue in distribution systems with high penetration of single phase solar PV units is presence of unacceptable levels of voltage unbalance. Normally, the electric utilities attempt to supply loads evenly in the three phases along the distribution feeder to minimise the voltage unbalance. Despite this fact, the primary source of voltage unbalance at the distribution level is the load asymmetry, especially the uneven distribution of single phase loads over the three phases. In addition, connection of single phase rooftop solar PV installations increase the existing voltage unbalance levels in the network as the single phase rooftop solar PV installations are randomly placed along the three phases where the potential solar customers are connected. However, it may even be possible to compensate the

background unbalance created by loads by connections of solar PV systems [6]. In addition, the increase/decrease in voltage unbalance depends on the location and size of the solar PV system and phase loading level.

The voltage unbalance level at the end of an LV feeder is higher than that of at the beginning of the feeder. This fact has been proven in analysis presented in [28, 29, 30, 31] which analyse the voltage unbalance in a residential distribution line with rooftop solar PV penetrations. Furthermore, several studies have been conducted to investigate new approaches to manage voltage unbalance in LV distribution networks caused by solar PV installations. For instance, [32] has proposed a new approach to manage voltage in unbalanced LV networks using demand response and on-load tap changing transformers (OLTC) considering consumer preference. An increase in voltage unbalance in LV distribution networks can result in malfunctioning of regulatory equipment and reduces the lifetime of customer appliances.

2.2.4 Protection Issues

In power systems, a fault is usually classified by an abnormal type of current. The networks employ protective devices to detect fault conditions and operate devices, such as circuit breakers and switch-gear, to isolate the affected part of network, limit the loss of service and ensure the normal operation of the unaffected part [33, 34]. Before the introduction of distributed generations, protection schemes were based on the traditional operation of the network, where the provision and co-ordination of protection devices were designed for uni-directional power flows which have direction insensitive characteristics [33]. However, the installation of solar PV systems can contribute to the fault-current and change its direction. Most of the existing protection relays in distribution networks usually have a directional insensitive characteristics at present and hence, LV networks with increasing solar PV penetration levels with bi-directional power flows may lead to unstable and malicious actions in operation of protection and thus reducing the reliability of the grid [34].

2.3 Assessment of Solar PV Hosting Capacity

Taking into account the power quality aspects, the evaluation of the maximum connectable solar PV generation has become necessary for the planning and operation of LV distribution grids. Determination of optimum level of solar integration based on hosting capacity approach is being researched at present and such a limit will be beneficial for the DNOs to amend the grid codes, to prevent violations of operational limits caused by solar PV systems in LV distribution networks. However, rudimentary knowledge exists at present in assessing hosting capacity based on power quality phenomenon addressing system uncertainties and simultaneous disturbances. In the interest of research context in this thesis, present knowledge on the assessment of solar PV HC is critically reviewed in this Section.

The concept of solar PV HC has been introduced to represent the maximum amount of solar PV capacity that can be connected to a distribution network or a feeder, without causing any adverse effects on normal system operations [8, 6]. This limit can help significantly in maintaining a healthy and secured electricity grid, and help avoid damages caused by violating operational limits set by standards during times of the high PV power generation.

The power quality operational criteria or limits and the network constraints in terms of power quality performance index or indices are the major factors in the determination of maximum permissible solar PV penetration in LV networks [8]. Appropriate power quality indices are chosen as performance indices including; voltage rise, thermal over-loading of feeders and transformers and voltage unbalance while complying with the operational limits of the network [6, 10, 13]. A performance index-based determination of solar PV HC is illustrated in Fig. 2.2, where the HC is the amount of PV generation at which the performance index reaches its stipulated limit first.

A comprehensive overview of the limiting factors for solar PV HC analysis starting from year 2013 is covered in [14] and the statistics show that the over-voltage violation as the most ubiquitously employed limiting factor for solar PV HC eval-

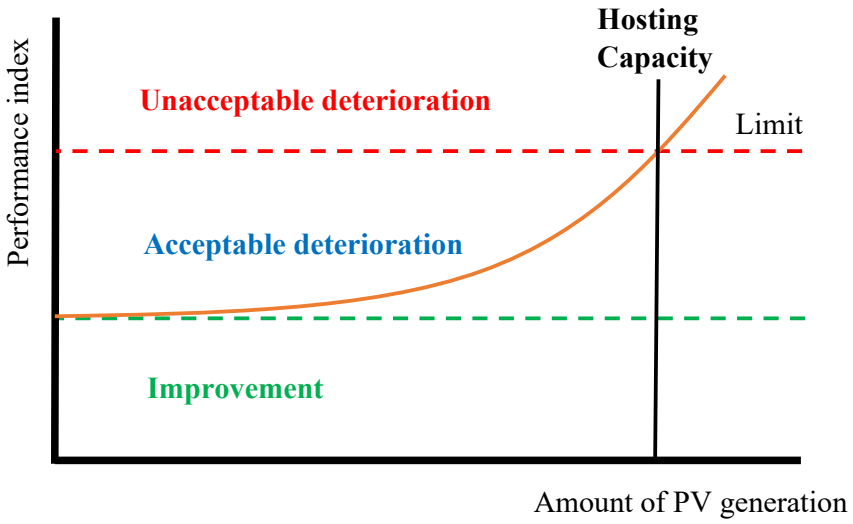

Figure 2.2: PV hosting capacity approach based on performance index [8]

uation and it is around 48% while thermal over-loading and voltage unbalance are around 26% and 19% respectively. Furthermore, harmonic and flicker have also been used as limiting factors for solar PV HC assessment studies where respective percentages being 4% and 3%. According to the statistics of over-voltage constraint limits presented in [14], there are different limiting ranges defined by utilities where widely utilised voltage standards are covered in; European Standard EN-50160 (±10% of nominal voltage (Un)) [35], German Standard VDE-AR-N 4105 (+3% of Un) [36], American Standard ANSI C84.1(±5% of Un) [37], Australian Standard (AS) (-6/+10% of Un) [38, 39] and Canadian Standards Association (CSA) (±6% of Un) [40]. The most widely employed voltage rise limits used in different countries for solar PV integration in line with standards are summarised in Table 2.1.

Table 2.1: Most widely employed voltage rise limits used in different countries for HC assessment [14]

Voltage rise	Countries
1.1 p.u.	Australia, Italy, Finland, Cyprus, South Africa, UK
1.06 p.u.	Sri Lanka, Qatar
1.05 p.u.	USA, Denmark, Sweden, Indonesia, Philippines
1.03 p.u.	Germany, China, Switzerland

Furthermore, uncertainty in solar PV HC calculations may arise due to factors

such as unknown PV locations and their rating, the intermittent nature of their power output, variations in customer demand and network configurations [13]. Accordingly, a single value cannot be determined to the solar PV HC for different LV networks. Moreover, a single performance index cannot be used to determine the solar PV HC and the influence made by different disturbances has to be investigated and such a HC can take multiple values when different performance indices are used as constraint limits.

Accurate evaluation of solar PV integration levels based on hosting capacity approach requires detailed network models, network measurements and assessment methodologies to address system uncertainties. These details can have a significant impact on the resulting value of the HC, mainly the HC quantification approaches. Solar PV HC assessment in LV distribution networks can be facilitated using mainly deterministic and stochastic/probabilistic methods [9, 14, 41, 42] which will be discussed in detail in Sections 2.3.1 and 2.3.2.

2.3.1 Stochastic Approaches for Solar PV Hosting Capacity Evaluation

Solar PV power generation is uncertain and depends on the irradiance level that is influenced by the changing weather conditions and cloud movements which make power generation to be stochastic in nature. Apart from that, solar PV location, size, type of solar PV i.e., either single phase or three phase, number of customers with solar PV and customer load are often unknown and these can be referred to as uncertainties in solar power generation and customer load [9]. Stochastic methods for solar PV HC evaluation include these randomness and uncertainties in solar PV power generation and variations in customer load, thus representing the realistic nature [9, 41].

MCS are used in the stochastic HC assessment approach in order to accommodate uncertainties in the solar PV generation and load variations [10]. A well-developed stochastic approach using MCS to assess the solar PV HC on distribution networks is

presented in [10] by proposing two levels of solar PV HC; minimum hosting capacity and maximum hosting capacity for a given performance index. Two levels of HC are shown in Fig. 2.3 for over-voltage criteria (ANSI voltage limit) where the minimum HC is the lowest amount of solar PV that can result in a criteria violation and maximum HC is the highest amount of solar PV that the network can be able to accommodate [10]. Further, three regions of concern are highlighted in Fig. 2.3; region A, B and C. Region A (up to minimum HC) includes all PV deployments that do not cause adverse impacts to the network and hence, all penetrations in this region are acceptable. In Region B (between minimum HC and maximum HC), acceptability of PV deployments depends on location and size of solar PV systems. Accordingly, some PV penetrations in region B cause the violation of over-voltage criteria. In Region C, all PV deployments cause the violation of over-voltage criteria and hence, all penetrations in this region are not acceptable.

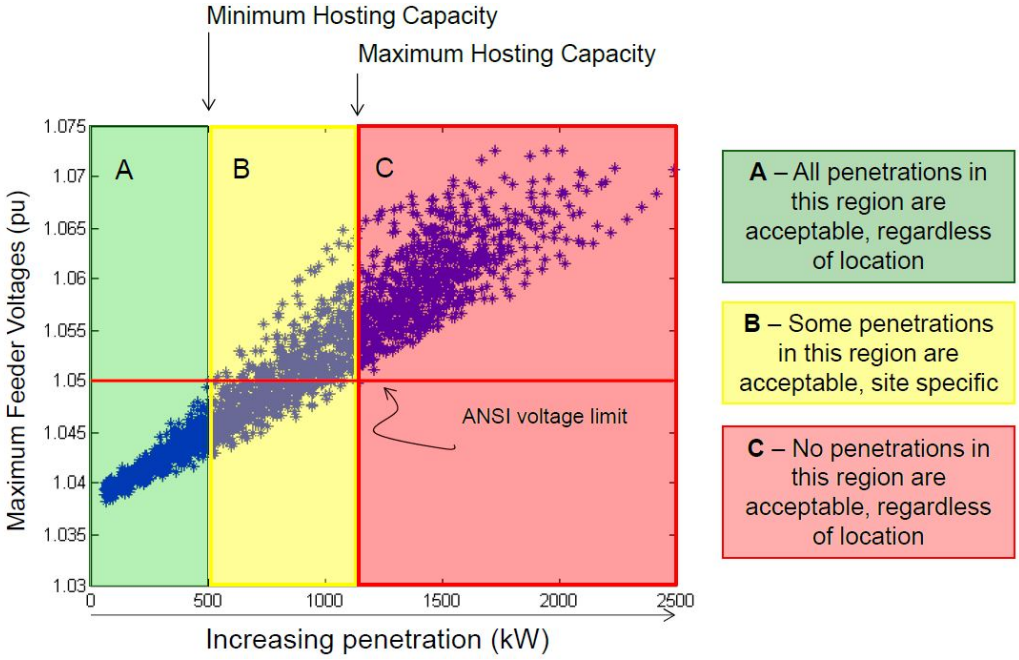

Figure 2.3: Two Levels of Solar PV Hosting Capacity [10]

In [11], a stochastic approach has been applied to determine the solar PV HC at feeder level covering four voltage quality criteria: over-voltage, voltage deviation, dynamic voltage drop and voltage unbalance, thus specifying a unique solar PV HC in accordance with different performance criteria.

Furthermore, a comprehensive review of impact studies presented in [9] states that the voltage rise and over-loading of feeders and transformers are the most influential performance indices used in stochastic methods to assess solar PV HC. For instance, [43] presents a stochastic analysis of PV integration in an 11.4 kV MV feeder in Taiwan considering feeder voltage impact as the main performance criterion with over-voltage limit as 1.03 p.u. (voltage deviation as 3% of Un) and [44] considers the over-voltage as the main limiting constraint complying with 0.92 p.u.–1.05 p.u. limits. Similarly, over-voltage and line over-loading limits are considered in [45] for solar PV HC assessment complying ±5% of Un and 100% of nominal rating, respectively, while introducing benefits from smart grid technologies to enhance the HC.

In [13], the Monte Carlo based simulations have been performed on a hypothetical network to determine solar PV HC and enhanced HC with network upgrade, subjected to over-voltage constraint. The authors claim that solar PV HC depends on the uncertainties including; the location and size of solar PV systems and the method of voltage control in the distribution grid.

In [12], a stochastic method is presented for hosting capacity determination constrained by voltage unbalance due to single phase connected solar PVs. Three different practical LV networks; two in Sweden and one in Germany are considered in this study and the risk of high-voltage unbalance is found to be reduced by a combination of controlled distribution over the phases and a reduction of the maximum size for a single phase PV inverter.

The accuracy of solar PV HC obtained from the traditional Monte Carlo method used in stochastic evaluation of HC depends significantly on the number of simulations and complexity of the network model. Furthermore, with more uncertainties considered, the computation time, storage and accuracy become challenges with the stochastic method. In addition, combining performance indices and operational limits in one model in a stochastic method brings out additional challenges that have not been addressed so far. The main drawback of the stochastic approach is that a

unique value does not fit for the HC as the one obtained for a particular distribution scheme cannot be generalised and applied to another network.

2.3.2 Deterministic Approaches for Solar PV Hosting Capacity Evaluation

Deterministic methods for solar PV HC evaluation are typically based on traditional power flow analysis, which can account for limitations and diversity of LV networks. Furthermore, deterministic methods use traditional power flow analysis tools where active power (P), reactive power (Q), conductor impedance (Z) and load models are used as input data [9]. Applying known and fixed input data to a model to analyse the impact of solar PV systems in an LV distribution network is a rule-based analysis and hence easy to generalise.

Deterministic methods for establishing the solar PV HC have been presented in [24, 46, 47, 48, 49] with regard to LV distribution networks constrained by voltage rise. In [49], the impact of single phase solar PV systems has been presented by modelling the solar PV as a PQ (constant active and reactive power) or PV (constant active power and constant voltage) models. A method following the feeder ampacity, authors in [50] propose a simple and a generic equation to estimate the maximum solar PV capacity without exceeding the thermal limit of 100% of the feeder as shown in (2.5).

$$P_{PV} = 2 * P_{LOAD} + (1 - S_{LOAD}) \tag{2.5}$$

where P_{LOAD} is the active power of the load and S_{LOAD} is the apparent power of the load in p.u. This eliminates the need for deterministic power flow calculations to determine the hosting capacity. However, this study focused on ampacity of feeders to evaluate solar PV HC, which is not the most prominent limiting factor for solar PV HC evaluation in LV distribution networks.

Furthermore, a comprehensive review on deterministic method on solar PV HC

assessment presented in [9] highlights that the voltage magnitude rise and overloading are the impacts most considered for the hosting capacity determination with deterministic approach. Moreover, the deterministic methods can give the first underestimated value of the hosting capacity based on snapshot worst-case (overestimated impacts) assessment of solar PV penetration levels [24]. In the worst-case scenario, the output of the solar PV is assumed to be maximum while the power demand of the load is assumed to be minimum. Furthermore, it is very easy to underestimate the HC when calculating it based on the worst-case scenario, due to the fact that minimum load consumption and maximum solar generation are unlikely to occur at the same time for most of the cases (during solar peak time).

2.4 Measures to Enhance Solar PV Hosting Capacity

Enhancement of the solar PV HC is desired by DNOs due to the increasing demand for solar PV deployment. In [51], the formulation of regulatory and normative recommendations to increase the network hosting capacity are presented and the technical solutions to enhance solar PV HC have been categorised into: DNO solutions, prosumer solutions and interactive solutions. Furthermore, various HC enhancement techniques presented in [51], investigates options for voltage rise mitigation along with congestion reduction in distribution networks while technical solutions have been evaluated considering various factors such as investment costs, impact on voltage, technology readiness, impact on congestion and compliance within existing regulations.

DNO solutions; network upgrade/reinforcement and reconfiguration are installed and managed on the grid side and do not require any interaction with the consumers or the PV plants. The category of prosumer solutions such as battery energy storage systems (BESS) installation with solar PV units, are installed beyond the point of common coupling and react on loads or generation units, without any interaction with the DNOs. The category of interactive solutions include control of active and reactive power of PV inverters via smart inverter technology and require a commu-

nication interface linking the PV system in different grid locations and grid voltage. To understand the challenges posed in this research area and for the purpose of investigating the relevant analysis methods, a literature review on the HC enhancement techniques that have been implemented is provided in Sections 2.4.1, 2.4.2 and 2.4.3.

2.4.1 Network Upgrade/Reinforcement Options

Network reconfiguration and reinforcement solutions ensure capability of networks to handle solar PV units in a safe and reliable manner. In this regard, reinforcement of feeders (which means using larger conductor sizes that have lower electrical resistance), replacement of distribution transformer with larger transformers are of the effective techniques that can be used, especially in congested distribution networks, to maintain appropriate voltage profiles and achieve higher solar PV HC levels, enhance power quality performance and reduce network losses [13].

However, feeder and distribution transformer reinforcement and reconfiguration are not free and certainly will incur extra material and installation costs. Furthermore, the network reconfiguration is a complicated optimisation problem, especially in practical LV distribution networks with a large number of customers [13].

A stochastic model for analysing the impact of network reconfiguration on improving PV HC of distribution networks is developed in [52]. However, this network reconfiguration process is complicated in the case of real-time complex distribution networks due to increased random PV installations. Practical considerations and the problem of selecting the optimal conductor for solar PV HC enhancement in a real radial distribution network in Egypt are covered in [53]. Another network solution is installation of OLTC transformers, which is expensive, causing a financial burden on utilities if a large number of transformers require to be changed. Most distribution transformers in the LV distribution network have manually adjusted tap settings, which cannot be used to address the cyclic over-voltages caused by solar PV during day-time and under-voltages caused by customer demand during peak.

Furthermore, OLTCs too may not practically provide continuous voltage support. However, in [54], regulation of the distribution transformer tap settings is proposed, which is based on the feeder loading level for solar PV HC enhancement.

Technical aspects of realistic distribution networks with varying solar PV penetration levels, and maximises the solar PV HC of the network that with over-voltage issues employing different voltage control strategies including; OLTC, reactive power control (RPC) of inverters, network reinforcement (NR), and hybrid approaches as examined in [55]. Authors in [55] show that the NR is the best approach to maximise the HC of a particular region but economically it is not proven to be feasible. Further, results indicate that the hybrid approach of OLTC and RPC will be the best strategy for HC enhancement. In addition, [56] shows that adoption of OLTC-fitted transformers in a real UK residential LV network which resulted in HC enhancement from 40% to 100%.

2.4.2 Smart PV Inverter

"Smart PV Inverters" have proven to be an efficient approach to manage the network operation providing operational advantages. Smart inverters can operate in all four quadrants of the P-Q plane by controlling active and reactive power in real time. They can monitor voltage and frequency at their terminals and control power outputs accordingly [57, 58].

As per Electric Power Research Institute's initiatives (EPRI smart inverter initiative) [15], a set of standard smart inverter capabilities has been developed for the control of local voltage, frequency and for grid protection. Table 2.2 illustrates the classification of smart inverter functions according to the purpose of use [15].

Following sections discuss the specific voltage support functions that can be provided by smart PV inverters.

Table 2.2: Categorisation of smart inverter functionalities [15]

Voltage support functions	Frequency support functions	Grid protection support functions (response to disturbances)
Constant power factor mode	Frequency-Watt mode	Connect/Disconnect mode
Voltage-reactive (Volt-VAr) power mode	Low/High Frequency Ride-Through Requirements	Low/High Frequency Ride-Through Requirements
Voltage-active (Volt-Watt) mode	Limit maximum real power output	Low/High Voltage Ride-Through Requirements
Active power-reactive power (Watt-VAr) mode	Ramp-Rate control function (charge/discharge)	Temperature-power factor behavior mode
Active power-power factor mode		
Dynamic reactive power factor mode		
Ramp-Rate control function (charge/discharge)		
Limit maximum real power output		

Constant Power Factor Function

In this control mode, a constant power factor is set to operate either as leading or lagging. This means as the real power output of PV inverter increases, based on the fixed leading/lagging power factor, the reactive power injection/absorption will increase proportional to the power factor as shown in Fig. 2.4. IEEE defines leading power factor as positive (capacitive) and lagging power factor as negative (inductive) [15]. Lagging (negative) power factor can help reduce voltage rise caused by PV system output. However, if the inverter is not large enough, it will only output the reactive power available and will not curtail the real power.

Volt-VAr Function

In this control mode, inverters either inject or absorb reactive power based on the grid voltages at the point of connection. Fig. 2.5 shows example settings for the Volt-Var control mode [17]. As shown in Fig. 2.5, for a certain voltage range (dead-

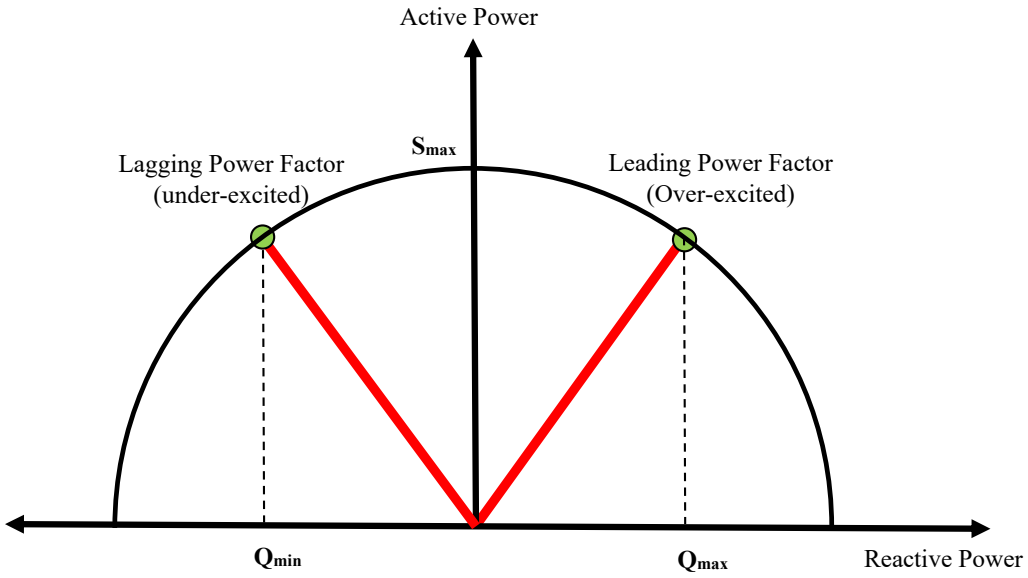

Figure 2.4: Generic constant power factor characteristic curve

band), inverters do not support reactive power and they operate in unity power factor control mode.

Capacitive VArs (injecting reactive power) are considered to be positive, while inductive VArs (absorbing reactive power) are negative. Absorption of reactive power occurs if the voltage begins to exceed a pre-determined upper level. Conversely, if the voltage begins to fall below the pre-determined lower level, reactive power can be delivered to the grid to help boost the voltage back to normal levels.

Further, Volt-VAr control mode could operate either on real power priority (Watt priority) or on reactive power priority (VAr priority) modes. Volt-VAr control in VAr priority mode outputs reactive power from the PV inverter, but limits the active power output based on the reactive power requirement. If the headroom for reactive power is incapable of delivering/consuming the required VArs to regulate the voltage, inverters with the VAr priority Volt-VAr control curtails some active power from the inverter. The active power output of PV inverter with VAr priority Volt-VAr control satisfy,

$$P_{PV} = \sqrt{S_{inv}^2 - Q_{Volt/VAr}^2} \tag{2.6}$$

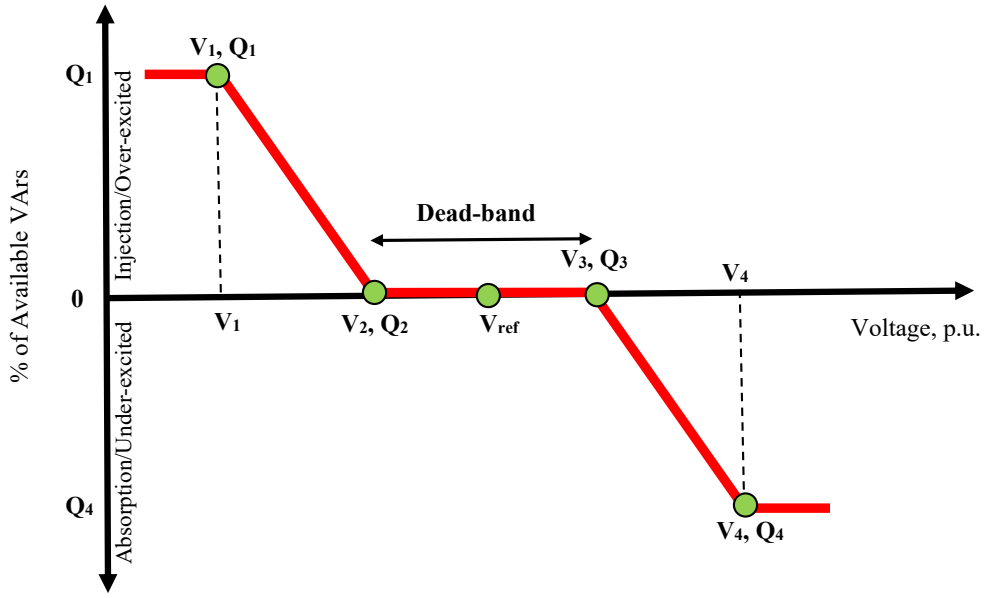

Figure 2.5: Generic Volt-VAr characteristic curve

where S_{inv} is the rating of the inverter and $Q_{Volt/VAr}$ is the required reactive power [17].

Watt priority Volt-VAr control provides all the active power generated by the PV system and is capable of delivering/consuming VArs based on available headroom for reactive power. Hence, available reactive power is

$$Q_{avail} = \sqrt{S_{inv}^2 - P_{PV}^2} \tag{2.7}$$

where S_{inv} is the rating of the inverter and P_{PV} is the real power available to the PV system from the irradiance [17]. If the inverter is operating at its full capacity, inverters with the Watt priority Volt-VAr control will not provide any voltage control.

Volt-Watt Function

This control mode of PV inverter manages the active power output of solar PV systems to maintain the voltage at the POC within predefined voltage limits. This

is illustrated in Fig. 2.6.

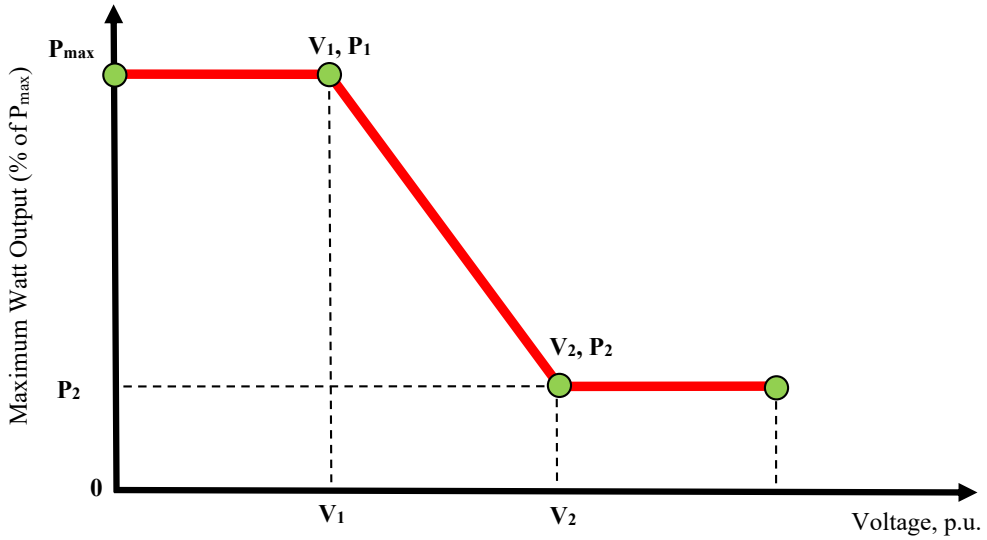

Figure 2.6: Generic Volt-Watt characteristic curve

Considering situations where high solar PV penetration and low load in distribution feeders that may result in high feeder voltages at certain times, the Volt-Watt control function can be used to limit the maximum active power output of the PV systems and bring voltages within the statutory limits. This control can also be beneficial in situations where existing controls (e.g., voltage control through OLTC transformer) are not able to prevent the occurrence of high voltages. Moreover, this control function can be used to manage thermal issues (provided that the over-voltages and the thermal over-loads occur at the same time) by adopting conservative Volt-Watt set-points, while managing voltages [59].

Watt-Power Factor Function

This control mode of inverters can either inject real power (positive real power) or absorb real power (negative real power) based on the power factor of the PV system. As illustrated in Fig. 2.7, positive values of x-axis are the real power relating to the Watts injected to the grid, while negative values are the real power absorbed from the grid. It is assumed that there is an energy storage system available to store real

power absorbed by the inverters [15].

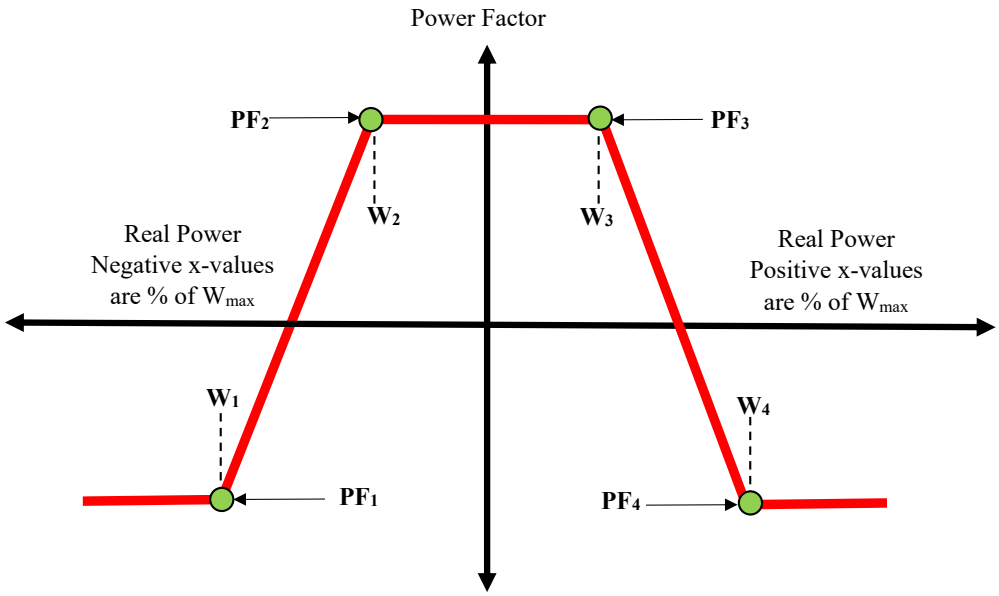

Figure 2.7: Generic Watt-Power Factor characteristic curve

Frequency-Watt Function

This control mode enables inverters to curtail their real power output and stabilise the system frequency. When there is a sudden load or generation change, the frequency of the system deviates from its nominal operating value and by allowing inverters to curtail their real power output, this function helps to lower and stabilise system frequency. The report by EPRI [15] gives two Frequency-Watt functions; Frequency-Watt Function 1 (given in Fig. 2.8) and Frequency-Watt Function 2 (given in Fig. 2.9). The Frequency-Watt Function 1 curtails active power at a specified rate when the frequency deviation is higher than 0.2 Hz. Power curtailment continues until frequency deviation returns to nominal operating conditions. If the frequency deviation starts to improve, power output does not start to increase and inverter waits until frequency deviation returns completely to nominal operating conditions.

Unlike Frequency-Watt Function 1, Frequency-Watt Function 2 does not wait until frequency deviation returns to nominal operating conditions to increase power

output of PV inverter.

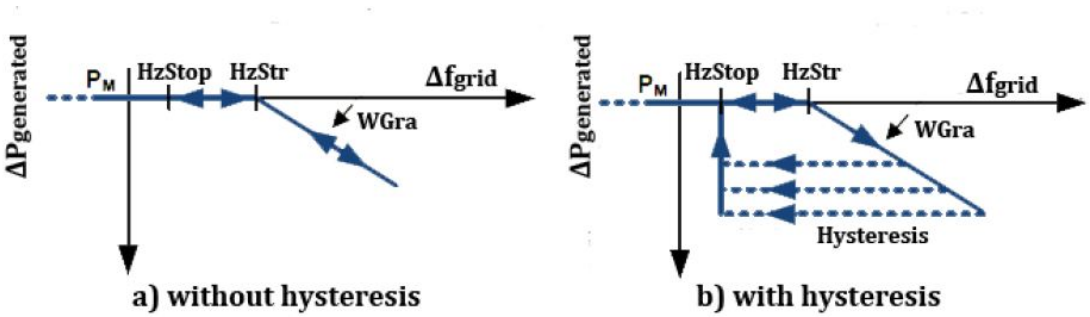

Figure 2.8: Generic Frequency-Watt Function 1 characteristic curve [15]

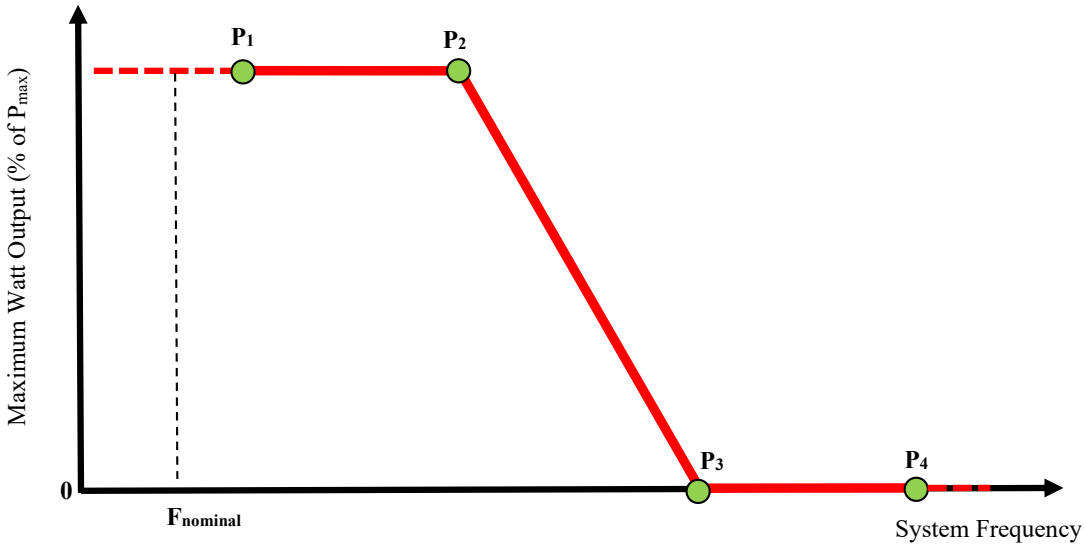

Figure 2.9: Generic Frequency-Watt Function 2 characteristic curve

The quantified benefits of smart inverter functions to increase solar PV HC and output would reduce the uncertainty of the decision making process. The capability of smart inverter functions to improve solar PV HC is presented in this thesis and a comparative evaluation of solar PV HC enhancement associated with different connection standards are provided in Chapter 6.

2.4.3 Battery Energy Storage Systems

Battery energy storage systems play a vital role in the adoption of renewable solar energy systems as they can handle the variability of production, which alternates

over the time and may not be fully predictable. BESSs are designed to store surplus energy during peak generation and low demand periods and later use during high power demand, thus not wasting the curtailed energy which cannot otherwise be used. Hence, distributed BESSs can be used for preventing over-voltage and voltage unbalance issues due to high solar PV penetration in LV residential networks [60, 61]. In [62], a technique to mitigate the voltage unbalance using BESS is proposed and shows that solar PV HC improved by 281.45 kW in a real LV distribution network in Victoria, Australia. Similarly, [63] has studied on BESS for over-voltage mitigation on an LV distribution feeder in Western Sydney, Australia. In [55], a coordinated control scheme has been proposed for a BESS with an OLTC transformer to mitigate voltage rise, which limits active power injections. The proposed controller sends charging/discharging operation commands to BESS in such a way to minimise the system losses and to shave the peak load. BESSs can also have the capability for reactive power compensation on the grid.

BESS not only can facilitate solar PV integration, but also useful to ensure continuity of supply, improve reliability and increase energy autonomy in distribution networks [64, 65].

2.5 Technical Requirements and Guidelines for Solar PV Connection

Considering the substantial impact of solar PV integration on distribution networks, technical requirements and guidelines for the connection processes and configurations are generally issued by network regulators. This section presents several regulatory standards to define the PV inverter operating modes for distribution networks and PV system interconnection requirements.

Solar PV HC approach and its assessment, current practices and technical requirements which worldwide DNOs follow are reviewed in [4]. Furthermore, CIGRE working group report C6.24 [7] titled "Capacity of distribution feeders for hosting

DER" has compiled recent HC assessment procedures practiced in many countries. However, many countries still apply their own practices, mostly based on rules of thumb, to limit impacts of PV interconnection on system performance [4, 7]. In general, DNOs presently use rules of thumb to quantify solar PV HC, such as, the percentage of the peak load of the feeder, percentage of transformer rating and thermal limit of relevant feeders [4, 7].

For example, the total penetration level of an LV network should not exceed 25% of the MV/LV transformer ratings in Portugal and South Africa, i.e. ($P_{DG} < 0.25P_{tr}$), whereas in Belgium the full MV/LV transformer rating should not be exceeded, i.e. ($P_{DG} < P_{tr}$) [7]. In Spain, the total PV capacity should be lower than 50% of the MV/LV transformer rating ($P_{DG} < 0.5P_{tr}$) and thermal limit of the affected feeders, i.e. ($P_{DG} < 0.5P_{thermal\_line}$) [7]. In Italy, the total PV capacity should be lower than 65% of the MV/LV transformer rating ($P_{DG} < 0.65P_{tr}$) and should be lower than 60% of the thermal limit of the affected feeders, i.e. ($P_{DG} < 0.6P_{thermal\_line}$) [7]. In Canada, the total PV capacity should be lower than 50% - 100% of the feeder capacity or transformer minimum load, i.e. ($P_{DG} < (0.5 - 1)$ Min. transformer load), or ($P_{DG} < (0.5 - 1)$ connected feeder capacity) [7]. In USA, total PV capacity on a 4-wire LV feeder should be lower than the 10% of the total line section peak load, i.e. ($P_{DG} < 0.1$ line section's peak load) [7]. However, these simple practices and rules of thumb do not address the locational impact of PV and other factors that determine solar PV HC.

In addition, most PV connection standards and guidelines have been revised in the recent years and have established a common set of smart inverter functions in order to manage network voltage levels related to PV integration at LV level. IEEE Std. 1547-2018[1] [66], AS/NZS 4777.2-2015[2] [67], California Rule 21-2018[3]

[1]IEEE 1547-2018 – IEEE Standard for Interconnection and Interoperability of DER with Associated Electric Power Systems Interfaces.

[2]AS/NZS 4777.2-2015 - Grid connection of energy systems via inverters, Part 2: Inverter requirements

[3]California Rule 21 - Version 1.5 – Simplified inverter configuration instructions to meet requirements

Table 2.3: Recent upgrades and recommendations for voltage and reactive power control in different standards

Standards / Control modes	IEEE 1547 -2018	AS/NZS 4777.2 -2015	California Rule 21 -2018	Hawaii Rule 14 -2018
Constant power factor mode	✓∗	✓	✓	✓
Voltage-reactive power (with reactive power priority) response mode	✓	✓	✓∗	✓∗
Voltage-active power response mode	✓	✓∗	✓	✓
Constant reactive power mode	✓			
Active power-reactive power mode	✓			
Active power-power factor mode		✓		
Frequency-watt mode			✓	✓

∗ Default control mode of standards

(Version 1.5) [68] and Hawaii Rule 14-2018[4] (Revised Sheet No. 34B-21) [69] are well known standards that have established such criterion and requirements for active and reactive power control, thus facilitating the mitigation of voltage related issues.

With regard to standardisation of new features in smart inverters, recommended practices/provisions of grid connected smart inverters have been recently amended in PV connection standards; IEEE Std. 1547-2018 [66], AS/NZS 4777.2-2015 [67], California Rule 21-2018 [68] and Hawaii Rule 14-2018 (Revised Sheet No. 34B-21) [69] as summarised in Table 2.3.

As given in the Table 2.3, IEEE 1547-2018 recommends the use of constant power factor mode with unity power factor set as the default mode unless or otherwise specified by DNOs. AS/NZS 4777.2-2015 specifies the inverters to operate with the Volt-Watt response mode as the default mode at the time of installation. California Rule 21 recommends the Volt-VAr control as the default mode with reactive power priority and Hawaii Rule 14 recently replaced 0.95 constant power factor requirement with reactive power priority Volt-VAr control mode as the default mode of operation. As a common feature to all standards, voltage and reactive power control functions are mutually exclusive and can activate only one of these modes at a time. However,

[4]Hawaii Rule 14 - Distributed Generating Facility Interconnection Standards Technical Requirements

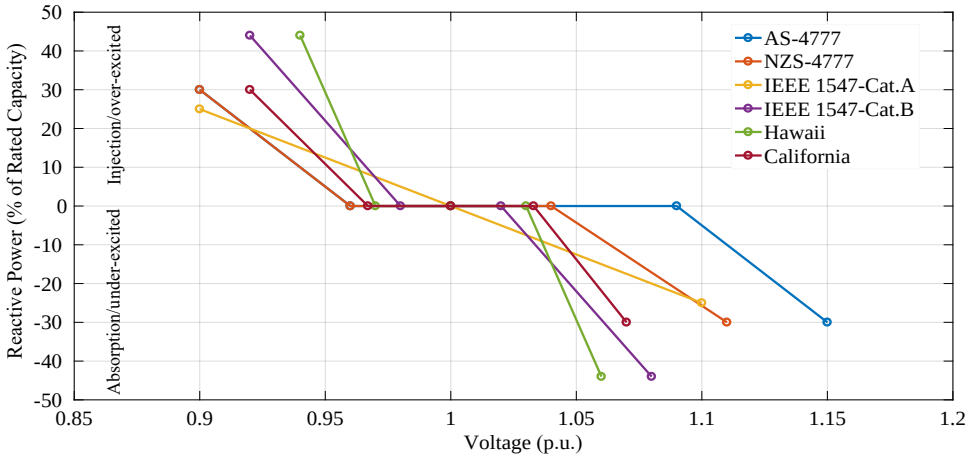

(a)

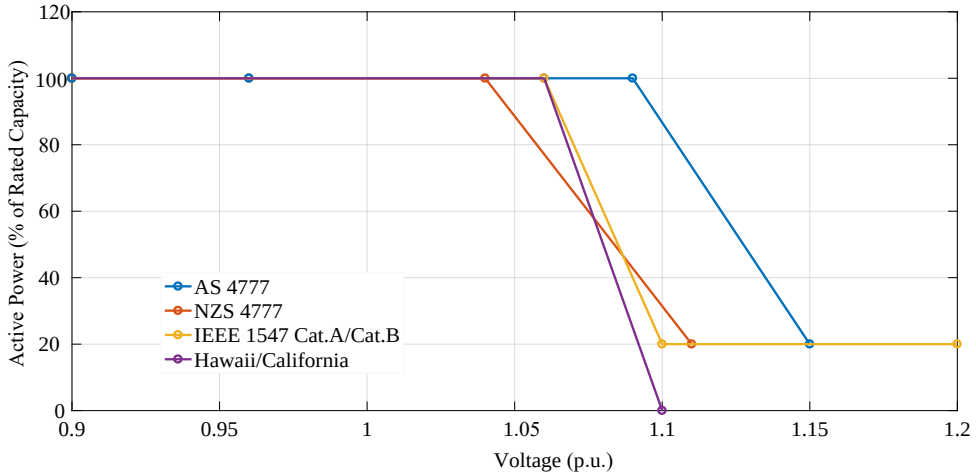

(b)

Figure 2.10: Power control function settings in different standards;(a) Volt-VAr control mode and (b) Volt-Watt control mode

the different suggestions/directions specified in various connection standards may be driven by regional practices and preferences.

The response curves for Volt-VAr and Volt-Watt control modes of aforementioned standards are illustrated in Figs. 2.10(a) and 2.10(b) respectively [66, 67, 68, 69]. It can be seen that set points of reactive and active powers are defined with or without a "dead-band" where no reactive or active power is absorbed or injected in Volt-VAr and Volt-Watt response curves respectively. The Volt-VAr and Volt-Watt control functions allow each individual PV system to provide a response according to (a) the voltage at the POC (the terminals of the PV system), (b) the available apparent power capacity of the PV system, and (c) the utility defined Volt-VAr and

Volt-Watt set points specified in different standards.

In general, voltage support functions of smart inverters can be used to manage over-voltage curtailments that often limit the solar PV hosting capacity in LV distribution networks. Therefore, potential HC enhancement options can be investigated by means of detailed analysis of smart PV inverter operation in Volt-VAr or Volt-Watt control modes. Further, smart inverter performance for over-voltage curtailment based on diverse recommendations made by solar PV connection standards need to be comparatively evaluated. Accordingly, the best fit control strategy and/or default setting/s of smart inverters for maximum HC enhancement for a given network configuration can be determined amongst the provisions given in different solar PV connection standards which may provide greater benefits to both customers and DNOs.

2.6 Chapter Summary

This chapter provided general information in relation to solar PV integration in LV distribution networks, which include impacts, basic concept of solar PV HC, HC enhancement techniques and current practices and standards for PV connections.

Key sections of this chapter have given critical discussion on the technical and operational issues with high solar penetration levels in LV distribution networks and the preliminary work in relation to the potential power quality assessment. With increased solar PV connections, their influence on power system performance cannot be neglected. Further, it has been discussed that voltage quality issues such as over-voltage is the major concern in relation to integration of solar PV systems in LV distribution networks. Therefore, it is important to investigate and quantify how the solar PV contributes to the network voltage levels and its operational impacts on network performance. Furthermore, general concept of solar PV HC is introduced and its assessment methods are critically discussed, establishing the background information relevant to the remaining chapters. Further, as enablers for solar PV HC enhancement approaches in cost-effective planning solutions; network

upgrade/reinforcement, smart grid and BESS technologies are outlined. Furthermore, general guidelines on the HC assessment at the pre-connection stage were discussed in detail to identify extended research scope for the development of systematic methodologies for solar PV HC assessment and enhancement which are strongly linked to the main thrust of this thesis.

Chapter 3

Potential Power Quality Impacts Associated with LV Distribution Networks with High Solar Penetration Levels: A Case Study

3.1 Introduction

LV distribution networks with high penetration levels of grid connected solar PV systems have been reported to experience operational challenges which could degrade a number of power quality related issues as discussed in Section 2.2.

The main objective of this chapter is to investigate the potential power quality issues of a practical LV distribution network with high solar penetration levels based on detailed analysis of an urban LV distribution network in Sri Lanka which was reported to have the highest levels of roof-top solar PV generation in 2017. The outcomes pave the path for identifying key parameters/indices which limit the maximum connectable solar PV capacity of LV distribution networks. Accordingly, the primary work covered in this chapter includes:

- Detailed simulations of the urban LV distribution network under different solar

penetration levels (present scenario and future estimated levels) thus exploring the network performance and limitations of increasing solar PV additions.

The power quality analysis is presented under different solar penetration levels by detailed modelling of the network. Accuracy of network modeling was verified employing measurements at the distribution transformer and smart meter readings at customer levels.

3.2 Modelling of LV Distribution Network

The 250 kVA, 11 kV/400 V LV distribution network in the study represents an urban LV network in Sri Lanka located in Kotte area which has more than a 40% of solar PV capacity (as a ratio of the distribution transformer capacity). The reproduced single line diagram of the network (the real LV system was simulated although the spur lines and individual pole locations are not shown in the single line diagram) is shown in Fig. 3.1 while, Tables 3.1 and 3.2 provide the details of the distribution network.

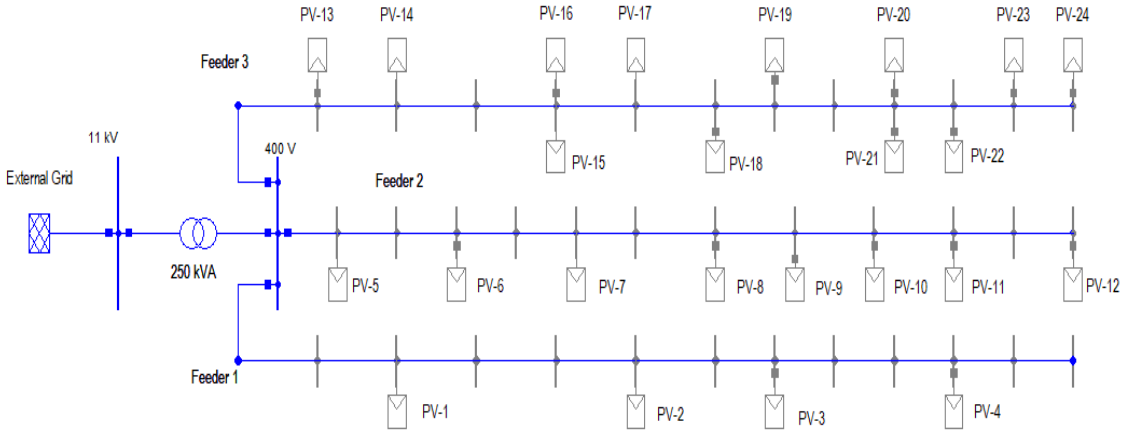

Figure 3.1: Single line diagram of the LV distribution network

The secondary per phase voltage of the distribution substation has been set at 240 V (1.04 p.u.) to ensure the voltage at customer connections is within the stipulated limits under maximum demand conditions. The distribution system consists of three LV (400 V) feeders and supplies a total 336 customers including 253 single

Table 3.1: Details of the case study

11 kV fault level	330 MVA
Transformer rating	250 kVA/11kV/400V
Present maximum demand (*)	154 kW
Present maximum demand as a % of transformer capacity	77%
Number of customers served	336
Number of customers with rooftop solar PV generators (Solar capacities vary in the range from 1 kWp to 15 kWp, eg : 1, 1.75, 3, 4, 6, 7.25, 15)	24
Number of outgoing LV feeders from the transformer	3

* Recorded Data for July 2017

phase customers and 83 three phase customers. More than 90% of the load is shared by 315 residential customers and remaining falls under commercial tariff category. In LV four-wire distribution networks, both zero sequence[1] and negative sequence[2] voltage unbalance components are present and this network has been reported exhibit voltage unbalance where measured maximum voltage unbalance factor[3] is around 1%. Voltage unbalance of LV network in Sri Lanka is permissible as the negative sequence voltage up to a maximum of 3% [20]. Details of the LV distribution scheme and related field measurements for this study were provided by the Lanka Electricity Company, the distribution licensee of the network.

The LV network was modelled in DIgSILENT PowerFactory simulation platform giving due consideration to following aspects:

- Single phase customers are distributed evenly among three phases
- Three phase customers are assumed to be balanced among three phases
- Single phase solar PV systems are distributed evenly among the three phases in each feeder

There is a higher potential for increase in the solar penetration levels across

[1]zero sequence voltage unbalance factor = $\frac{zero\ sequence\ voltage}{positive\ sequence\ voltage}$*100

[2]negative sequence voltage unbalance factor = $\frac{negative\ sequence\ voltage}{positive\ sequence\ voltage}$*100

[3]Quantified in terms of negative sequence voltage unbalance factor.

Table 3.2: Feeder vise customer details

	Feeder 1	Feeder 2	Feeder 3
Length of main feeder	510 m	400 m	610 m
No. of single phase customers	134	51	68
No. of three phase customers	20	26	37
Total no. of customers	**154**	**77**	**105**
No. of solar customers	4	8	12
Cumulative solar capacity	17 kW	35 kW	50 kW
Conductor type	3 Phase Aerial Bundle Cable (ABC) Type : $3 \times 70\ mm^2 + 54\ mm^2$ R = 0.443 Ω/km , X = 0.08 Ω/km Type : $3 \times 50\ mm^2 + 54\ mm^2$ R = 0.641 Ω/km , X = 0.08 Ω/km		

the network, following the recent government initiatives on net metering options. Net-metered[4] solar PV customers generally select their rooftop solar PV capacity in such a way that the electricity generation matches their monthly electricity consumption. With two newly introduced schemes, namely Net-Accounting[5] and Net Plus[6], customers have the freedom to over-size their rooftop solar PV capacity up to their contract demand to generate more electricity than what they consume, if they have sufficient roof area.

3.2.1 Load Modelling

Load profiles of more than 30% of the total of 336 customers were derived based on the actual energy data recorded in 15 minute time intervals, obtained from the remote metering facilities. The remaining load profiles were obtained by deriving an average load profile (using measured load profiles) for each tariff block in a given tariff category.

Average load profiles derived for each tariff block are given in Fig. 3.2. These average load profiles were used to generate load profiles of the remaining customers (those who did not have remote metering to provide actual load profiles) based on

[4]The consumer has to pay only for the net amount of electricity that is consumed.

[5]This allows customers to be paid in cash for any surplus electricity they generate from the solar PV system at the end of their monthly billing cycles.

[6]This allows customers to sell total electricity generated from the solar PV system to the utility while the customers pay for the electricity they consume based on the existing tariff structure.

the monthly energy consumption data taken from individual customer accounts. Further, a constant power factor of 0.8 lagging was assumed for all customers. The total customer demand was assumed to be constant for different solar PV penetration levels. It is a justifiable assumption to use with regard to all simulated scenarios since the solar penetration level was reported to have reached 40% in a very short time span.

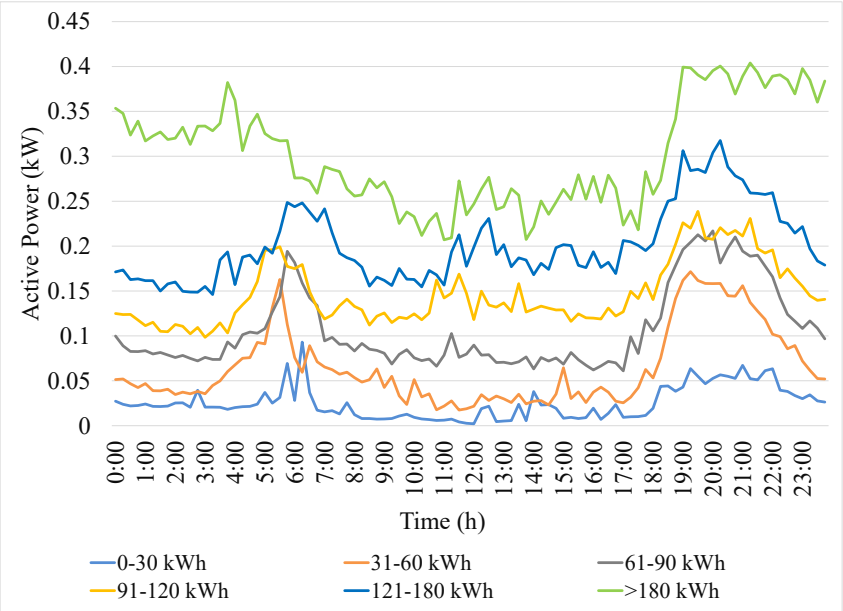

Figure 3.2: Averaged load profiles for customers in different tariff blocks

3.2.2 Solar PV Modelling

All installed solar PV units are assumed to provide active power at unity power factor which is compliant with IEEE 1547-2003 [70]. Solar irradiance profiles were developed using the System Advisor Model (SAM) software considering the irradiance data applicable to Sri Lanka where high solar radiation (5.5 to 6 kWh/m^2) is available throughout the year [71]. In practice, solar PV system's direct current (DC) capacity does not reach its rated value even when the solar irradiance is maximum. This mismatch is typically avoided by increasing DC capacity of the system to be higher than the alternating current (AC) capacity of the inverter by introduc-

ing a DC to AC design ratio of 1.2 [72]. However, considering the fact that the AC capacity of the inverter is equal to the installed solar PV output at the POC, a DC to AC ratio of unity was used in modelling solar PV systems.

3.3 Network Performance Analysis under Increasing Solar Penetration Levels

The LV network is simulated to cover a 24 hour period under different solar penetration levels as shown in Table 3.3. The base case scenario which is the case without any solar installation (0% penetration) is simulated under scenario 1. The present network was simulated under scenario 2 (40% penetration) with existing 24 solar PV customers of cumulative solar PV capacity of 102 kW. In scenarios 3, 4, 5 and 6, the network was simulated with increasing penetration levels of 50%, 60%, 75% and 100% of the transformer rating respectively. At increasing solar penetration levels, individual solar PV capacities were assumed to be connected as net metered connections. Further, customers with higher monthly energy consumption levels were assumed to install solar PV systems early in the capacity built-up. Cumulative solar PV capacity for different penetration levels used for simulations are shown in Table 3.3.

Table 3.3: Installed solar capacity under various scenarios

Scenario	Penetration level	No. of solar customers	Cumulative capacity (kW)
1	0%	0	0
2	40%	24	102
3	50%	28	127
4	60%	34	150
5	75%	45	187
6	100%	83	250

Subsections; 3.3.1, 3.3.2, 3.3.3, 3.3.4 and 3.3.5 present the simulation outcomes of the LV network performance under different solar penetration levels in terms of power flow, voltage profiles, negative sequence and zero sequence voltage unbalance components, power loss and power factor at the secondary of the distribution

transformer for a 24 hour period.

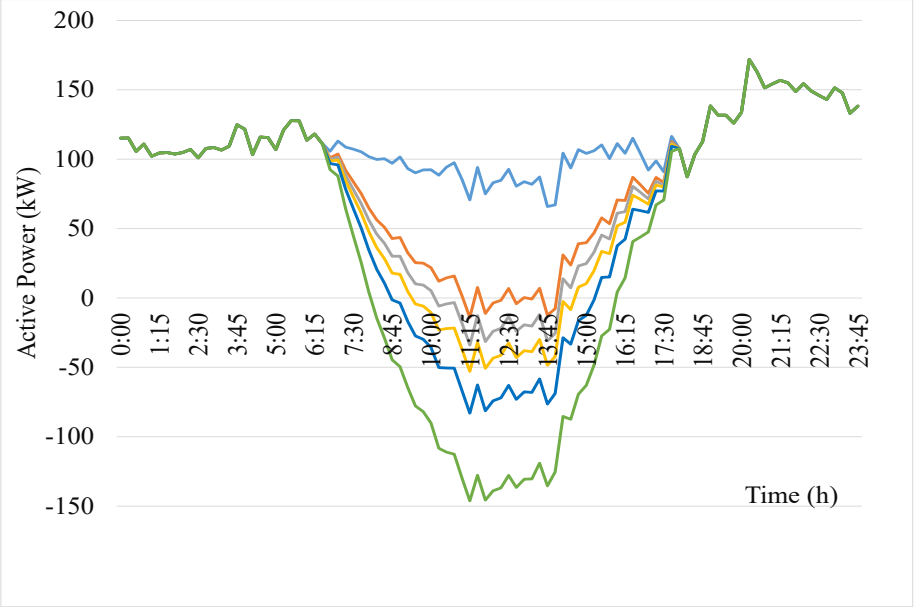

(a)

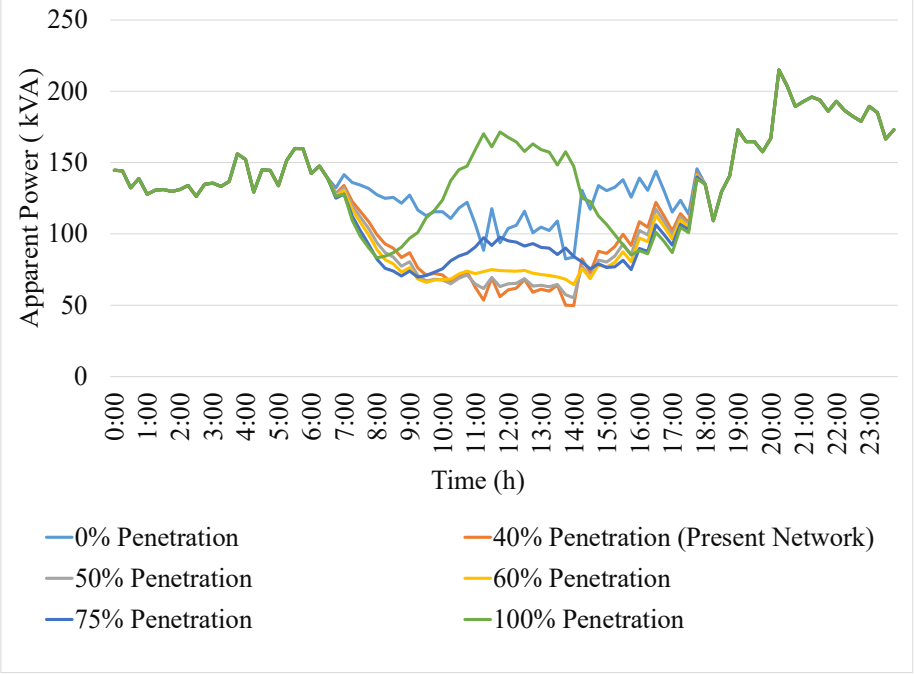

(b)

Figure 3.3: Power flow at the distribution transformer for different solar penetration levels (a) Active power (b) Apparent power

3.3.1 Active Power Flow

Fig. 3.3(a) shows the active power (kW) at the transformer secondary for different solar PV penetration levels for 24 hour period. Reverse power flow is visible when the solar penetration is 40% of transformer capacity (i.e. Scenario 2 representing the present network operation) when the solar power generation is maximum during 11:00 am to 1:00 pm which can be used to verified the accurate network modelling. Increasing levels of PV penetration beyond 40% causes higher reverse power to flow towards the transformer thus affecting the 11 kV network. A reverse power flow of around 80 kW which is almost equal to day time average demand load can be seen at 75% of the solar PV penetration level. Corresponding to present network operation, the transformer loading level has only been reduced to 22% (54 kVA) as shown in Fig. 3.3(b) as the total reactive power is still supplied by the grid.

The accuracy of network modeling was tested by comparing the net power flow, assessed based on the measurements at the transformer secondary and the simulated net power flow variation as shown in Fig. 3.4. Moreover, the selected distribution transformer has recorded a reverse power flow for a short period of time on certain days when the solar generation is maximum. Fig. 3.5 shows the reverse power flow incident recorded on a day in July 2017. Measured imported and exported energy (kWh) levels are shown in 15 minutes time intervals.

3.3.2 Feeder Voltage Rise

Maximum feeder voltages were observed at a time when the solar power generation is maximum and customer demand is minimum. Accordingly, Fig. 3.6 shows the variation of phase voltages along the three feeders (the maximum voltage levels were observed in phase “c” of all three feeders). Voltages of feeder 1 and feeder 2 do not violate any stipulated limits under any solar penetration level considered. However, the longest feeder, feeder 3 (610 m) has shown an over voltage situation (upper voltage limit - 1.06 p.u.) towards the end of the feeder at a solar PV penetration level of 50% (Scenario 3). In scenario 6, where the solar PV penetration level is

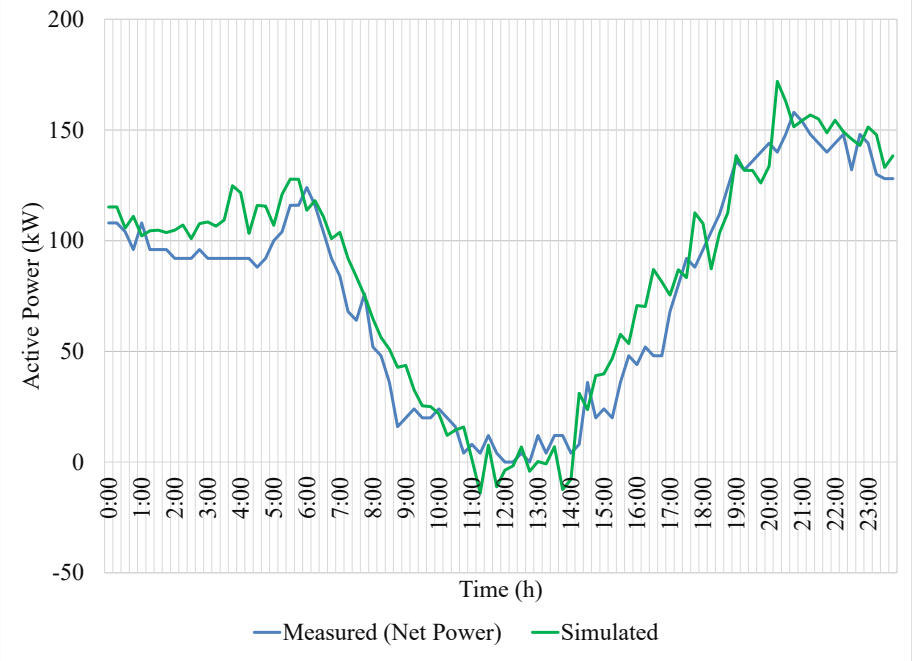

Figure 3.4: Measured and simulated net power flow at the distribution transformer for the present scenario (Scenario 2)

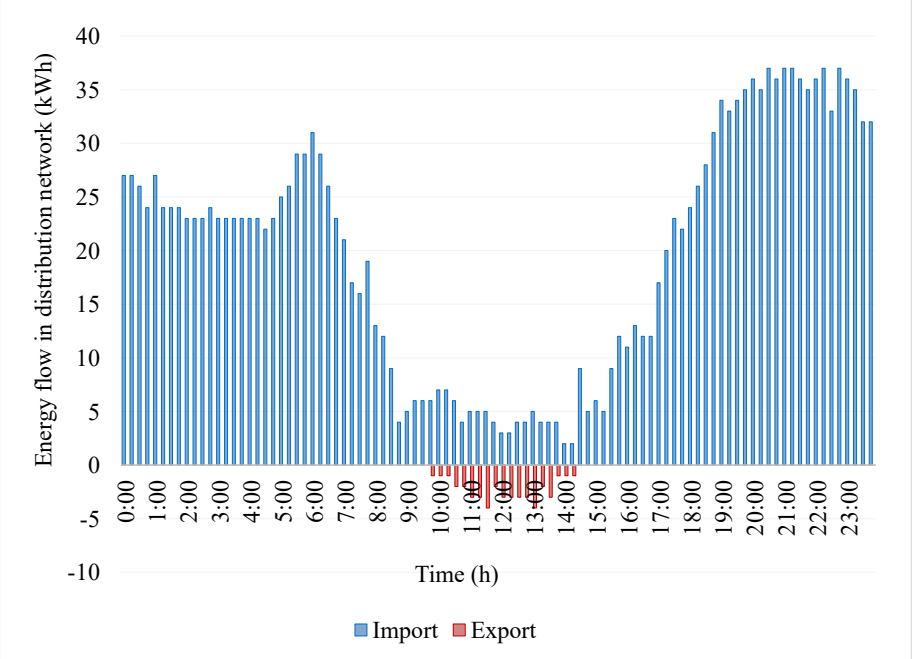

Figure 3.5: Measured imported and exported energy at the distribution transformer secondary

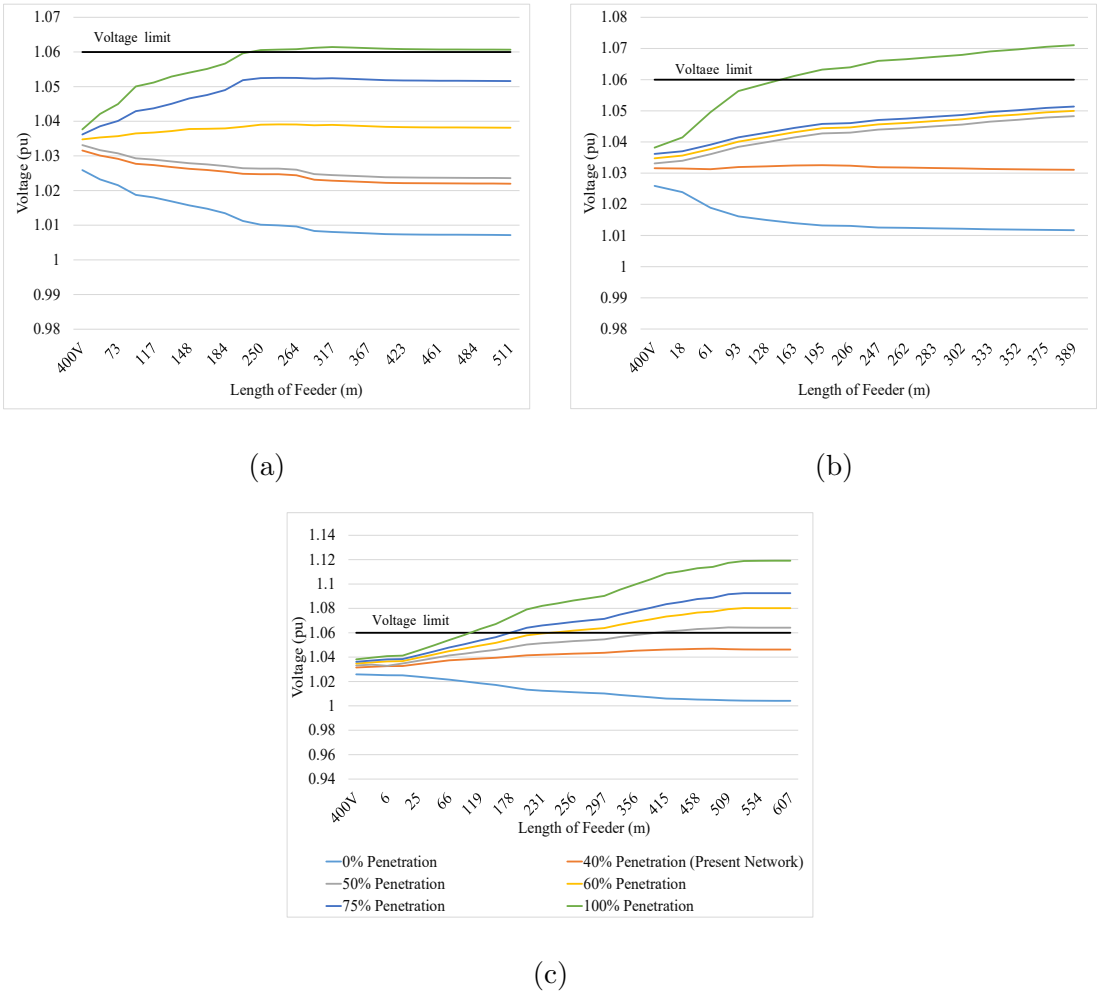

Figure 3.6: Voltage profiles at different solar penetration levels (a) Feeder 1 - phase c (b) Feeder 2 - phase c (c) Feeder 3 - phase c

100%, around 80% of the feeder 3 exhibits an over-voltage situation.

3.3.3 Voltage Unbalance

The LV distribution system under study was modelled in such a way that loads were equally distributed in the three phases to account for a balanced network (a relatively smaller zero sequence and negative sequence voltage unbalance factors between 0.1% and 0.84%). During the night peak, the same system is reported to exhibit more than 1% negative sequence voltage unbalance based on available field measurements. The simulated model also confirms the same night peak voltage unbalance conditions. Table 3.4 gives maximum zero sequence and negative sequence voltage unbalance factors at the feeder end calculated based on the simu-

lated voltages (V_0 - zero sequence voltage component, V_1 - positive sequence voltage component, V_2 - negative sequence voltage component) for the five different scenarios considered. At higher solar penetration levels, a tendency exists for higher voltage unbalance levels, mainly because of higher number of single phase solar PV inverter connections. Location of connections and size of the inverters can be seen to influence the resultant feeder voltage unbalance level.

Table 3.4: Zero sequence and negative sequence voltage unbalance components

	Feeder 1		Feeder 2		Feeder 3	
	V_0/V_1 (%)	V_2/V_1 (%)	V_0/V_1 (%)	V_2/V_1 (%)	V_0/V_1 (%)	V_2/V_1 (%)
Scenario 1	0.82	0.84	0.10	0.22	0.24	0.16
Scenario 2	1	1	0.50	0.47	0.46	0.55
Scenario 3	0.95	1.07	0.26	0.20	1.13	1.17
Scenario 4	0.85	1.30	0.48	0.51	1.20	1.16
Scenario 5	1.82	1.94	0.53	0.66	2	1.50
Scenario 6	1.79	1.92	0.58	0.71	1.98	1.05

3.3.4 Total Network Power Loss

Fig. 3.7 shows the total network power loss associated with the LV system including transformer loss for different solar PV penetration levels for the 24 hour time period. Network power loss during day time (when the solar PV generation is maximum) varies due to different solar penetration levels and is seen to be minimum at 40% penetration level. However, further increase in solar PV to 100% has resulted in a higher power loss compared to scenario 1 (without solar). Considering all scenarios in the study, the present solar penetration level (40%) leads to minimum power loss during day time.

3.3.5 Power Factor at the Transformer Secondary

Referring Figs. 3.3(a) and 3.3(b) (reactive power and apparent power flow), net active power demand at the transformer secondary has significantly reduced during the day time where solar PV generation is maximum. Since the inverters are man-

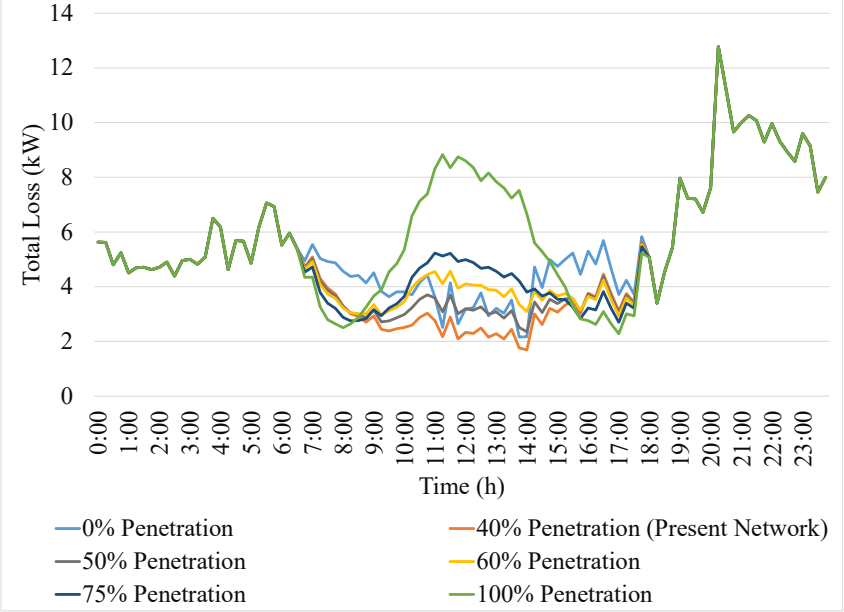

Figure 3.7: Network power losses

dated to operate at unity power factor and the total reactive power demand is being supplied by the transformer, a poor power factor is visible at the supply side. At the present solar PV penetration level, power factor varies from 0.0 to 0.4 lagging during the time period when solar PV generation is at its maximum, whereas at the maximum solar PV penetration level (100%), leading power factor in the range of 0.8 to 0.9 can be observed. However, poor power factor in itself does not present any operational impact for the network.

The following conclusions can be drawn in reference to the Sections 3.3.1, 3.3.2, 3.3.3, 3.3.4 and 3.3.5.

- Unacceptable voltage rise is evident with higher solar penetration levels
- 40% solar penetration level (present network) is the optimal PV level in respect to reverse power flow, minimum power loss and reduced transformer loading level to 22%
- Network voltage unbalance increases with single phase PV connections and depends on the PV location and size of the PV systems

- Experiencing poor power factor at the distribution transformer is significant with higher solar penetration levels
- Maximum connectable solar PV capacity is primarily limited by unacceptable voltage rise

The general observation which can be made from this case study is that, the high solar penetration levels increase the over-voltage situations in a significant manner.

3.4 Voltage Rise Analysis based on Smart Meter Measurements

Smart meter readings of the urban LV distribution network discussed in Section 3.2 was analysed to examine the customer voltage profiles as the over-voltage issue is the major concern with increasing solar penetration levels.

Voltage profiles of selected six customers connected to feeders 2 and 3 at different locations (customer locations are marked as A, B, C, D, E and F in Fig. 3.8) are analysed in relation to the over-voltage problem as shown in Fig. 3.8. These smart meter readings over a 24 hour period were recorded in April 2018 and the cumulative solar capacity in the network was noted to be 116 kW on the day of observation.

Total rooftop solar PV systems connected to feeders 2 and 3 have increased to 42 kW and 57 kW (7 kW increase from the value in July 2017 for both feeders) respectively while cumulative solar capacity in feeder 1 has unchanged. Table 3.5 gives a summary of the solar PV installations in the network.

Table 3.5: Feeder wise solar PV installations in 2017 and 2018

	Feeder 1	Feeder 2	Feeder 3
As at July 2017			
No. of solar customers	4	8	12
Cumulative solar capacity	17 kW	35 kW	50 kW
As at April 2018			
No. of solar customers	4	11	13
Cumulative solar capacity	17 kW	42 kW	57 kW

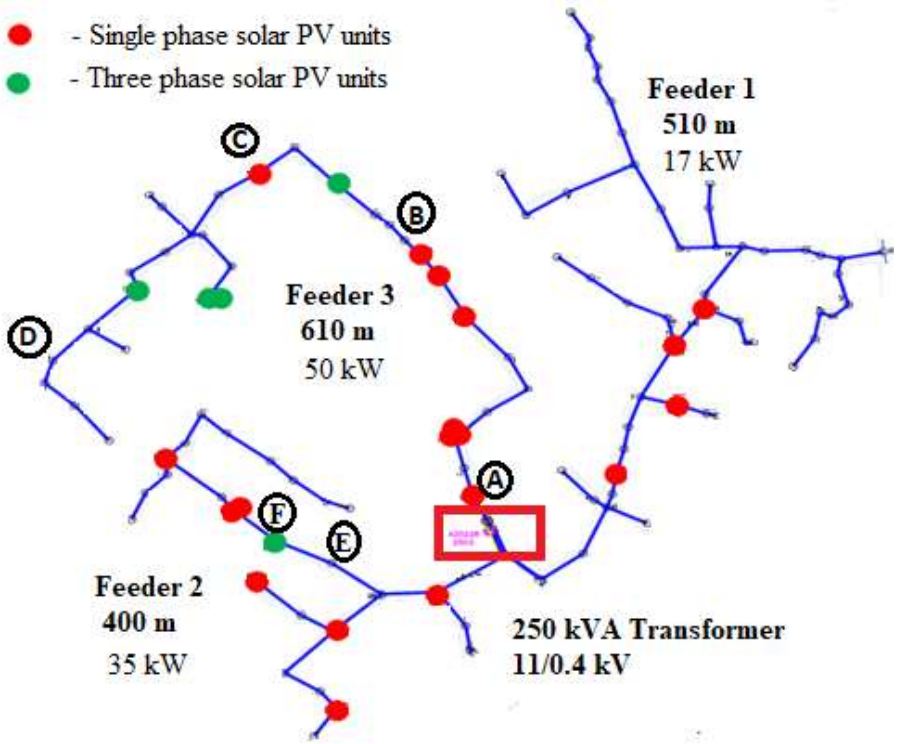

Figure 3.8: Distribution network with solar PV map

Fig. 3.9(a) shows voltage profiles of a solar customer (at location F as shown in Fig. 3.8) and a non-solar customer (at location E as shown in Fig. 3.8), located half way of the feeder 2, affected by over-voltage condition. Further, Fig. 3.9(b) shows four selected customer voltage profiles for both solar and non-solar in feeder 3, where a solar customer (at location C as shown in Fig. 3.8) and a non-solar customer (at location D as shown in Fig. 3.8) towards the feeder end are affected by over-voltage condition during the solar peak times. However, customers who are close to the transformer end (both solar customer at location A and non-solar customer at location B) are not affected. It is to be noted that the upper voltage limit stipulated by the distribution network service provider in Sri Lanka is in the range +/- 6% of the nominal voltage.

Overall, customer voltage profiles obtained from smart meter readings provide clear evidence on unacceptable voltage rise during solar peak times (10 am to 2 pm).

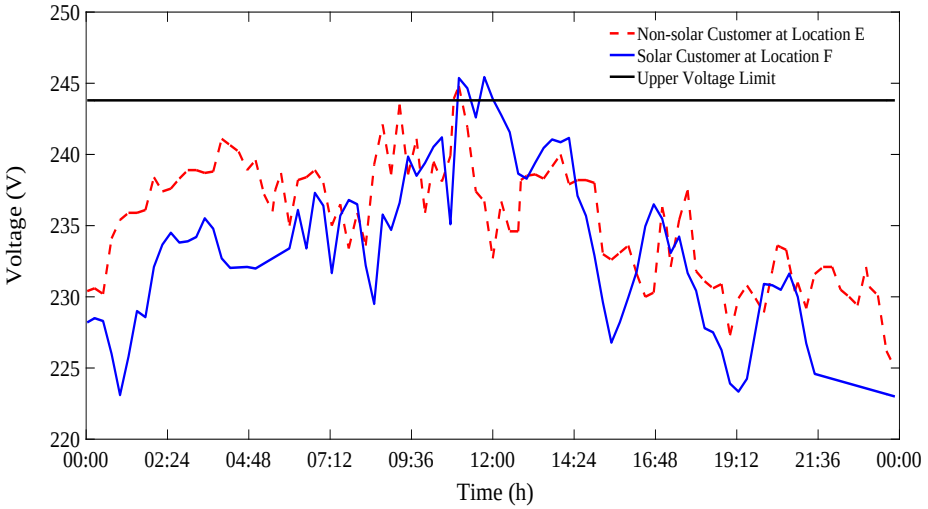

(a)

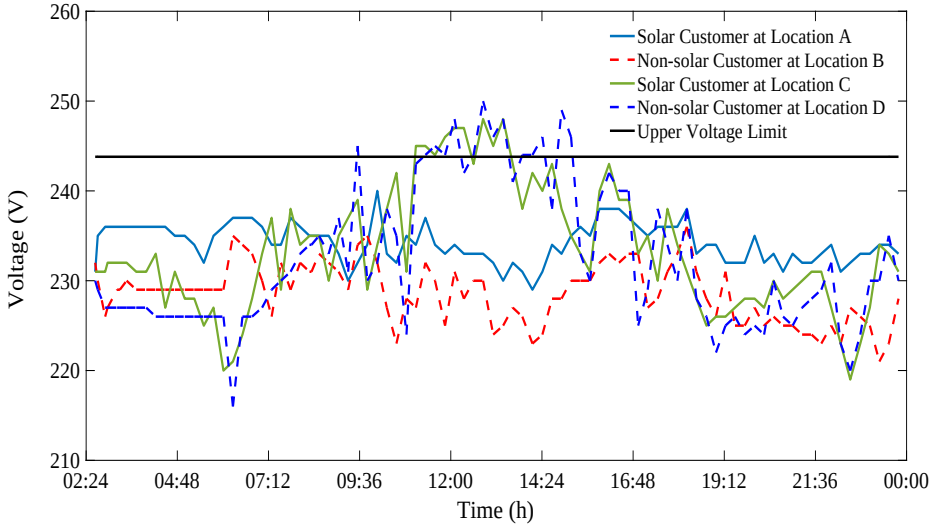

(b)

Figure 3.9: Voltage profiles of solar/non-solar customers at different locations (a) Feeder 2 (b) Feeder 3

3.5 Discussion

The analysis presented in this chapter helped identify the limiting factors on maximum solar PV penetration level in a practical urban LV distribution network.

Effects of increasing solar connections which are realistic have been analysed considering discrete levels of future solar penetration levels. Results of this study reveal that the maximum solar penetration level of the study network is primarily limited by the unacceptable voltage rise towards the feeder ends. Furthermore, voltage rise analysis based on smart meters measurements provides clear evidence

of over-voltage conditions in LV distribution feeders during peak PV generation on the same practical urban LV network. Thus, the smart meter data analysis validates the case study results obtained for the LV distribution network. Thus, voltage rise and consequent violation of statutory limits become the most influensive constraint limit for maximum connectable solar PV capacity in LV distribution networks.

3.6 Chapter Summary

This chapter has presented the technical impacts caused by higher penetration levels of roof top solar PV systems on the operating performance of the LV distribution networks based on a case study of an urban LV distribution network in Sri Lanka which has a 40% solar penetration level (based on transformer capacity). Effects of increasing solar connections which are realistic have been further analysed.

Several major observations can be drawn from the work presented:

- Simulation results covering the present scenario (case study) were validated with available field measurements and voltage levels at the feeder ends were found to be within network stipulated limits
- 40% solar penetration level (present network) was the optimal PV level in respect to reverse power flow and minimum power loss and hence, further connection of solar PV systems will cause increase in network losses and reverse power flow
- Network voltage unbalance increases with single phase PV connections which depend on the location of PV systems
- Experiencing poor power factor at the distribution transformer is maximum with 40% solar penetration level (present network)
- Unacceptable voltage rise is evident with higher solar penetration levels and hence, the maximum connectable solar PV capacity is primarily limited by the voltage rise

The work presented in this chapter has led to identify the limiting factors on maximum solar PV penetration level in LV distribution networks. A systematic evaluation of the solar PV HC of the considered LV distribution network will be covered in Chapter 4.

Chapter 4

Solar PV Hosting Capacity Evaluation: Stochastic Approach

4.1 Introduction

As discussed in Chapter 2 (Section 2.3.1), stochastic approaches are widely used to evaluate the solar PV HC as the uncertainties of solar PV location, sizes can be more accurately represented. The work presented in this chapter covers a stochastic approach to evaluate the solar PV HC in LV distribution networks based on Monte Carlo simulations. The practical urban LV network discussed in Chapter 3 where over-voltage issues were reported has been primarily studied for solar PV HC evaluation considering over-voltage and thermal over-loading limits as performance indices.

A methodology based on stochastic approaches can determine the net solar PV HC on the entire network, however does not provide locational information or feeder wise connection capabilities. Further, from a distribution network planning perspective, advanced HC assessment methods which give information with regard to locational variation of solar PV units are important in accepting new connection applications. Thus, influential factors/considerations on maximum solar penetration level are analysed while identifying the limitations and shortcomings of such stochastic methods through detailed analysis of the network in consideration. Fur-

thermore, a feeder based solar PV HC evaluation method is proposed based on the outcomes of sensitivity analysis of influential factors on HC. The work presented in this chapter includes:

- Assessment of solar PV HC in a practical urban LV distribution network subjected to voltage rise and thermal limit violations based on Monte Carlo simulations.
- Analysis on limiting factors on maximum connectable solar PV capacity in LV distribution networks.
- Development of a feeder based solar PV HC evaluation method.

Accordingly, Section 4.2 describes a stochastic approach of solar PV HC assessment of the practical urban LV distribution using Monte Carlo simulation method and Section 4.3 provides a detailed analysis on limiting factors on solar PV HC employing sensitivity analysis of locational variation of solar PV units and feeder characteristics. Further, Section 4.4 proposes a feeder based solar PV HC evaluation approach for LV distribution networks based on the findings in Section 4.3.

4.2 Stochastic Approach for Hosting Capacity Analysis in Practical Urban LV Network

This section covers the development of stochastic analysis framework followed using conventional Monte Carlo Simulation (MCS) method to assess solar PV HC of the practical LV distribution network discussed in Chapter 3. The performance indices are selected as over-voltage of the feeders and over-loading of the feeders and distribution transformer with regard to the selection of an appropriate solar PV HC level.

Accurate analysis of solar PV HC requires the development of solar deployment scenarios for all possible future PV locations and corresponding PV installation size in the network. However, it is not feasible to simulate all possible PV deployment

scenarios for a given network. Thus, to represent the impact of the location of a new solar PV connection, the MCS approach is used with a limited number of PV deployment scenarios at a particular level of penetration.

The overall stochastic analysis framework developed for creating M solar deployment scenarios for each of the N penetration levels is illustrated in Fig. 4.1. In the proposed approach, solar PV penetration level (N) is defined as the ratio of the number of customers with PV units and the total number of customers. With increasing penetration levels, a number of stochastic solar PV deployment scenarios (M) is considered in such a way that in each scenario the locations of the solar PV customers are randomly selected from the pool of solar customers in the network. Capacity of each solar PV system is determined as a net metered customer. Therefore, each simulated scenario is unique in the way how the solar PV units are deployed with solar PV location and size of PV system.

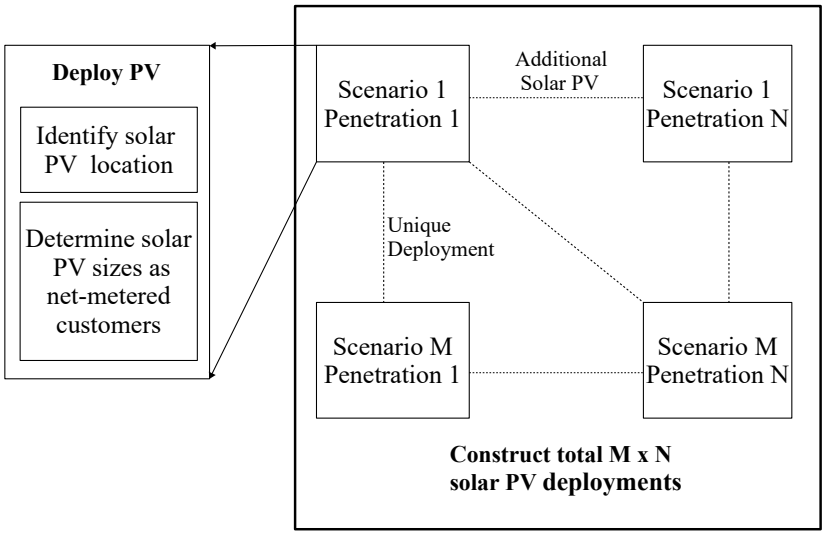

Figure 4.1: Stochastic analysis framework for solar PV deployment

Since this systematic approach is applied to a practical distribution network, solar PV connections are only allocated to customers with energy consumption greater than 120 kWh per month, with the assumption that the solar PV installations are financially feasible for these customers. Following the same rationale, capacity of the

solar PV system is determined based on the monthly energy consumption of each consumer and assigned as a net metered customer. The total customer demand is assumed to be constant for different solar PV penetration levels. Following this method, several deployment scenarios are systematically developed, until all financially feasible solar deployments are implemented in the network. It is assumed that all installed solar PV units are to provide active power at unity power factor which is a common practice.

The network model was prepared in DiIgSILENT PowerFactory simulation platform to run Monte Carlo simulations.

4.2.1 Over-Voltage and Over-Loading Criteria

Maximum feeder voltage violation and thermal over-loading of feeders and transformers are commonly reported as the deciding and critical factors in assessing solar PV HC in distribution networks. The considered test network is already associated with over-voltage violation issues as discussed in Chapter 3. Accordingly, solar PV HC was evaluated for the test network by defining the maximum feeder voltage in addition to considering the feeder and transformer loading violations. In each PV deployment scenario, network power flows were monitored and the corresponding network voltages and feeder and transformer loading levels were calculated in order to verify whether any performance standards are violated. The threshold values for each performance index considered in this analysis are given in Table 4.1. It is important to highlight that threshold value for a given performance index is mutually exclusive of the rest of performance indices.

Table 4.1: Operational limits for evaluating solar PV hosting capacity

Criterion	Definition	Limit
Over-voltage	Feeder bus voltage	$\geq$ 1.06 p.u.
Thermal loading	Feeder and transformer loading	$\geq$ 100 %

MCS results shown in Figs. 4.2(a), 4.2(b) and 4.2(c) elaborate the resulting maximum feeder voltage, maximum feeder loading and transformer loading levels

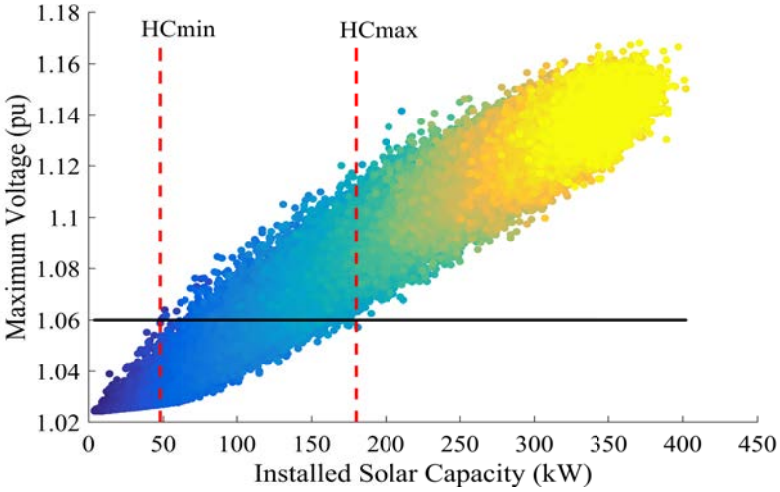

(a)

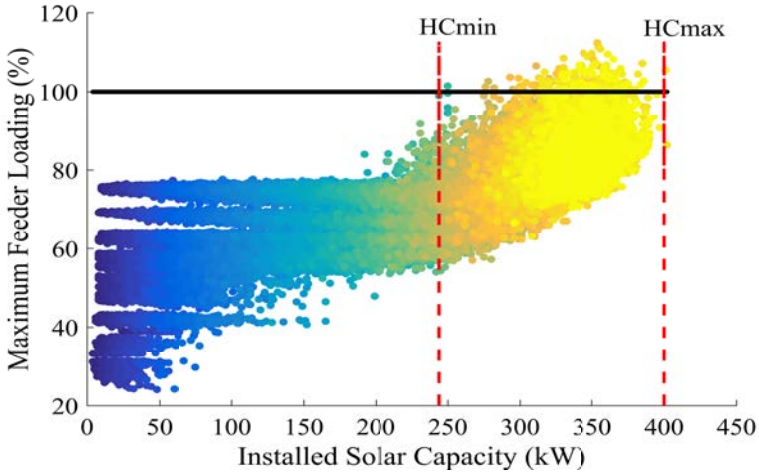

(b)

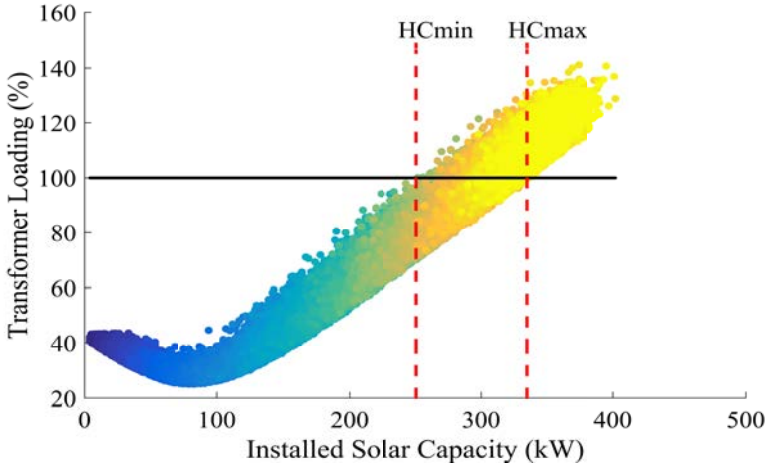

(c)

Figure 4.2: Hosting capacity limits for performances index (a) Maximum feeder voltage criterion (b) Maximum feeder loading criterion (c) Transformer loading criterion

Table 4.2: Solar deployment limits for test network

Criterion	HC_{min} (kW)	HC_{max} (kW)
Over-voltage	48	178
Thermal loading - Feeder over-loading - Transformer over-loading	 244 250	 >400 332

respectively, under different solar penetration levels for a total number of 66,000 solar deployment scenarios. Based on the MCS results, two levels of solar PV HC can be identified as minimum hosting capacity (HC_{min}) and maximum hosting capacity (HC_{max}) compliant with the given performance index, as shown in Fig. 4.2 and summarised in Table 4.2. With the minimum hosting capacity level, none of the solar penetration levels violates the criteria of the performance index, i.e. 48 kW of solar PVs can be integrated to the test network without violating the steady-state maximum feeder voltage limits without any concern of the PV location. Similarly, considering only the thermal over-loading limits of feeders and transformer, the same network can withstand up to 244 kW solar PVs (note that the voltage violation criterion is excluded in thermal loading analysis, and vice-versa). Solar penetration levels in excess of the maximum hosting capacity limit, independent of the location of the solar installation will violate the relevant operational limits. Moreover, between minimum and maximum hosting capacity levels, certain solar penetration levels which arise from random PV locations may violate network constraints. Therefore, detailed studies are necessary with precise solar PV locations to verify that a given level of penetration is safe.

The dependency of the number of solar PV deployments on the accuracy of the results obtained through MCS method was tested by changing the number of solar deployment scenarios and repeating the process for over-voltage criterion as shown in the Fig. 4.3.

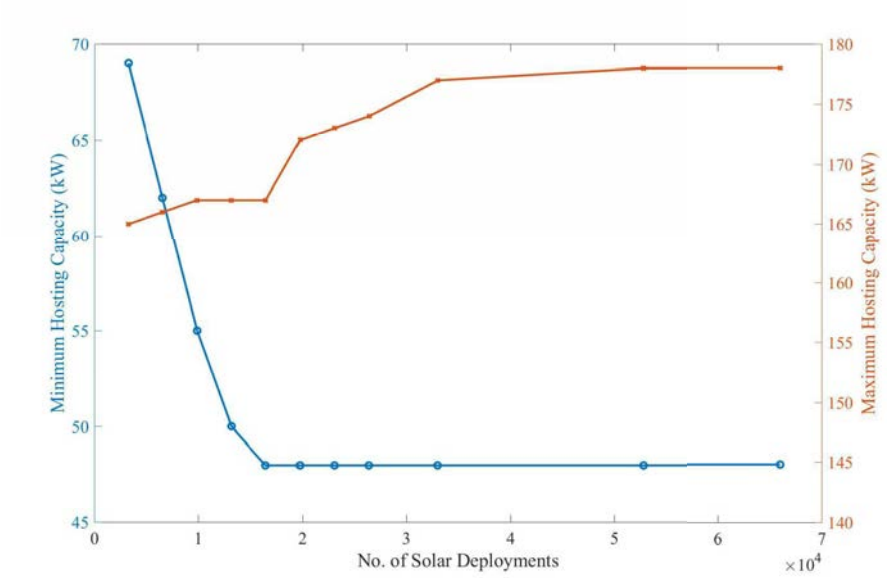

Figure 4.3: Variation of hosting capacity limit with the number of solar deployment scenarios for over-voltage criterion; minimum hosting capacity and maximum hosting capacity

4.2.2 Limitations with Stochastic Evaluation Framework

Evaluation of solar PV HC is a complex task that requires accurate network modelling requiring extensive data. A major drawback of Monte Carlo based studies is the higher computational time and data storage requirements in order to reach superior convergence of the final output. Furthermore, stochastic assessment methodologies for addressing the randomness of the position and rating of solar PV systems are not easy to implement due to complexity and high computational times in the evaluation procedures. In addition, solar PV HC of a network depends on the characteristics of the network (feeder length, type of the conductor, level of loading etc.). Therefore each network will have a distinctive solar PV HC level. From a network planning perspective, evaluation of the solar PV HC of LV distribution networks through stochastic method is a complicated task and not practical. Thus, there is a need for systematic approaches to assess the solar PV HC together with theoretical verification where possible.

4.3 Influencive Factors on Solar PV Hosting Capacity

This section presents necessary sensitivity analysis on solar PV HC influencing factors in order to broaden the stochastic approach of solar PV HC assessment and assess HC in an accurate and effective manner.

Solar PV HC depends on many factors including the characteristics of the network and solar PV systems. Therefore, sensitivity analysis should be performed on each individual influencing factor to examine their effects on the hosting capacity. The major factors that influence solar PV HC are solar PV system rating, solar PV location [4] and feeder characteristics including are operating voltage, loading level, topology, conductor type, length and existing power/voltage control mechanisms [13].

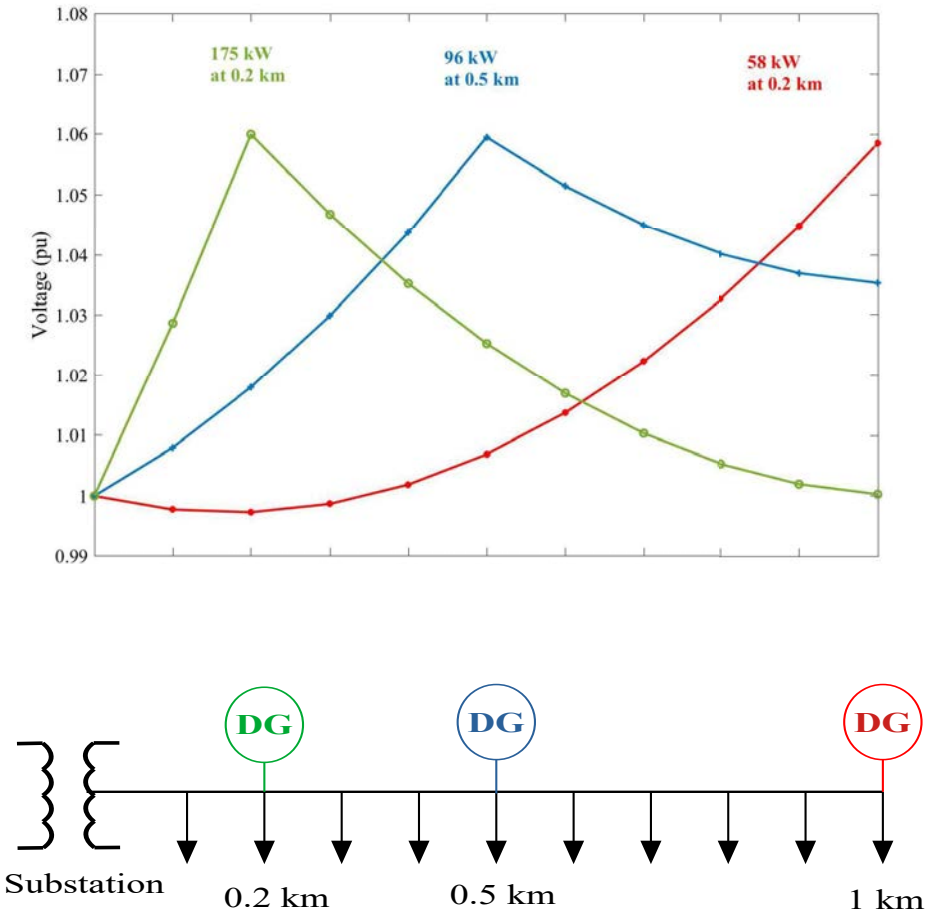

Figure 4.4: Feasible solar PV generation levels at different locations for over-voltage limit of 1.06 p.u.

All hypothetical network analysis presented in this section assumes uniform load distribution on the feeder for simplicity. This assumption agrees with the practical networks due to the fact that LV feeders with larger number of customer base are tapped with short pole span.

4.3.1 Influence of PV Location and Capacity on Hosting Capacity

Solar PV location and their aggregated capacity along the feeder are vital factors in assessing hosting capacity for a given distribution network. A simple case study is presented to show the influence of solar PV system location and aggregated capacity on maximum penetration level. The 1 km long single feeder network shown in Fig. 4.4 (conductor type: AAC - Fly type (All Aluminium Conductor), $R = 0.4505\ \Omega/km$, $X = 0.292\ \Omega/km$) is considered with the daily peak demand of 40 kW and 30 kVAr. The total load is assumed to be divided equally between three phases and evenly distributed along the feeder. Fig. 4.4 also shows the voltage profile of the feeder for maximum solar power that can be injected at three different locations, where an aggregated capacity is considered at a given location (distance is measured from the transformer end) without violating over-voltage conditions. The results clearly show how the power injection levels tend to reduce when solar PV system is connected towards the feeder end.

Location Sensitivity Analysis

Influence of solar PV location system and aggregated capacity on the solar PV HC levels is assessed by considering a simple LV distribution network which has two feeders. The study network comprises an 11 kV/400 V, 100 kVA transformer with a loading level of 50%. Two different feeder lengths; 500 m and 1000 m (conductor type: AAC - Fly type) are considered to analyse the effect of feeder length on the solar PV HC. To assess the impact of loading levels on solar PV HC, two cases are considered;

- Case 1: 60% of total load is allocated to feeder 1 and the rest (40%) is assigned to feeder 2
- Case 2: 40% of total load is allocated to feeder 1 and the remaining (60%) is assigned to feeder 2

In addition, a constant power factor of 0.8 lagging is assumed for all connected loads. For simplicity, balanced and evenly distributed loads are considered. Each feeder length is analysed by dividing into three equal-length segments as shown in the Fig. 4.5 where the randomness of the solar PV deployment is applied to each seg

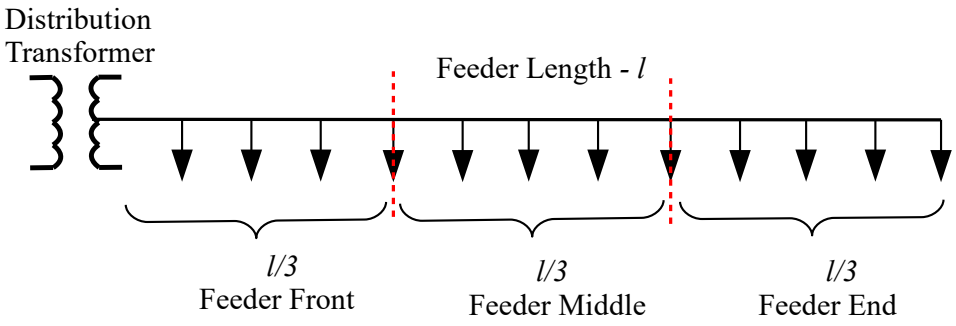

Figure 4.5: Feeder segments for hosting capacity analysis

Accordingly, four solar deployment scenarios are considered by changing the locations of the solar PV connections in relation to the Case 1 and 2:

- Scenario 1: Solar PVs are distributed in the feeder end segment;
- Scenario 2: Solar PVs are distributed in the feeder middle segment;
- Scenario 3: Solar PVs are distributed in the feeder front segment;
- Scenario 4: Solar PVs are distributed over all segments of the feeder.

As a specific case, solar PV HC at a pre-determined location is also investigated by evaluating the maximum connectable solar capacity in three phases at the boundaries of each segment such that voltage limit is not violated.

Outcomes of Location Sensitivity Analysis

Initial values of maximum feeder voltage drop and feeder loading levels of the network are given in Table 4.3 for both Case 1 and Case 2 (without any solar PV connections).

Table 4.3: States of feeders without solar PVs

	Case 1 (F1-60%/F2-40%)		Case 2 (F1-40%/F2-60%)	
	Feeder 1	Feeder 2	Feeder 1	Feeder 2
Max. voltage drop	3%	4%	2%	6%
Max. feeder loading	0.3 p.u.	0.2 p.u.	0.2 p.u.	0.3 p.u.

The test network was analysed to examine the maximum connectable solar PV capacity at different segments ensuring that the voltage upper limit is not violated. Fig. 4.6 shows the maximum connectable solar PV capacities at the boundaries (the specific case of fixed locations of PV) of the three segments for both Case 1 and Case 2 (hosting capacity values are given in per unit using a base, S_b =100 kVA which is the step down transformer rating thus allowing the feeder loading level to be compared against). Further, solar PV units are to provide only active power operating at unity power factor. The voltage at the secondary of the transformer was maintained to a constant value of 1 p.u.

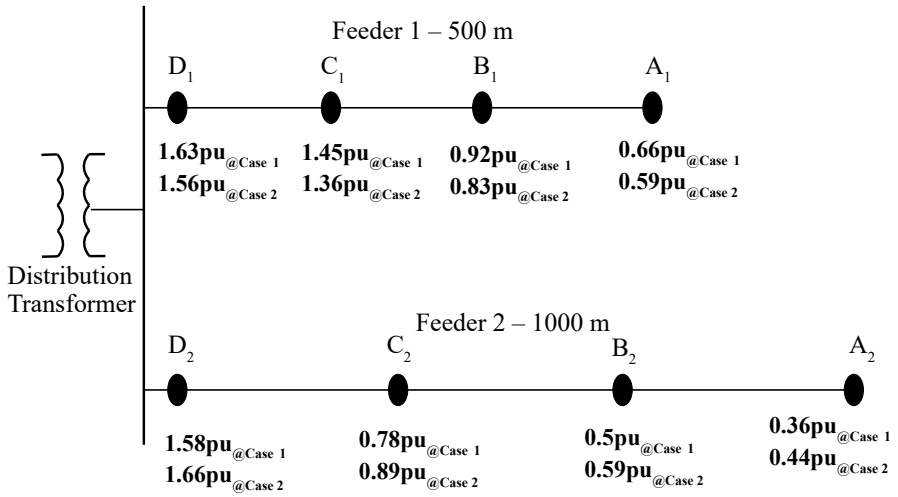

Figure 4.6: Maximum connectable solar capacity at different locations of two feeder network without violating over-voltage limit

The two feeder network of Fig. 4.6 was analysed using MCS method and for illustrative purposes, results obtained for Case 1 scenarios are shown in Fig. 4.7 and Fig. 4.8 with regard to over-voltage and feeder over-loading criteria respectively. The limit for over-voltage exceedance is 1.06 p.u. and the acceptable feeder loading limit is considered to be 100% of the thermal loading of the conductor. Transformer loading level was not considered in the analysis as the aim was to consider the feeder level solar PV HC.

To be complied with HC constraints limits; feeder over-voltage and over-loading, minimum (HC_{min}) and maximum (HC_{max}) hosting capacity levels for considered scenarios must not violate HC limits of each constraint as illustrated in Fig. 4.9. Here, HC_{min} and HC_{max} are defined as the HC levels where 0% and 100% of violation of penetration limits under the given constraint respectively. Thus, the minimum hosting capacity of a given scenario is the maximum connectable solar capacity at 0% of constraint limit violation and the maximum hosting capacity is the maximum connectable solar capacity at 100% of constraint limit violation.

Referring to Fig. 4.9, it can be seen that when solar PV systems are distributed in the feeder front segment, the connectable maximum solar PV capacity level is essentially limited by the feeder over-loading due to minimal voltage rise caused by solar PVs. Table 4.4 gives the summary of minimum and maximum hosting capacity values (considering feeder over-voltage and over-loading criteria) derived using MCS for both Case 1 and Case 2 (detailed results obtained from MCS method for Case 2 are given in Appendix A).

Table 4.4: Solar deployment limits for the two feeder network in per unit

	Case 1		Case 2	
	HC_{min}	HC_{max}	HC_{min}	HC_{max}
Scenario 1: End segment	0.4	1.4	0.45	1.4
Scenario 2: Middle segment	0.5	2.3	0.6	2.3
Scenario 3: Front segment	0.8	3.4	0.9	3.4
Scenario 4: All over the feeder	0.7	2.5	0.9	3.0

Referring to Fig. 4.6, maximum connectable solar capacity at different locations, without violating the over-voltage limit of two feeder network, clearly indicates

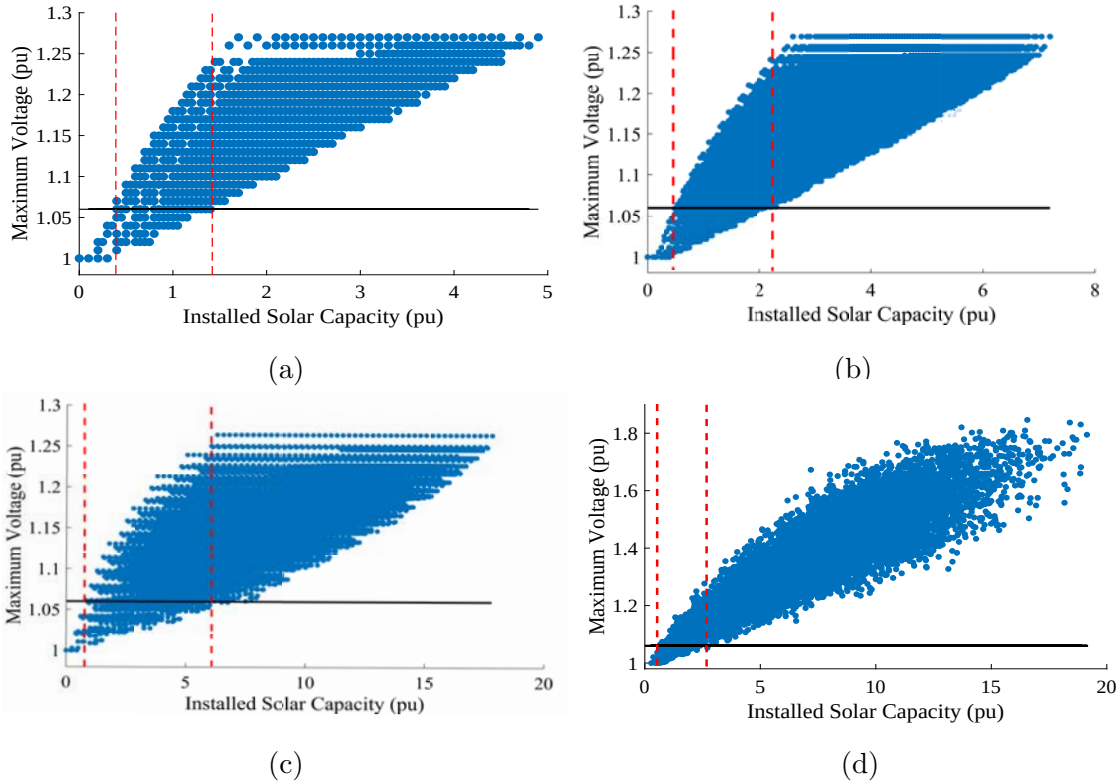

Figure 4.7: Variation of segment wise hosting capacity levels for over-voltage criterion; Case 1, Solar PVs are distributed in; (a) Feeder end segment (b) Feeder middle segment (c) Feeder front segment (d) Over all segments of the feeder

that the maximum connectable PV capacity increases as the solar PV systems are distributed towards the feeder front (closer to the distribution transformer). Further, in Case 1, for the end segment, the lowest hosting capacity was obtained at the feeder end as 0.36 p.u. (at point A_2 in the feeder 2) and for the same case, the summation of the hosting capacities at the nearest end to the transformer of both feeders in the end segment is 1.42 p.u. (hosting capacities at the points B_1 and B_2). These values are equal to minimum and maximum solar PV HC values obtained from MCS method. Same argument is valid for all three segments. Hence, for a multi-feeder network, minimum hosting capacity of the entire network is the lowest of the minimum hosting capacities of all feeders. Thus, considering a single feeder network, minimum hosting capacity can be defined as the maximum connectable solar PV capacity at the far end of the given feeder while, maximum hosting capacity is the maximum connectable solar PV capacity at the nearest end to the transformer. The same argument is valid for segment wise analysis as well. In other words, the

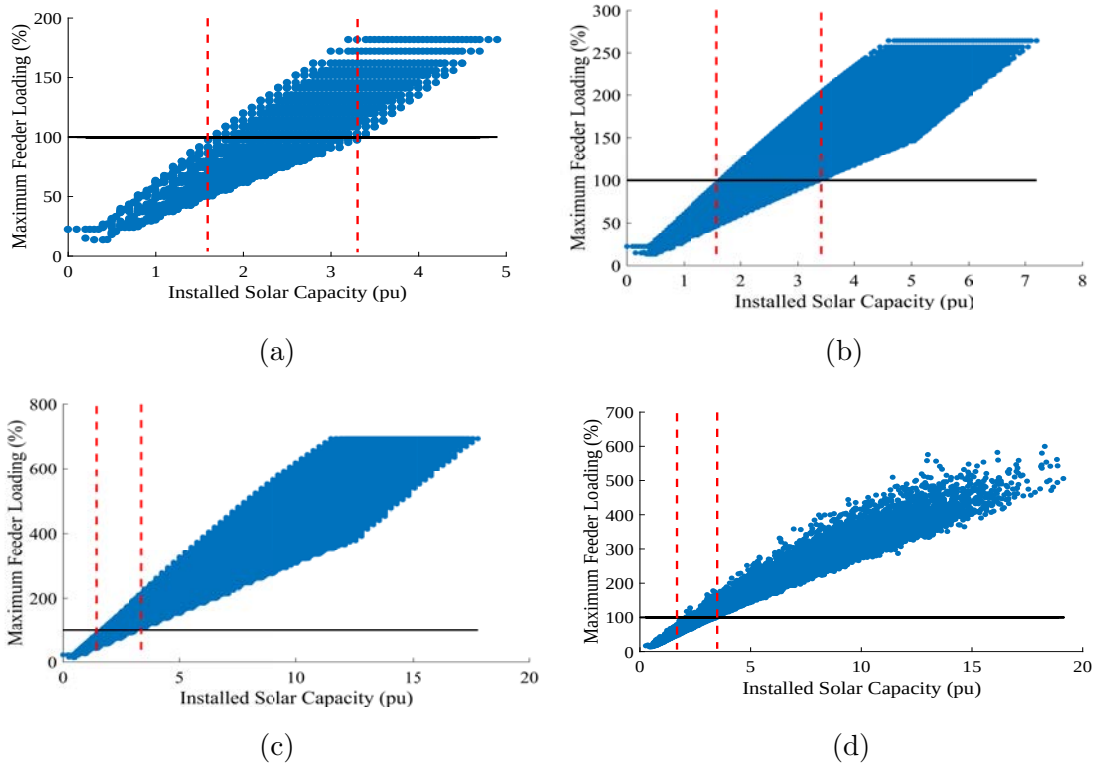

Figure 4.8: Variation of segment wise hosting capacity levels for feeder over-loading criterion; Case 1, solar PVs are distributed in; (a) Feeder end segment (b) Feeder middle segment (c) Feeder front segment (d) Over all segments of the feeder

minimum and maximum hosting capacities are the connectable maximum solar PV capacity at the boundaries of each segment, far end of the feeder segment and nearest end to the transformer respectively.

4.3.2 Influence of Feeder Characteristics on Hosting Capacity

Multi-feeder LV distribution networks with different feeder characteristics were simulated in DIgSILENT simulation platform in order to analyse the influence of feeder characteristics on solar PV HC. In this study, all test networks comprise an 11 kV/400 V, 100 kVA transformer with a loading level of 50% (all multi-feeder scenarios consider at the same transformer loading level). In addition, a common network classification of urban and rural networks is represented by selecting different lengths of feeders. Same analysis is repeated for different types of conductors in order to examine the effect of R/X ratios on hosting capacity. For simplicity, balanced and evenly distributed loads are assumed. Furthermore, it is assumed all

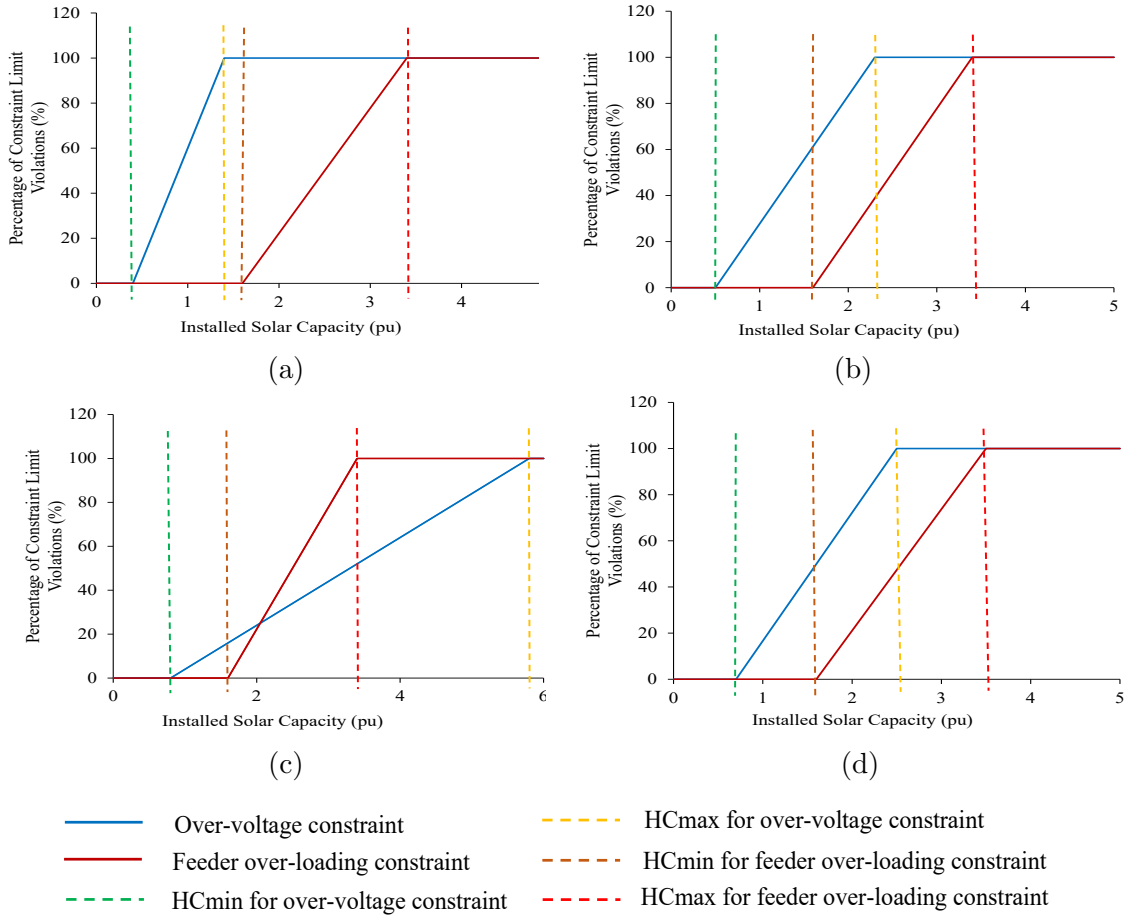

Figure 4.9: Segment wise minimum and maximum hosting capacity levels; Case 1, Solar PVs are distributed in; (a) Feeder end segment (b) Feeder middle segment (c) Feeder front segment (d) Over all segments of the feeder

loads to have a power factor of 0.8 lagging. Voltage at the transformer terminal is maintained at a constant value of 1 p.u. This analysis is mainly focused on the maximum connectable solar PV capacity at the feeder end (i.e. the minimum hosting capacity level) where the results are given in the Table 4.5.

Number of Parallel Feeders

To estimate the effect of number of parallel feeders on solar PV HC, the analysis is carried out by increasing number of parallel feeders. Total loading level of the network (in terms of transformer loading level) is maintained at a constant value (50% of the transformer capacity) and identical feeders are used to observe the impact only of number of parallel feeders.

Feeder Length

In order to distinguish urban and rural networks with different feeder lengths, 600 m long feeders are used to represent urban networks whereas 1200 m long feeders are used to represent rural networks. Total network loading level is maintained at a constant value of 50% by the transformer capacity.

Conductor Type

Analysis described in Section 4.3.2 is repeated for different conductor types; $AAC - Fly$, $ABC - 70\ mm^2$ and $ABC - 50\ mm^2$, in order to examine the effect of R/X ratio on solar PV HC. The relevant conductor specifications are given in first column of Table 4.5.

Loading Level

Feeder loading level is one of the vital factors which governs the solar PV HC. In the analysis of impact of multi-feeders on hosting capacity, each feeder is applied with different loading levels while maintaining the same total transformer loading level of 50% of the transformer rating. The corresponding results are analysed to investigate the impact of loading level on the solar PV HC.

Outcomes of Feeder Characteristic Sensitivity Analysis

The estimated solar PV hosting capacities considering the influencing factors are given in the Table 4.5. Since a number of factors are simultaneously influencing on the hosting capacity, it is difficult to derive a direct correlation between solar PV HC and individual parameters. Nevertheless, it can be seen that for a given radial feeder, the minimum hosting capacity decreases as the feeder length increases. In addition, the minimum hosting capacity decreases with high R/X ratio and increasing number of parallel feeders. Furthermore, the minimum hosting capacity of a given feeder increases with feeder loading level.

Table 4.5: Safe limit of hosting capacities for different network configurations

Type of the conductor	Number of parallel feeders	Urban network (feeder length - 600 m), kW	Rural network (feeder length - 1200 m), kW
AAC – Fly	1	73	55
R = 0.4505 Ω/km	2	55	36
X = 0.292 Ω/km	3	50	30
R/X = 1.5	4	46	28
ABC – 70 mm^2	1	64	45
R = 0.441 Ω/km	2	51	32
X = 0.08 Ω/km	3	47	27
R/X = 5.5	4	45	25
ABC – 50 mm^2	1	51	38
R = 0.641 Ω/km	2	38	26
X = 0.08 Ω/km	3	34	21
R/X = 8	4	32	19

4.4 Outcomes of Feeder Level Approach for Solar PV Hosting Capacity Constrained by Voltage Rise

With regard to stochastic analysis employing MCS method, two levels of solar PV HC compliant with the given performance index can be identified as minimum hosting capacity (HC_{min}) and maximum hosting capacity (HC_{max}). The detailed analysis of location sensitivity and feeder characteristics on solar PV HC shows that the HC limits; HC_{min} and HC_{max} essentially depends on the size and location of a solar PV system, feeder loading level, feeder length and conductor type. Furthermore, the minimum and maximum hosting capacity levels further can be defined based on a distribution feeder and a multi-feeder distribution network levels.

Accordingly, for a given feeder, the minimum and maximum solar PV HC can be defined as follows;

- Minimum hosting capacity of a given feeder is the connectable maximum PV capacity at the feeder end and known as the safe limit of hosting capacity (referred to as $HC_{Feeder,Min}$)

- Maximum hosting capacity of a given feeder is the connectable maximum PV capacity at the feeder front (to the transformer) and primarily limited by

the thermal over-loading limits of components: eg. feeders and transformer (referred to as $HC_{Feeder,Max}$)

However, for multi-feeder networks, individual feeders will exhibit different PV hosting capacities. Hence, the minimum solar PV HC of a given LV distribution network, HC_{min_LV} is the minimum of the safe limits of each feeder. Thus, for a given LV distribution network, the minimum solar PV HC can be formulated as given in (4.1).

$$HC_{min\_LV} = \begin{cases} HC_{F1\_End} \\ HC_{F2\_End} \\ . \\ . \\ HC_{Fn\_End} \end{cases} \tag{4.1}$$

where, HC_{Fn_End} is the maximum connectable solar PV capacity at the feeder end of n^{th} feeder (n = 1, 2, 3,. . . . .).

Further, maximum solar PV HC of a given LV distribution network, HC_{max_LV} is the summation of the hosting capacities at the nearest end to the transformer of each feeder and can be formulated as given in the (4.2);

$$HC_{max\_LV} = HC_{F1\_Front} + HC_{F2\_Front} + ... + HC_{Fn\_Front} \tag{4.2}$$

where, HC_{Fn_Front} is the maximum connectable solar PV capacity at the feeder front of n^{th} feeder (n = 1, 2, 3,. . . . .).

Furthermore, comparison of hosting capacity levels obtained from spot simulations (hosting capacities at boundaries of the feeder segments) and MCS method in Section 4.3.1, segment wise minimum and maximum solar PV HC can be defined as;

- Minimum hosting capacity of a given segment is the connectable maximum PV capacity at the furthest end (from the transformer) of that segment;

- Maximum hosting capacity of a given segment is the connectable maximum PV capacity at the nearest end (to the transformer) of that segment.

It is evident that extensive analytical efforts are required for accurate hosting capacity evaluation process because of the complexity associated with distribution networks. Thus, there should be generalised approaches that are extendable to address various aspects of concern. Thus, feeder based solar PV HC approach is the most suitable as individual hosting capacity of each feeder has to be established in multi-feeder networks. Such a methodology needs to be extended in order to better capture the complexity of network modelling, constraints and technologies that will enable the greatest potential in generalisation.

In essence, the development of a new deterministic approach for the evaluation of solar PV HC in a feeder level is important from a distribution planning perspective. Further, such an approach will facilitate the connection of solar PV systems in a cost-effective way, thus enhancing the associated environmental and social benefits. In this regard, Chapter 5 presents a generalised deterministic approach that can be used to evaluate the feeder level solar PV HC levels.

4.5 Chapter Summary

This chapter has critically evaluated the factors which affect the solar PV HC of LV distribution networks which are constrained by unacceptable voltage rise, which is a common issue with increasing solar penetration levels. Accordingly, no single value can be defined as the hosting capacity for a given network as it mainly depends on the location of solar PV, feeder loading levels, feeder lengths and conductor type. Based on the sensitivity analysis on solar PV HC, a novel concept of feeder based solar PV HC approach was presented. Accordingly, for a given feeder, the minimum and maximum solar PV HC were defined as follows;

- Minimum hosting capacity of a given feeder is the connectable maximum PV capacity at the feeder end and known as safe limit of hosting capacity;

- Maximum hosting capacity of a given feeder is the connectable maximum PV capacity at the feeder front (to the transformer) and primarily limited by the thermal loading of the conductor.

For a multi feeder network, minimum hosting capacity is the lowest of all individual feeder minimum hosting capacity levels and maximum hosting capacity is the summation of all individual feeder maximum hosting capacity levels.

The outcomes of the work presented in this chapter have established the need for the development of novel conceptual approaches in relation to solar PV HC assessment in LV networks. Accordingly, a deterministic methodology for solar PV HC evaluation is proposed in Chapter 5 and a nomographic tool for solar PV HC evaluation is proposed in Chapter 7.

Chapter 5

Solar PV Hosting Capacity Evaluation: A Deterministic Approach

5.1 Introduction

This chapter presents a generalised deterministic approach to evaluate the solar PV HC in LV distribution networks considering over-voltage as the constraining criterion and the performance parameter. The maximum connectable solar PV capacity (the total aggregated capacity) of a given distribution feeder is evaluated subjected to locational and operational aspects of the solar PV units employed.

From a distribution system planning perspective, the use of such a deterministic approach is convenient and practical compared to the use of extensive simulation studies. Furthermore, the proposed method can be used as an approximate guide or a rule of thumb to evaluate solar PV HC at a given location of an LV distribution feeder without using complex stochastic techniques.

The work presented in this chapter elaborates the extended use of fundamental power flow equations to evaluate solar PV HC at a given point in LV distribution feeders under different operating conditions. Thus, the primary work covered in this chapter include:

- Development of generalised mathematical models for evaluation of solar PV HC at a given point of a distribution feeder for different operating conditions of PV inverters: unity, leading and lagging power factor.

This chapter is organised as follows. Section 5.2 presents the operational regimes of a distribution feeder with solar PV systems. Mathematical modelling of solar PV HC is given in section 5.3. Further, the proposed deterministic approach is validated using two case studies; a typical distribution feeder model and with the practical LV distribution network presented in Chapter 3 with the aid of DIgSILENT PowerFactory simulation software. The error minimisation approach for the solar PV HC evaluation with lagging power factor operated PV inverters is further proposed in Section 5.4.

5.2 Four-Quadrant Operation of Distribution Networks with Solar PVs

Under high solar penetration levels, bi-directional power flow can be visible in distribution networks since the local generation by solar systems is higher than the local load. As stated previously, the most common issue of concern with high solar integration levels is the voltage at the POC which tends to increase during the midday (during peak solar power generation periods) due to reverse power conditions.

Further, modern day solar PV systems possess reactive power capability allowing inverters to control the voltage at their POC. Thus, injection and absorption of both real and reactive power is achievable at the POC, such an operational capability referred to as four-quadrant operation. As shown in Fig. 5.1, P_{PV} and Q_{PV} are real and reactive power outputs of the solar PV system and P_L and Q_L are real and reactive power demand of the connected load (this may include a battery). The operating scenarios of the distribution feeder can be listed as below;

- I^{st} Quadrant - POC operating at a lagging power factor while both net P ($P_L - P_{PV}$) and net Q ($Q_L - Q_{PV}$) are positive

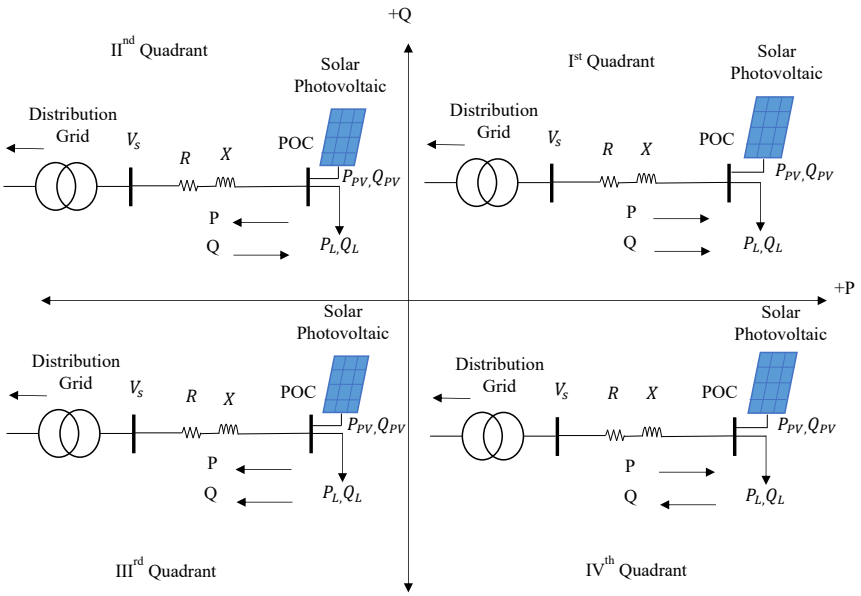

Figure 5.1: Four-quadrant operation at POC of a distribution feeder

- II^{nd} Quadrant - POC operating at a lagging power factor while net P ($P_L - P_{PV}$) is negative and net Q ($Q_L - Q_{PV}$) is positive
- III^{rd} Quadrant - POC operating at a leading power factor while both net P ($P_L - P_{PV}$) and net Q ($Q_L - Q_{PV}$) are negative
- IV^{th} Quadrant - POC operating at a leading power factor while net P ($P_L - P_{PV}$) is positive and net Q ($Q_L - Q_{PV}$) is negative

The steady state voltage rise with grid connected solar PV systems can be explained employing a model of a simplified distribution feeder with a single lumped load and a PV system as shown in Fig. 5.2 where the total load is modelled as a concentrated load drawing a current I_L at the feeder end having an impedance $R+jX$. The voltage of the PV system is V_{PV} and the source voltage is V_S. The PV system injects active and reactive power, P_{PV} and Q_{PV} respectively, to the network resulting in current of I_{PV} that is considered constant to examine the impact of the variation of the operating power factor of the inverter.

The relationship between the voltage at the POC, V_{PV}, and voltage at distribution transformer, V_S, can be written as;

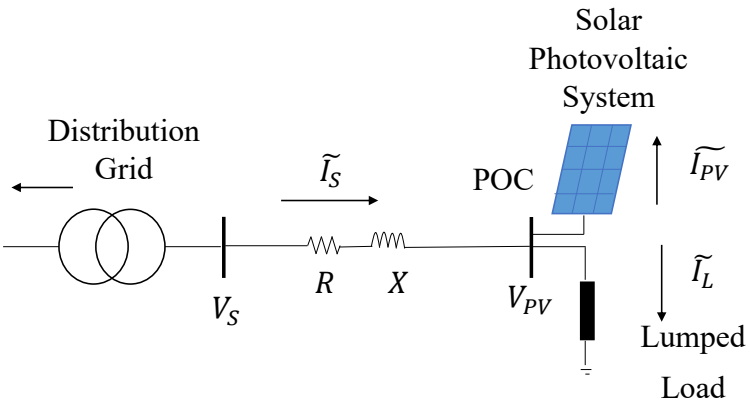

Figure 5.2: Simplified model of distribution feeder considered in the model development

$$\vec{V_S} = \vec{V_{PV}} + \vec{I_S}\,(R + jX) \tag{5.1}$$

where I_S is the net current flowing through the line.

The II^{nd} quadrant operation in Fig. 5.1 depicts realistic network conditions, wherein majority of the solar PV systems in LV networks inject P into the grid. Voltage rise phenomena in II^{nd} quadrant operation of solar PV inverter for three of its different operating conditions considered include (a) unity power factor, (b) lagging power factor and (c) leading power factor respectively while maintaining its injected current constant as stated previously.

The voltage at the POC is taken as the reference phasor as real power/reactive power/power factor are independently controlled. Real and imaginary parts of the load current I_L are I_{pl} and I_{ql} respectively.

5.2.1 Solar PV System Operating at Unity Power Factor

Fig. 5.3 shows voltage and current phasors when solar PV is operating at unity power factor injecting only active power[1] to the network. Hence, I_{PV} is the active current injected to the network where $I_{PV} > I_{pl}$. Voltage at POC, V_{PV} is defined

[1]Note that active power injection to the network is considered as negative.

as V_{PV1}. The resultant current[2] flow through the feeder is given by (5.2).

$$\vec{I_S} = \vec{I_L} + \vec{I_{PV}}$$

$$I_S = I_{pl} - jI_{ql} + (-I_{PV})$$

$$I_S = I_{pl} - I_{PV} - jI_{ql} = -I_{p1} - jI_{q1} \tag{5.2}$$

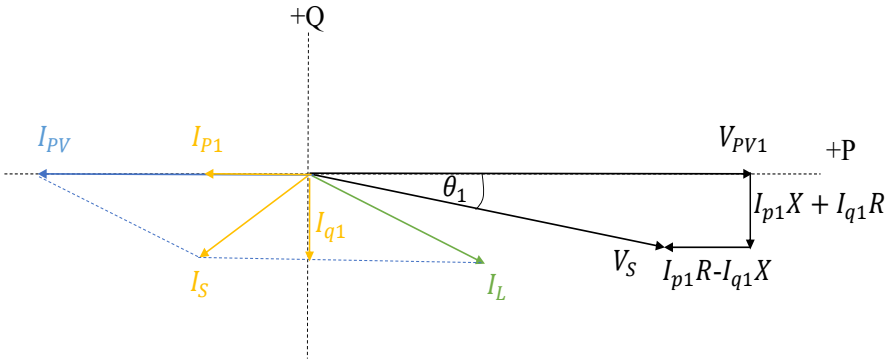

Figure 5.3: Phasor diagram for the distribution feeder with solar PV inverter operating at unity power factor

5.2.2 Solar PV System Operating at Lagging Power Factor

Fig. 5.4 shows voltage and current phasors when solar PV is operating at lagging power factor. In this case, the PV system is injecting active power (refers to I_{PVp}, ($I_{PVp} > I_{pl}$)) to the network and absorbing reactive power[3] (refers to I_{PVq}) from the network. Voltage at POC, V_{PV} is defined as V_{PV2}. The resultant current flow through the feeder is given by (5.3).

$$\vec{I_S} = \vec{I_L} + \vec{I_{PV}}$$

$$I_S = I_{pl} - jI_{ql} + (-I_{PVp} - jI_{PVq})$$

$$I_S = I_{pl} - I_{PVp} - j(I_{ql} + I_{PVq}) = -I_{p2} - jI_{q2} \tag{5.3}$$

[2]Note that load current, I_S is reactive wherein current phasor operates in quadrant IV. Thus imaginary part of the net load current is negative.

[3]The complex power at the POC of the PV system is, $V_{PV}I^*_{PV} = -P_{PV} + jQ_{PV}$. Hence, imaginary part of the current, I_{PV} is negative.

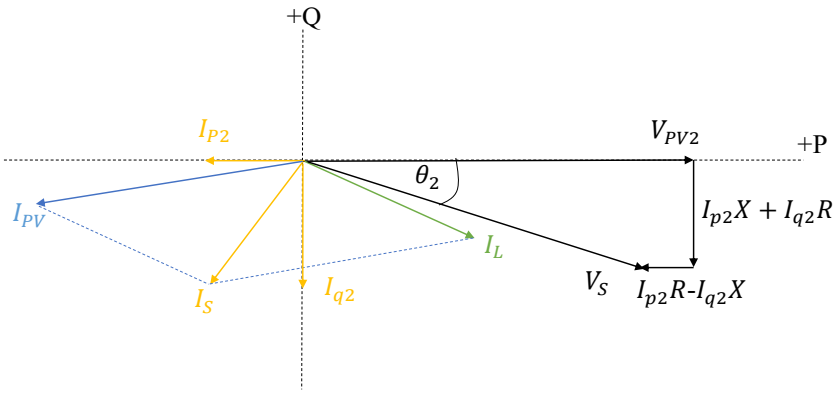

Figure 5.4: Phasor diagram for the distribution feeder with solar PV inverter operating at lagging power factor

As shown in Fig. 5.4, lagging power factor operation of solar PV inverter will cause an additional voltage drop in the feeder which affects the angle between V_{PV2} and V_S to increase with compared to unity power factor operation of PV inverters. Thus, this case results a lower voltage rise at the POC ($V_{PV1} > V_{PV2}$).

5.2.3 Solar PV System Operating at Leading Power Factor

Fig. 5.5 shows voltage and current phasors when solar PV is operating at leading power factor. Voltage at POC, V_{PV} is defined as V_{PV3}. However, leading power factor operation of the PV inverter will inject both active and reactive power that result in an increase in the voltage V_{PV3}. In this case, active and reactive power current[4] component of solar PV system are taken as I_{PVp}, (where, $I_{PVp} > I_{pl}$) and I_{PVq}, (where, $I_{PVq} < I_{ql}$) respectively. The resultant current flow through the feeder is given by (5.4).

$$\vec{I_S} = \vec{I_L} + \vec{I_{PV}}$$

$$I_S = I_{pl} - jI_{ql} + (-I_{PVp} + jI_{PVq})$$

$$I_S = I_{pl} - I_{PVp} - j(I_{ql} - I_{PVq}) = -I_{p3} - jI_{q3} \tag{5.4}$$

[4]The complex power at the POC of the PV system is, $V_{PV}I^*_{PV} = -P_{PV} - jQ_{PV}$. Hence, imaginary part of the current, I_{PV} is positive.

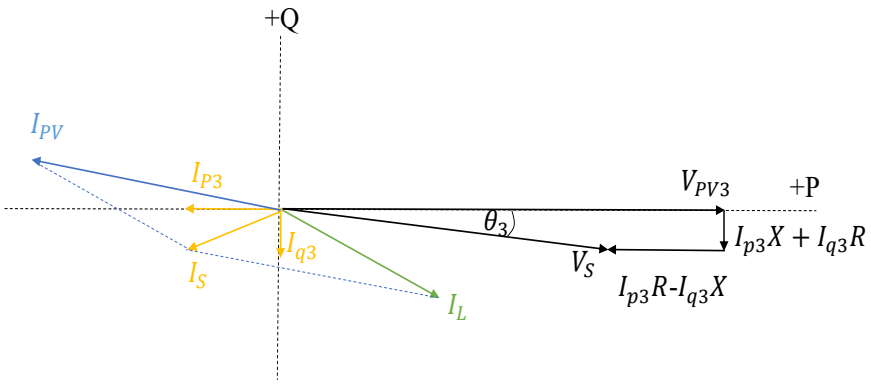

Figure 5.5: Phasor diagram for the distribution feeder with solar PV inverter operating at leading power factor

As shown in Fig. 5.5, leading power factor operation of the solar PV inverter will lead to a reactive power compensation in the feeder load which affects the angle between V_{PV3} and V_S to decrease with compared to unity power factor operation of PV inverters. Thus, this case results a higher voltage rise at the POC ($V_{PV3} > V_{PV1}$).

5.3 Mathematical Modelling of Solar PV Hosting Capacity

This section explores a novel deterministic approach which facilitates the evaluation of maximum solar PV penetration level constrained by over-voltage limits. Solar PV HC of a given network depends on network characteristics, solar PV location, size of the inverter and the voltage maintained at the distribution transformers. These factors are taken into consideration when developing the mathematical formulation.

In general, deterministic models should be developed in such a way that they can represent the four quadrant operation of the solar PV system (which may include a battery) where possible. In specific terms, the operation at unity power factor or at a fixed leading or lagging power factor must be considered.

The principles underlying power flow and voltage calculations for the mathematical model formulation in this section used a simple feeder model with balanced and uniformly distributed loads as shown in Fig. 5.6. The principles are then extended to deal with distribution feeders embedded with solar PV generation.

Consider the single line diagram of a single feeder network shown in Fig. 5.6. The resistance and reactance of the feeder are R and X in Ohm per unit length respectively. V_S is the supply voltage at the secondary of the transformer.

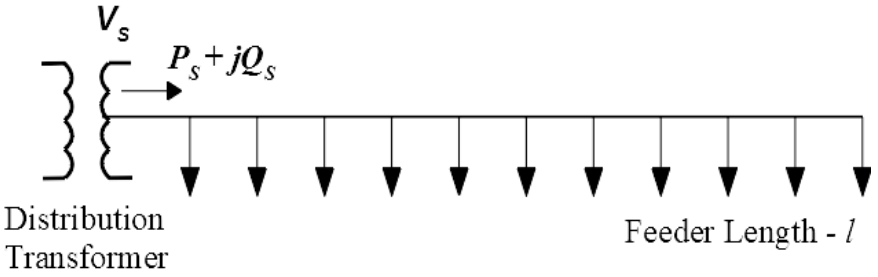

Figure 5.6: Simplified distribution feeder model

The total voltage drop VD_l in per unit (p.u.) of the feeder can be written as [73];

$$VD_l = \frac{l\,(RP_S + XQ_S)}{2V_b^2} + j\frac{l\,(XP_S - RQ_S)}{2V_b^2} \tag{5.5}$$

where, V_b is the nominal line-line voltage and P_S and Q_S are the total real and reactive power components of the total load in three phases that is uniformly distributed in the feeder, and l is the total length of the feeder.

Active power and reactive power flow at a distance d from the transformer can be written as (5.6).

$$P_d = P_S\left(1 - \frac{d}{l}\right), \quad Q_d = Q_S\left(1 - \frac{d}{l}\right) \tag{5.6}$$

where P_d and Q_d are the active and reactive power flow at distance d from the transformer. Fig. 5.7 illustrates P_S and Q_S distribution in (5.6) graphically.

As the actual voltage of the feeder is affected by the connection of solar PV in the feeder, (5.5) can be modified subjected to different operating conditions of the solar PV inverter as discussed in following sections.

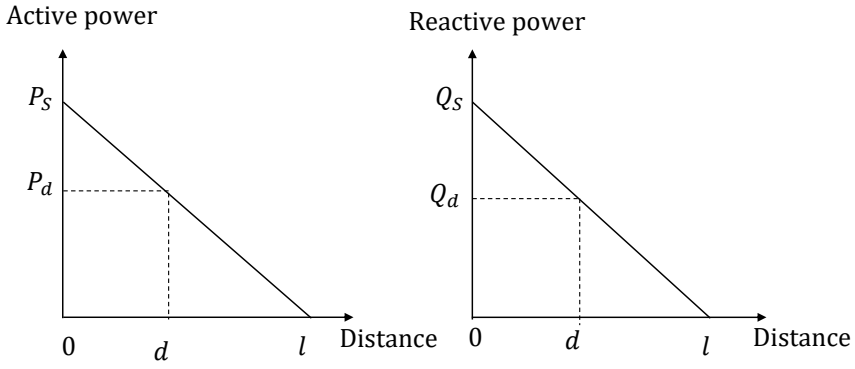

Figure 5.7: Active and reactive power profile along the feeder (without solar PV)

5.3.1 Solar PV Inverter Operation at Unity Power Factor

Suppose that a solar PV generator installed at a distance d from the distribution transformer produces only real power output (finite P_{PV}) and zero reactive power ($Q_{PV} = 0$). At the POC, the voltage is V_{PV}. For the condition $P_{PV} > P_d$, active and reactive power flows along the feeder are illustrated in Fig. 5.8. Zero crossing point denoted by $d^{'}$ in Fig. 5.8 is where the transition of the direction of active power flow occurs. Just to the right of zero crossing point, active power flows towards the transformer and just to left of the zero crossing point, active power flows from the transformer. The zero crossing point can be established as,

$$d^{'} = \left(1 - \frac{P_{PV}}{P_S}\right) l \tag{5.7}$$

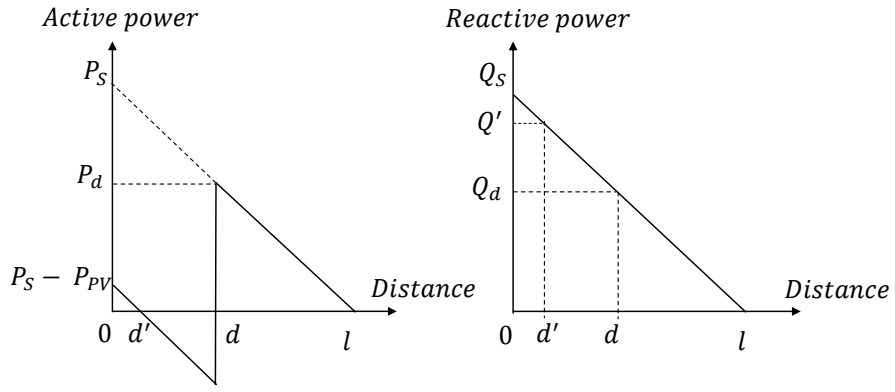

Figure 5.8: Active and reactive power profile along the feeder (with unity power factor solar inverter)

Using (5.5), the new magnitude of the voltage drop from 0 to $d^{'}$ can be shown to be:

$$VD_{0-d'} = \frac{d^{'}}{2}\left(\frac{R\left(P_S - P_{PV}\right) + X\left(Q_S + Q^{'}\right)}{V_b^2}\right) + j\frac{d^{'}}{2}\left(\frac{X\left(P_S - P_{PV}\right) - R\left(Q_S + Q^{'}\right)}{V_b^2}\right) \tag{5.8}$$

The magnitude of the rise in voltage from $d^{'}$ to d can be expressed as:

$$\begin{aligned} VR_{d'-d} = \frac{\left(d - d^{'}\right)}{2}\left(\frac{R\left(P_{PV} - P_d\right) - X\left(Q^{'} + Q_d\right)}{V_b^2}\right) + \\ j\left(\frac{\left(d - d^{'}\right)}{2}\frac{X\left(P_{PV} - P_d\right) + R\left(Q^{'} + Q_d\right)}{V_b^2}\right) \end{aligned} \tag{5.9}$$

where, $Q^{'} = Q_s\left(1 - \frac{d^{'}}{l}\right)$

The total voltage rise from distribution transformer to the POC can be established by subtracting (5.8) from (5.9);

$$VR_{0-d} = \left(\frac{dRP_{PV}}{V_b^2} - \left(2\lambda - \lambda^2\right)VD_l^{re}\right) + j\left(\frac{dXP_{PV}}{V_b^2} - \left(2\lambda - \lambda^2\right)VD_l^{im}\right) \tag{5.10}$$

where, $\lambda = d/l$, VD_l^{re} - real component of voltage drop and VD_l^{im} - reactive component of voltage drop.

The magnitude of the voltage rise in (5.10) is a linear function of the capacity of the solar PV system as well as its location on the feeder. Hence, the maximum connectable solar PV capacity at a fixed location can be derived theoretically that correspond to the maximum allowable voltage rise in the feeder. Furthermore, by neglecting the phase angle deviation of V_{PV} from V_S, (5.10) can be written as in (5.11).

$$V_{PV} - V_S = \left(\frac{dRP_{PV}}{V_b^2} - \left(2\lambda - \lambda^2\right)\Delta V\right) \tag{5.11}$$

where, ΔV is the total voltage drop across the feeder which arise as a result of

the load.

For an inverter with unity power factor operation, the maximum connectable solar PV capacity in the three phases at a distance d from the distribution transformer can be formulated as given in (5.12) where V_{PV}, V_S and ΔV are in p.u.

$$P_{PV} = \frac{V_b^2}{Rd}\left\{(V_{PV} - V_S) + \left(2\lambda - \lambda^2\right)\Delta V\right\} \tag{5.12}$$

For a given feeder, the safe limit of hosting capacity which represents the maximum connectable solar PV capacity at the feeder end as discussed in Section 4.4 of Chapter 4 can be calculated when $d = l$ as given in (5.13).

$$P_{PV} = \frac{V_b^2}{Rl}\left\{(V_{PV} - V_S) + \Delta V\right\} \tag{5.13}$$

5.3.2 Solar PV Inverter Operating at a Leading Power Factor

Suppose that a solar PV generator is installed at a distance d from the distribution transformer and let P_{PV} and Q_{PV} be the real and reactive power outputs of the PV system.

When the solar inverter is operating at a leading power factor, the reversal of both active and reactive power flows can happen as shown in Fig. 5.9. Zero crossing point of reactive power flow profile along the feeder can be formulated similar to (5.7) as in (5.14).

$$d'' = \left(1 - \frac{Q_{PV}}{Q_S}\right) l \tag{5.14}$$

The total voltage rise from distribution transformer to the POC can be decomposed using active and reactive power flows as:

$$\begin{aligned} VR_{0-d} = &\left(\frac{dP_{PV}\left(R + X\tan\left(\cos^{-1} pf_{pv}\right)\right)}{V_b^2} - \left(2\lambda - \lambda^2\right) VD_l^{re}\right) \\ &+ j\left(\frac{dP_{PV}\left(X - R\tan\left(\cos^{-1} pf_{pv}\right)\right)}{V_b^2} - \left(2\lambda - \lambda^2\right) VD_l^{im}\right) \end{aligned} \tag{5.15}$$

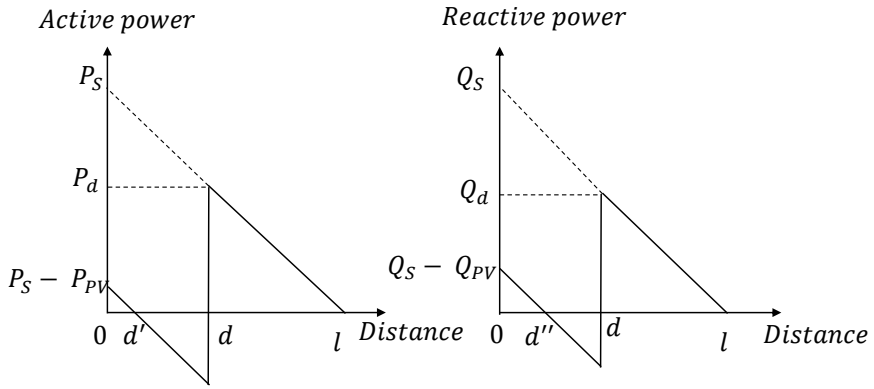

Figure 5.9: Active and reactive power profile along the feeder (with leading power factor solar inverter)

If the PV inverter operating at a fixed power factor, then the reactive power becomes; $Q_{PV} = P_{PV} \tan\left(\cos^{-1}\left(pf_{pv}\right)\right)$.

By neglecting the phase angle deviation of V_{PV} from V_S, (5.15) can be rewritten as:

$$V_{PV} - V_S = \left(\frac{dP_{PV}\left(R + X\tan\left(\cos^{-1} pf_{pv}\right)\right)}{V_b^2} - \left(2\lambda - \lambda^2\right)\Delta V \right) \tag{5.16}$$

Maximum amount of solar power generation in the three phases that will cause the voltage to reach the over-voltage limit at a distance d from the transformer for a leading power factor operation can be formulated as in (5.17). Here, V_{PV} , V_S and ΔV are in p.u.

$$P_{PV} = \frac{V_b^2}{d\left(R + X\tan\left(\cos^{-1}\left(pf_{pv}\right)\right)\right)} \left\{ \left(V_{PV} - V_S\right) + \left(2\lambda - \lambda^2\right)\Delta V \right\} \tag{5.17}$$

For a given feeder, the safe limit of hosting capacity can be calculated when $d = l$ as given in (5.18).

$$P_{PV} = \frac{V_b^2}{l\left(R + X\tan\left(\cos^{-1}\left(pf_{pv}\right)\right)\right)} \left\{ \left(V_{PV} - V_S\right) + \Delta V \right\} \tag{5.18}$$

5.3.3 Solar PV Inverter Operating at a Lagging Power Factor

Suppose that a solar PV generator is installed at a distance d from the distribution transformer and let P_{PV} and $-Q_{PV}$ be the real and reactive power outputs of the PV system.

As shown in Fig. 5.10, reactive power supplied by the grid is increased due to solar PV inverter is operating as an inductive load. In this case, solar PV inverter will cause an additional voltage drop in the feeder.

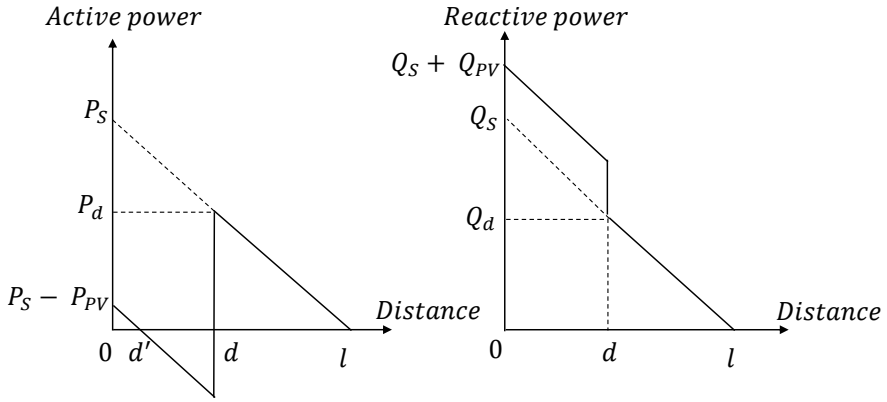

Figure 5.10: Active and reactive power profile along the feeder (with lagging power factor solar inverter)

The total voltage rise from distribution transformer to the POC can be decomposed using active and reactive power flows as:

$$\begin{aligned} VR_{0-d} = &\left(\frac{dP_{PV}\left(R - X\tan\left(\cos^{-1} pf_{pv}\right)\right)}{V_b^2} - \left(2\lambda - \lambda^2\right) VD_l^{re} \right) \\ &+ j\left(\frac{dP_{PV}\left(X + R\tan\left(\cos^{-1} pf_{pv}\right)\right)}{V_b^2} - \left(2\lambda - \lambda^2\right) VD_l^{im} \right) \end{aligned} \tag{5.19}$$

By neglecting the phase angle deviation of V_{PV} from V_S, (5.19) can be rewritten as:

$$V_{PV} - V_S = \left(\frac{dP_{PV}\left(R - X\tan\left(\cos^{-1} pf_{pv}\right)\right)}{V_b^2} - \left(2\lambda - \lambda^2\right) \Delta V \right) \tag{5.20}$$

Similar to Section 5.3.2, maximum amount of solar power generation in the three phases that will cause the voltage to reach the over-voltage limit at a distance d from

the transformer for lagging power factor operation can be formulated as in (5.21). Here, V_{PV} , V_S and ΔV are in p.u.

$$P_{PV} = \frac{V_b^2}{d\left(R - X\tan\left(\cos^{-1}\left(pf_{pv}\right)\right)\right)}\left\{\left(V_{PV} - V_S\right) + \left(2\lambda - \lambda^2\right)\Delta V\right\} \tag{5.21}$$

For a given feeder, the safe limit of hosting capacity can be calculated when $d = l$ as given in (5.22).

$$P_{PV} = \frac{V_b^2}{l\left(R - X\tan\left(\cos^{-1}\left(pf_{pv}\right)\right)\right)}\left\{\left(V_{PV} - V_S\right) + \Delta V\right\} \tag{5.22}$$

From (5.12), (5.17) and (5.21), it is clear that the maximum level of solar power generation that can be connected to a given location in a distribution feeder is seen to depend on following factors:

- Feeder characteristics (length of the feeder, type of the conductor)
- Distance from the distribution transformer
- Demand on the feeder
- Voltage at the distribution transformer
- Stipulated voltage limit on the feeder

5.3.4 Verification of the Proposed Mathematical Model

For verification purposes, the proposed deterministic approach is used to evaluate the solar PV HC of the practical distribution network discussed in Chapter 3 (Case 1) and of the simple distribution feeder (Case 2) with the aid of DIgSILENT PowerFactory simulations.

Case 1: Practical LV Distribution Network

The total midday peak demand of the distribution network is (P_S and Q_S) 82 kW and 60 kVAr respectively (40% by the transformer capacity). Based on the assumption

that all three feeders are loaded equally, the total voltage drop along each feeder can be calculated using (5.5). Accordingly, total voltage drops of feeder 1 ($ABC - 50\ mm^2$), feeder 2 ($ABC - 70\ mm^2$) and feeder 3 ($ABC - 70\ mm^2$) are 3%, 1.7% and 2.6% respectively at the solar peak time. The safe limits of the solar PV hosting capacities of each feeder are calculated using (5.12) considering unity power factor operation of inverters. Table 5.1 gives safe limits of hosting capacity values calculated using the mathematical models and spot simulations constrained by over-voltage for each feeder. As an example, detailed calculations relevant to safe HC limit calculation of feeder 1 is given below:

The total voltage drop in feeder 1 (510 m) is approximately 3%. The secondary line-line voltage at the distribution transformer is set at 1.04 p.u. to ensure that the voltage is within the stipulated limits under maximum demand conditions at night peak. At this loading level (40%), supply voltage[5] of the distribution transformer is 1.024 p.u.

Using (5.12), the maximum connectable solar PV capacity at feeder end is,

$P_{PV,Feeder1} = \frac{400^2}{0.641*051}\{(1.06 - 1.024) + 0.03\} \approx 32$ kW

Table 5.1: Safe limits of solar PV hosting capacity - Practical urban LV network

	Safe limit for HC calculated using mathematical model (kW)	Safe limit for HC simulated using PowerFactory (kW)
Feeder 1	32	30
Feeder 2	48	41
Feeder 2	37	40

Case 2: A Single Feeder Test Network

The test network consists of a 100 kVA, 11 kV/400 V transformer connected to a 1 km long feeder as shown in Fig. 5.11. The total midday peak demand on the feeder is (P_S and Q_S) 40 kW and 30 kVAr (50% by the transformer capacity). Total load

[5]Secondary voltage of the transformer depends on the transformer loading level.

is assumed to be balanced and uniformly distributed on 10 nodes along the feeder. Further, secondary side voltage of the transformer is assumed to be at a constant voltage of 1 p.u. The test network is analysed for maximum connectable solar PV capacity at two different locations so that the upper voltage limit stipulated by the utility (taken as +6%) is not violated.

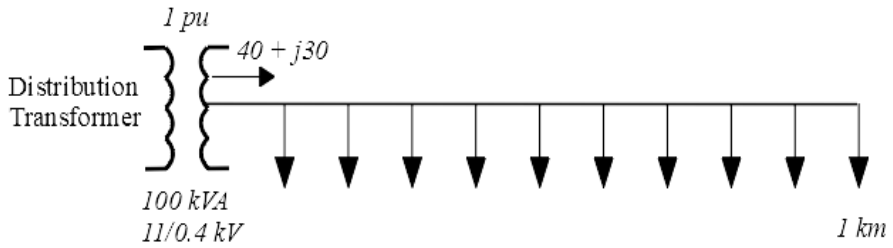

Figure 5.11: Single distribution feeder model-Case 2

Table 5.2: Maximum connectable solar capacity when solar PV system operating at unity power factor

	HC at feeder end		HC at feeder middle	
	simulated	calculated	simulated	calculated
AAC - Fly	0.58	0.57	0.96	0.96
ABC - 70 mm^2	0.49	0.49	0.84	0.84
ABC - 50 mm^2	0.41	0.41	0.69	0.69

Table 5.3: Maximum connectable solar capacity when solar PV system operating at 0.9 leading power factor

	HC at feeder end		HC at feeder middle	
	simulated	calculated	simulated	calculated
AAC - Fly	0.48	0.48	0.79	0.81
ABC - 70 mm^2	0.50	0.50	0.84	0.85
ABC - 50 mm^2	0.43	0.43	0.71	0.73

Table 5.4: Maximum connectable solar capacity when solar PV system operating at 0.9 lagging power factor

	HC at feeder end		HC at feeder middle	
	simulated	calculated	simulated	calculated
AAC - Fly	1.41	0.92	1.98	1.55
ABC - 70 mm^2	0.63	0.59	1.06	1.02
ABC - 50 mm^2	0.52	0.49	0.85	0.82

Maximum connectable solar PV capacity was evaluated for different types of conductors; $AAC - Fly$, $ABC - 70\ mm^2$ and $ABC - 50\ mm^2$ in order to investigate the effect of R/X ratio on solar PV HC. Accordingly, three cases are presented for different operating scenarios of the PV inverters; unity power factor, 0.9 leading power factor and 0.9 lagging power factor. In each case, hosting capacity values relevant to feeder end and middle of the feeder were evaluated and compared against the results from the mathematical models as given in Tables 5.2, 5.3 and 5.4. All solar PV capacity values are given in per unit with transformer ratings as base values. As shown in Tables 5.2 and 5.3 when solar PV inverters are operating at unity power factor and leading power factor conditions, solar PV hosting capacities obtained from simulations and the proposed deterministic method are in close agreement verifying the accuracy of the deterministic approach. However, there is a considerable difference with simulated and calculated hosting capacities for the case lagging power factor operating inverters with low R/X ratio conductors ($AAC - Fly$ conductor given in Table 5.4).

The deterministic approach for feeder level solar PV HC offers substantial benefits over a stochastic approach which have high variability in accuracy that depends on the number of simulations and complexity of the network model.

5.4 Error Minimisation of Hosting Capacity with Lagging Power Factor Operating PV Inverters

Accuracy of the proposed deterministic method for inverters operating with lagging power factor varies with the R/X ratio, inverter operating power factor and PV locational variation. Thus the influence of these on the maximum HC level is examined in detail in the following section.

5.4.1 Influence of R/X Ratio, PV Location and Inverter Operating Power Factor on Hosting Capacity

This study comprises an 11kV/0.4kV, 100 kVA transformer connected to a 1 km long single feeder with a loading level of 50 kVA (40 kW and 30 kVAr, 50% of transformer capacity). The total load was assumed to be balanced and uniformly distributed along the feeder. In order to analyse the effect of R/X ratio, aforementioned conductors in Section 5.3.4 were considered; AAC-Fly, $ABC - 70mm^2$ and $ABC - 50mm^2$. The percentage error[6] of the solar PV HC was calculated by comparing HC values established using simulations and analytical model. To analyse the effect of locational variation on solar PV HC, the HC was calculated at three different locations on the feeder (at 1 km, 0.75 km and 0.5 km from the distribution transformer) for each type of conductor. Furthermore, operating power factor of the PV inverter was also varied from 0.9 lagging to 1 in order to observe the impact on the error of solar PV HC. Fig. 5.12 shows the percentage error of solar PV hosting capacities with locational variation of PV system together with PV inverter operating power factor for considered three types of conductors.

It is clear that the distribution of solar PV towards the distribution transformer, high R/X ratio feeders and higher PV inverter operating power factor decrease the percentage error of solar PV HC. Furthermore, Fig. 5.13 gives a comparison of minimum hosting capacity values obtained using the proposed deterministic method and simulations.

Fig. 5.13 shows that the LV conductors with low R/X ratios lead to a higher percentage error of HC. The reason being, solar PV inverters with lagging power factor operation will cause an additional reactive voltage drop in the feeder leading to an increase in the angle deviation between the voltage at the POC and the voltage at the supply end. Thus, the error minimisation only needs for the mathematical models with the conditions of low R/X ratio conductor types and PV inverters which

[6]Percentage error of HC, $\% = \frac{HC_{Calculated} - HC_{simulated}}{HC_{Calculated}} * 100$, where, $HC_{Calculated}$ - HC obtained from the proposed analytical approach and $HC_{Simulated}$ - HC obtained from the DIgSILENT simulations

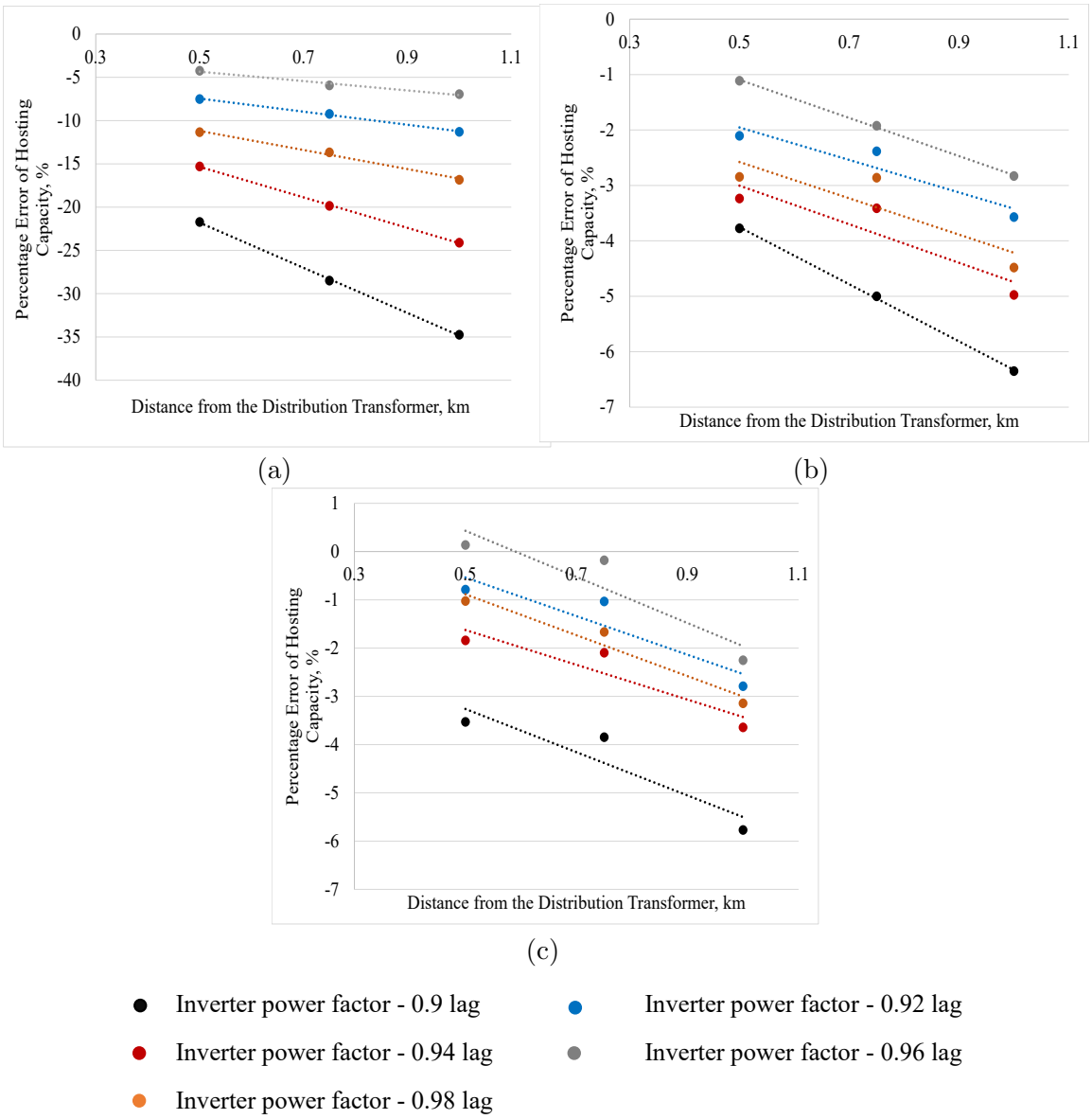

Figure 5.12: Percentage error of solar PV hosting capacity at different locations in a different conductor types (a). AAC-Fly (b). ABC-70 mm^2 (c). ABC-50 mm^2

are operating at lagging power factor.

The error of solar PV HC associated with the mathematical equation for lagging power factor operating PV inverters proposed in Section 5.3 is associated with the assumption which was the negligible angle deviation between the voltage at the POC and the voltage at the supply end. Hence, an error minimisation approach for solar PV HC assessment is proposed in the following section by accommodating the voltage angle deviation to the mathematical model in (5.21).

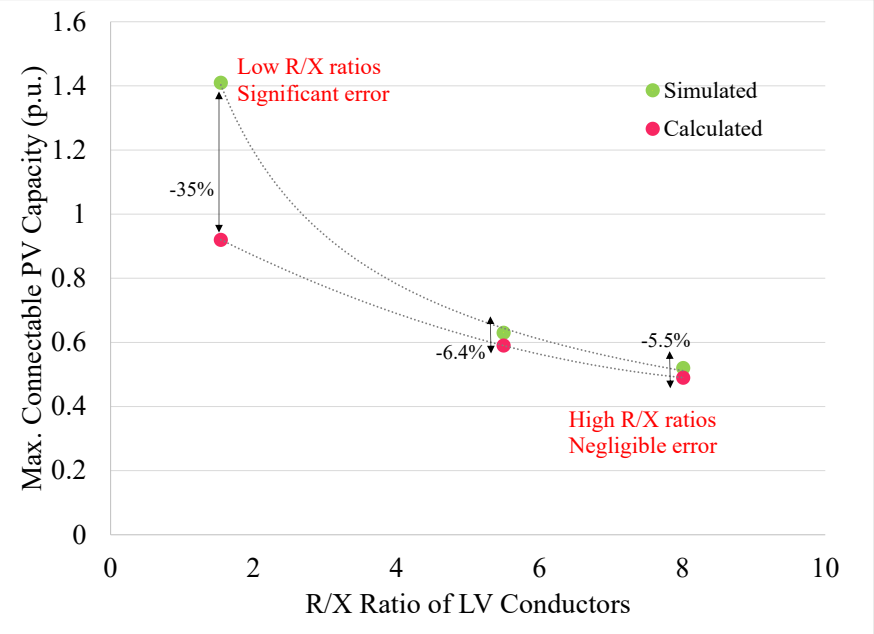

Figure 5.13: Percentage error of solar PV hosting capacity with R/X ratio of LV conductors

5.4.2 Characteristics Curve of Voltage Angle Deviation; θ and Solar PV Capacity; P_{PV}

Voltage angle deviation, θ (between the voltage at the solar terminal, V_{PV} and the voltage at supply end, V_S) has the relationship with the solar PV capacity as given in (5.23) (see Appendix B for the detailed derivation of (5.23)).

$$\theta = sin^{-1}\left(\frac{P_{PV}d(X + R\tan(cos^{-1}(pf_{pv})))}{V_b^2 V_S}\right) \tag{5.23}$$

Fig. 5.14 illustrates the voltage angle deviation (θ) and solar PV capacity (P_{PV}) characteristic curve in relation to variable PV location in the feeder, different type of conductors and inverter operating power factor.

The mathematical formulae given in (5.21) can be updated as given in (5.24) to include the voltage angle deviation, θ (see Appendix B for the detailed derivation).

$$P_{PV} = \frac{V_b^2}{d\left(R - X\tan\left(\cos^{-1}\left(pf_{pv}\right)\right)\right)}\left\{\left(V_{PV} - V_S cos\theta\right) + \left(2\lambda - \lambda^2\right)\Delta V\right\} \tag{5.24}$$

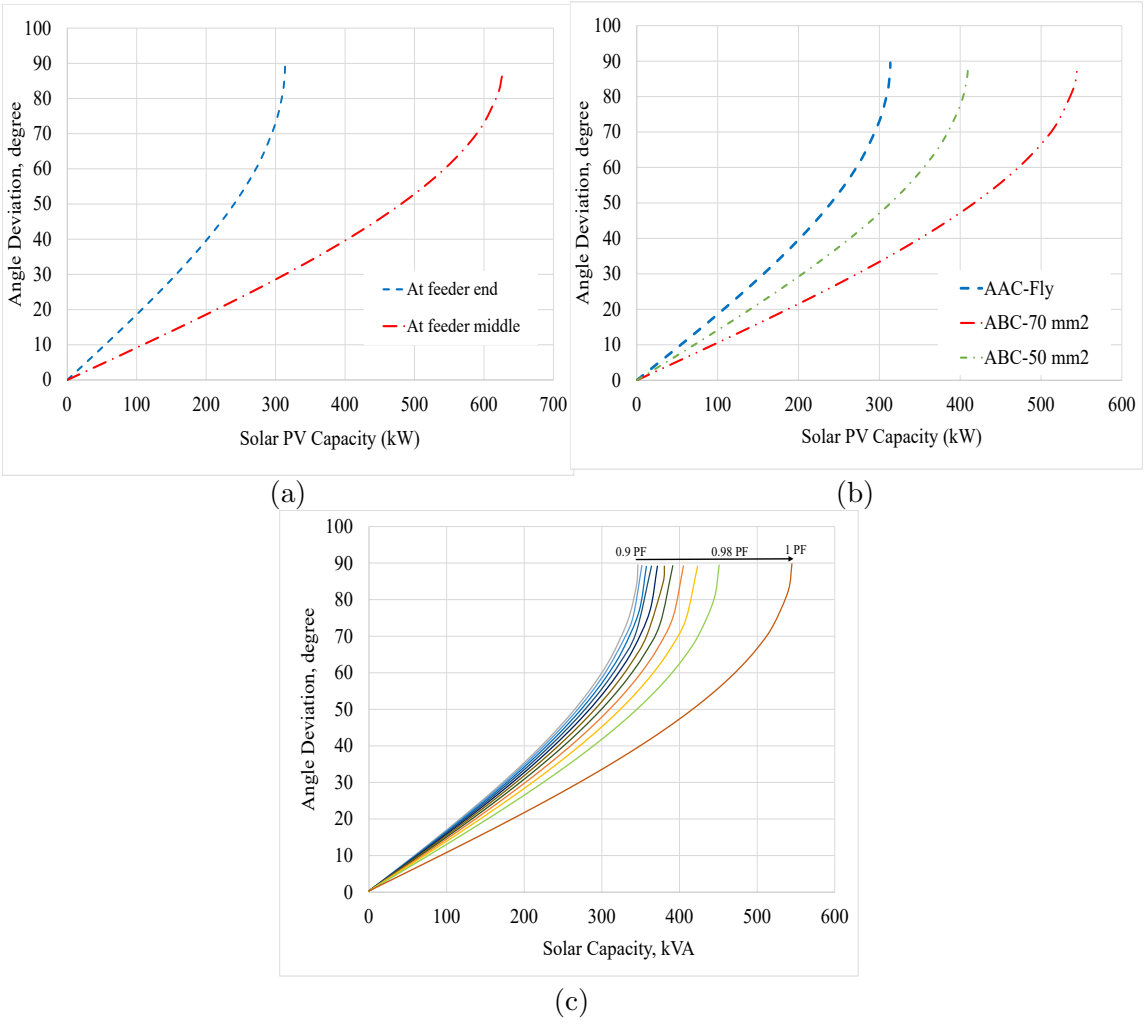

Figure 5.14: Solar PV capacity vs voltage angle deviation for different scenarios (a). AAC-Fly type conductor at two distinct locations (b). Different types of conductors at feeder end (c). AAC-Fly type conductor and solar PV connected at feeder end: PV inverter operating power factor varies from 0.9 lagging to 1

Solar PV HC can be calculated using (5.24), with reference to the voltage angle deviation shown in Fig. 5.14 until the voltage at POC, V_{PV} reaches to the maximum allowable upper voltage limit.

5.4.3 Verification of the Modified Deterministic Method

As discussed in Section 5.4.2, a modified formulae has been developed accounting for the voltage angle deviation in the solar PV HC calculation process presented in 5.3.3. The single feeder distribution network model in Section 5.3.4 (Fig. 5.11) was used for validation of the mathematical model given in (5.24). The test network was

analysed for maximum connectable solar PV capacity at two different locations; end of the feeder and middle of the feeder without violating the upper voltage limit of 1.06 p.u.

The analysis was repeated for different types of conductors in order to investigate the effect of R/X ratio on solar PV HC. Accordingly, solar PV HC values which were obtained from the simulations and mathematical model are given in Table 5.5 for two different locations; feeder end and middle of the feeder respectively. All solar PV capacity values are given in p.u. (transformer rating was taken as the base value) value.

Table 5.5: Maximum connectable solar capacity when solar PV system operating at 0.9 lagging power factor

	At 1 km from transformer		At 0.5 km from transformer	
	simulated	calculated	simulated	calculated
AAC - Fly	1.41	1.38	1.98	2
ABC - 70 mm^2	0.63	0.62	1.06	1.05
ABC - 50 mm^2	0.52	0.51	0.85	0.85

As shown in the Table 5.5, solar PV HC levels obtained from the simulations and the proposed mathematical model in (5.24) are in close agreement verifying the accuracy of the modified approach.

5.5 Chapter Summary

In this chapter, a feeder based deterministic approach was proposed for the evaluation of the solar PV HC in LV distribution networks constrained by over-voltage limits. Compared to well established stochastic approaches of solar PV HC evaluation (Monte Carlo type approaches) are not practical in distribution network planning perspective due to extensive network modelling efforts and the complexity. Thus, individual feeder based analysis approach is recommended and considered to be effective. Furthermore, the proposed deterministic method for solar PV HC assessment has been accommodated following uncertainties; PV location and size of

PV system, feeder characteristics, demand on the feeder, voltage at the distribution transformer and stipulated voltage limits on the feeder in the distribution network.

Table 5.6 summarises the mathematical models developed for evaluation of solar PV HC at a given point in a feeder considering three different operating conditions of a PV inverter. The simplified equation for the HC at the feeder end which gives safe limit (i.e. when $d = l$) is also shown in the same Table 5.6 for clarity.

Table 5.6: Generalised mathematical models for different operating conditions of PV inverters

PV inverter operation mode	At a distance d from the transformer	At the feeder end ($d = l$)
Unity power factor	$\frac{V_b^2}{Rd}\left\{(V_{PV} - V_S) + \left(2\lambda - \lambda^2\right)\Delta V\right\}$	$\frac{V_b^2}{Rl}\left\{(V_{PV} - V_S) + \Delta V\right\}$
Leading power factor	$\frac{V_b^2}{d\left(R + X\tan\left(\cos^{-1}\left(pf_{pv}\right)\right)\right)}*$ $\left\{(V_{PV} - V_S) + \left(2\lambda - \lambda^2\right)\Delta V\right\}$	$\frac{V_b^2}{l\left(R + X\tan\left(\cos^{-1}\left(pf_{pv}\right)\right)\right)}*$ $\left\{(V_{PV} - V_S) + \Delta V\right\}$
Lagging power factor	$\frac{V_b^2}{d\left(R - X\tan\left(\cos^{-1}\left(pf_{pv}\right)\right)\right)}*$ $\left\{(V_{PV} - V_S) + \left(2\lambda - \lambda^2\right)\Delta V\right\}$	$\frac{V_b^2}{l\left(R - X\tan\left(\cos^{-1}\left(pf_{pv}\right)\right)\right)}*$ $\left\{(V_{PV} - V_S) + \Delta V\right\}$

Under this framework, distribution network operators and planners can investigate the capability and limitations of solar PV penetration. The proposed feeder based solar PV HC evaluation approach can be seen to capture all influencing factors on solar PV HC and diversity of LV networks. Thus, this can be used as an approximate guide or a rule of thumb to evaluate solar PV HC at a given point of LV feeders for over-voltage curtailment without using complex stochastic techniques.

The mathematical formulation presented in this Chapter is further extended in Chapter 7 to develop a nomogram based solar PV HC assessment approach.

Chapter 6

Solar PV Hosting Capacity Enhancement with Smart Inverter Capabilities

6.1 Introduction

As discussed in Chapters 4 and 5, development of systematic approaches to evaluate solar PV HC in LV distribution networks is of benefit for both DNOs and consumers in enhancing solar PV generation while improving the quality of power. In addition, it is worthwhile investigating how to enhance solar PV HC existing network conditions. With the latest technological advancements, smart solar PV inverters have become popular over the last few years, which can operate in all four quadrants of the P-Q plane by controlling active and reactive power compared to the conventional solar PV inverters.

Modern smart inverters are equipped with fast and flexible active and reactive power control functions; Volt-VAr and Volt-Watt controls which can assist in the management of network voltage levels. Furthermore, these voltage support functions of smart inverters can be used to manage over-voltage conditions that often limit the solar PV HC in LV distribution networks and hence help enhance the solar PV HC.

Although a smart inverter can be configured to manage the voltage at the POC by controlling the necessary reactive and active power using Volt-VAr and Volt-Watt control modes, distributed nature of solar PV resources and different network characteristics/configurations may limit the HC enhancement as comprehensive understanding of such advanced coordinated control strategies is not available to-date. Further, various provisions/approaches facilitated by different standards pose challenges in the selection of the best practice for solar PV HC enhancement with smart inverters. In this regard, most solar PV connection standards and guidelines have been revised in the recent years and have established a common set of smart inverter functions in order to manage network voltage levels related to PV integration at LV level. IEEE Std. 1547-2018 [66], AS/NZS 4777.2-2015 [67], California Rule 21-2018 [68] and Hawaii Rule 14-2018 [69] are well known standards/guidelines that have established such criterion and requirements for active and reactive power control thus facilitating the mitigation of voltage related issues. Thus, there is a need for detailed analysis of different practices/rules imposed by widely used solar PV connection standards/guidelines on solar PV HC enhancement.

Therefore, this chapter presents a detailed analysis of different Volt-VAr and Volt-Watt control regimes and their influence on solar PV HC enhancement by comparative evaluation of the outcomes associated with each standard/guideline using the feeder based solar PV HC assessment approach proposed in Chapter 4. Furthermore, the most suitable operating mode and settings of a smart inverter that can in turn mitigate over-voltage issue is investigated in order to enhance solar PV HC at feeder level.

The major objectives of the work presented in this chapter are:

- Investigation of smart inverter capabilities of Volt-VAr and Volt-Watt control strategies for over-voltage curtailment in LV distribution networks.
- Solar PV HC enhancement using smart inverter capabilities subjected to locational aspects of PV systems.

- Comparative evaluation of solar PV HC enhancement facilitated by different connection standards/guidelines.

This chapter is organised as follows: Section 6.2 presents a detailed analysis of operational aspects of Volt-VAr and Volt-Watt control strategies on voltage regulation based on a smart inverter model developed in DIgSILENT PowerFactory simulation platform. Analysis of solar PV HC enhancement with different Volt-VAr and Volt-Watt control strategies covered in a number of standards/guidelines is presented in Section 6.3 using two network models; a typical distribution feeder model and with a practical urban LV distribution network which was presented in Chapter 3. Furthermore, this section extends the understanding on the solar PV HC improvement by employing advanced inverter control functions where such improvements are subjected to locational aspects of inverters in distribution feeders.

6.2 Smart Inverter Capabilities of Volt-VAr and Volt-Watt Control Strategies for Over-Voltage Curtailment in LV Distribution Networks

As per Electric Power Research Institute's initiatives (EPRI smart inverter initiative) [15], a set of standard smart inverter capabilities has been in developed for the control of local voltage, frequency and for grid protection (see Section 2.4.2). Furthermore, smart inverters can monitor voltage and frequency at their terminals and change their power outputs accordingly [57, 58]. Moreover, those functions fully utilise capabilities of solar PV inverters in order to comply with operational limits of networks and hence prevent costly network augmentations.

The specific voltage support is mainly facilitated by means of adjusting either or both reactive and active power using Volt-VAr and Volt-Watt control of smart PV inverters [74]. The Volt-VAr control mode dynamically regulates voltage at POC by injecting or absorbing reactive power during under-voltage and over-voltage conditions respectively. Further, Volt-VAr control mode could operate either on real

power priority (Watt priority) or on reactive power priority (VAr priority) modes (see Section 2.4.2). However, Volt-Watt control mode is only capable of responding to over-voltage conditions by curtailing active power output.

In general, voltage support functions of smart inverters can be used to manage over-voltage conditions that often limit the solar PV HC in LV distribution networks. Therefore, potential HC enhancement options can be investigated by means of detailed analysis of smart PV inverter operation in Volt-VAr or Volt-Watt control modes.

Scope of smart inverter modelling exercise presented in this section is focused on investigating the applicability of Volt-VAr and Volt-Watt control functions of smart inverters to address over-voltage limit violation issues and their impact on solar PV HC enhancement.

6.2.1 Modelling of Smart PV Inverter Functions

The generic PV system in DIgSILENT PowerFactory simulation platform [75] is used with modifications to incorporate the Volt-VAr and Volt-Watt control functions of smart PV inverters. Its highly customisable PV system template contains four main blocks: solar PV array, the DC bus-bar and capacitor model, PQ controller and the static generator. In addition, some measurement blocks available can be used for voltage, frequency, phase and power measurements. The schematic of the DIgSILENT PowerFactory generic PV model is shown in Fig. 6.1 which allows the user to implement specific models that are not standard in the DIgSILENT library and allows development of blocks either as modifications of existing models or as completely new models. Specifics of each block of the generic PV system model are described below.

Solar Irradiance and Temperature (Blocks 1 & 2)

Solar irradiance and ambient temperature are important factors that influence the power output of the PV system by affecting the output voltage of the solar panel.

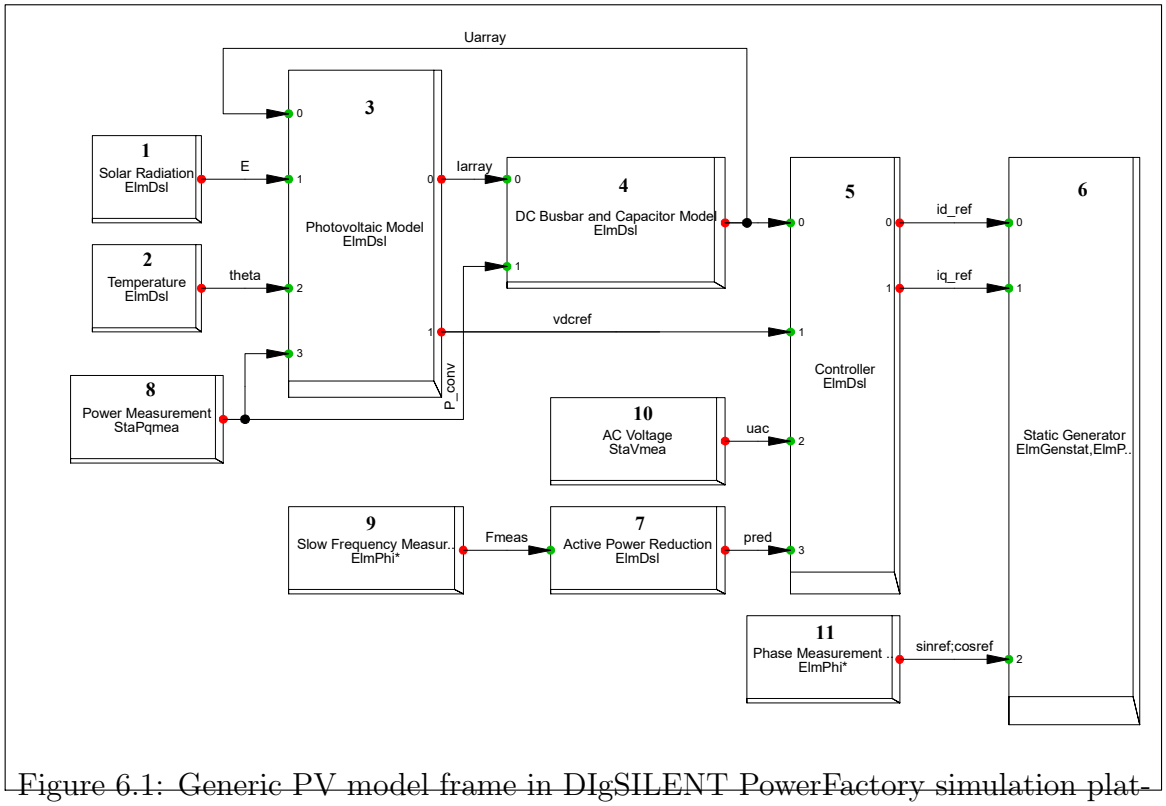

Figure 6.1: Generic PV model frame in DIgSILENT PowerFactory simulation platform

The purpose of these blocks is to accumulate the rate of change of irradiance and the temperature and integrate them over a period of time. The outputs of these blocks are provided as inputs to the photovoltaic model. However, the temperature that is used in DIgSILENT PowerFactory is 25 °C which is the STC (standard test condition) temperature.

Photovoltaic Model (Block 3)

The photovoltaic model which detailed in Fig. 6.2 takes the voltage of the PV array, V_{array} (V), the irradiation, E (W/m^2), active power signal from power measurement device, P_{conv} and the module temperature, theta (25 °C) as inputs and provides two outputs; the array current I_{array} (A) and voltage at the maximum power point, $V_{mmp-array}$ (V). The purpose of this model is to determine the $V-I$ characteristic of a single panel, particularly the magnitudes of the voltage (V_{mpp}) and current (I) at the maximum power point which assist in the determination of the current and voltage of the entire solar PV system which incorporates a number of series and

parallel PV panels.

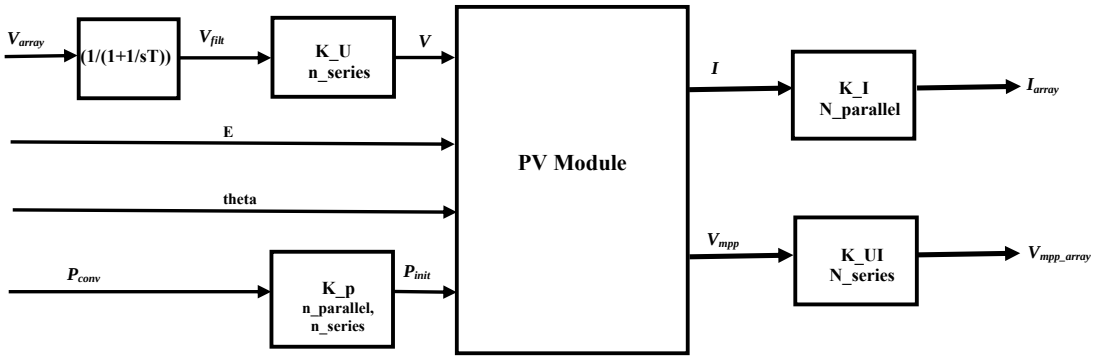

Figure 6.2: Photovoltaic array model

DC Busbar and Capacitor Model (Block 4)

This block is modelled as a DC link of which the details are shown in Fig. 6.3. The purpose of this block is to calculate the input DC link voltage of the inverter utilising the magnitudes of the array current, I_{array} (from the PV model) and active power, P_{conv} (from power measurement device). DC capacitor is modelled as the equation given in (6.1).

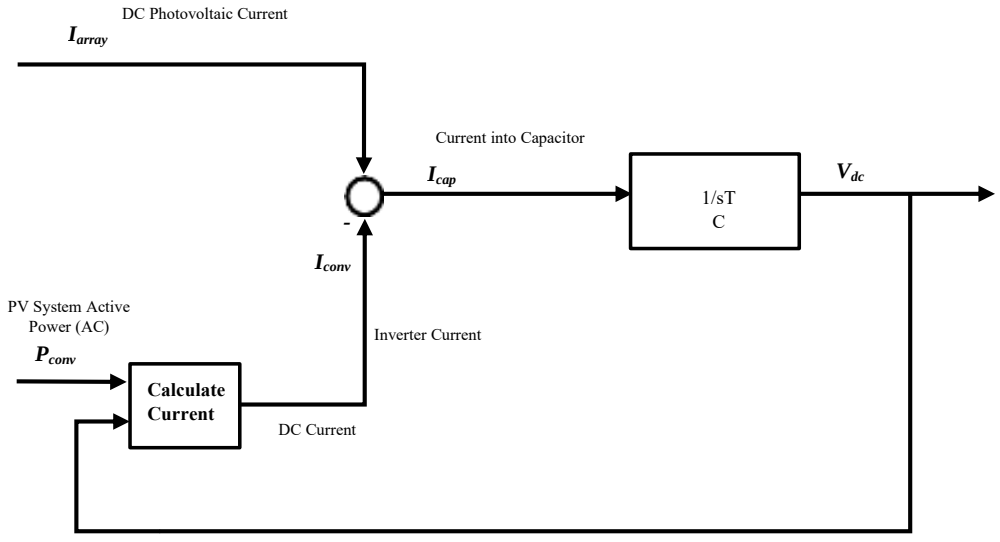

Figure 6.3: DC busbar and capacitor model

$$I_{conv} = I_{array} - \frac{1}{sC} V_{dc} \tag{6.1}$$

PQ Controller Block (Block 5)

The PQ controller is the most important part of the PV system and regulates the active and reactive power outputs of the static generator according to the DC side output of the PV system. As shown in Fig. 6.4, this block takes DC voltage from the capacitor model as actual DC voltage (V_{dcin}), reference DC voltage from PV model (V_{dcref}), measured AC voltage at the output of the inverter (V_{ac}) and reference AC voltage (V_{ref}) as the inputs. This block essentially determines the reference values for active power current, Id_ref and reactive power current, Iq_ref which are fed to the static generator block which operates as the interface for power converter.

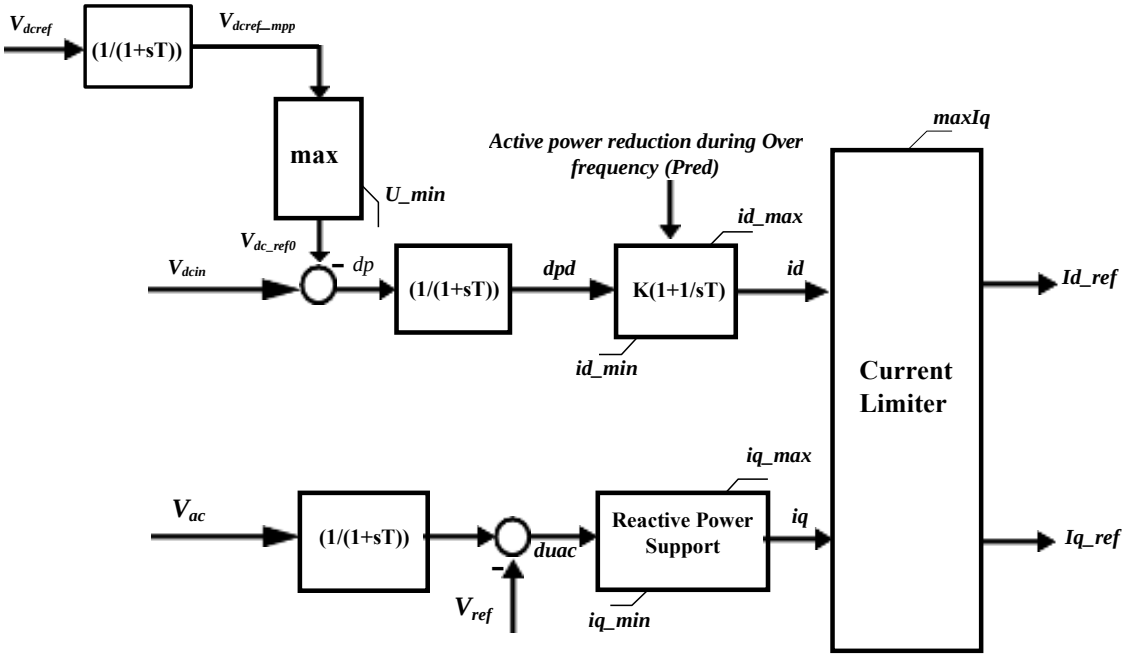

Figure 6.4: PV controller model

Static Generator Block (Block 6)

The static generator acts as the interfacing of the converter. The output from the controller block that is the d-q axis reference currents from the controller (Id_ref and Iq_ref) and d-q reference angles (cos_ref and sin_ref) from the phase measurement unit are given to the static generator block as inputs. Based on the inputs, the active and reactive power outputs of the static generator are regulated.

Active Power Reduction Block (Block 7)

Increase in power system frequency is a good indicator of surplus real power. In over frequency situations, the solar PV plant must be capable of reducing the active power delivered to the grid. The purpose of this block is to adjust active power injection according to the system frequency. If the frequency is above 50.2 Hz, the inverter reduces the injected power and if the frequency reaches 51.5 Hz, the inverter is switched off and when the frequency falls below 50.05 Hz, the inverter regains its real power injection capability.

Measurement Blocks (Blocks 8, 9, 10 & 11)

These measurement blocks represent the measurement of the instantaneous active and reactive power from the AC side of the PV system, AC voltage and frequency and provides the corresponding measured values to the controller block and the active power control block.

6.2.2 Local Volt-VAr and Volt-Watt Control Strategies

The DIgSILENT generic model of Fig. 6.1 can only be used for reactive power control and does not facilitate active power curtailment for management of over-voltage conditions [75]. Thus, the controller block was modified in order to facilitate active power curtailment along with the existing reactive power control as shown in Fig. 6.5, and are elaborated below:

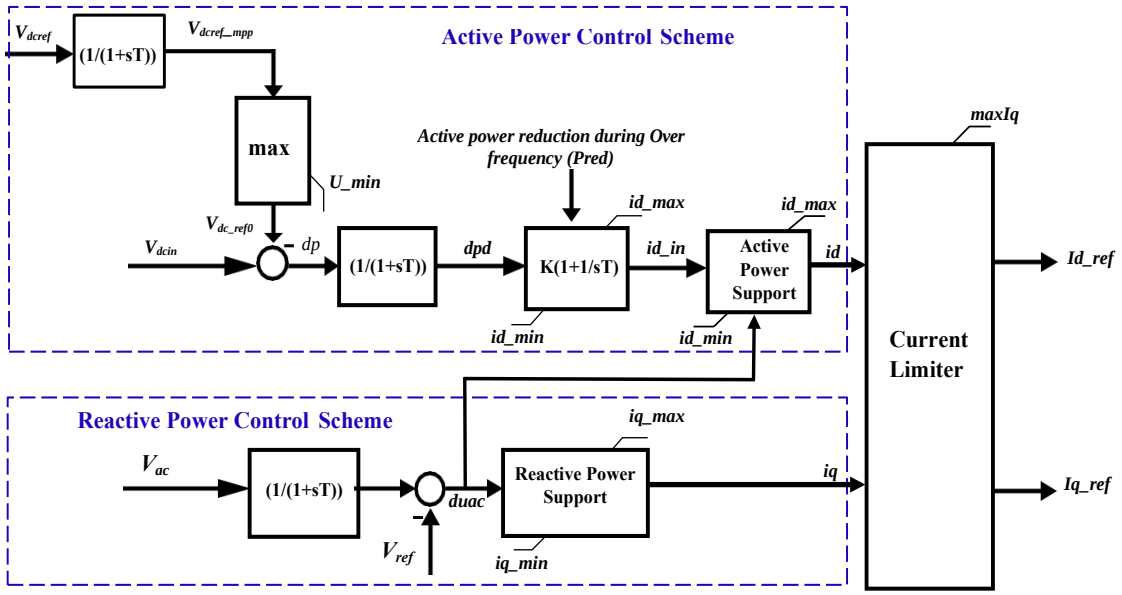

Figure 6.5: Real and reactive power control loops of solar PV inverter model

Reactive Power Control Scheme

The existing model of reactive power control scheme in DIgSILENT operates in accordance with the Volt-VAr response curve shown in Fig. 6.6. By comparing the voltage reference, V_{ref} with the voltage measurement, V_{ac},(terminal voltage at the POC), q-axis current, iq in the range of iq_max (referred to Q_1 given in Fig. 6.6) and iq_min (referred to Q_4 given in Fig. 6.6) is generated and fed to the current limiter of the controller block.

As per the Volt-VAr characteristic curve shown in Fig. 6.6, a set of points is defined as, (V_1, Q_1), (V_2, Q_2), (V_3, Q_3) and (V_4, Q_4) depending on the DNO requirements. The middle point of the statutory voltage limits is used as a reference voltage, V_{ref}. Based on a "dead-band" range (db) where no reactive power is absorbed or injected in Volt-VAr response curve (as given in Fig. 6.6), V_2 and V_3 voltages can be calculated using (6.2) and (6.3), respectively.

$$V_2 = V_{ref} - db \tag{6.2}$$

$$V_3 = V_{ref} + db \tag{6.3}$$

Further, the voltages V_1 and V_4 can be calculated as given in (6.4) and (6.5)

respectively.

$$V_1 = V_2 - \left| \frac{Q_1}{K_{iq}} \right| \tag{6.4}$$

$$V_4 = V_3 + \left| \frac{Q_4}{K_{iq}} \right| \tag{6.5}$$

where, K_{iq} is the reactive current droop gain in the "active-band" range (ab) which is defined in Fig. 6.6 and Q_1 and Q_4 are the maximum possible reactive power injection and absorption levels of the inverter respectively.

Required reactive power absorption or injection, Q (referred to iq) at a measured voltage, V_{ac}, can be computed using the expressions given in (6.6) .

$$Q = \begin{cases} \frac{V_0}{|V_0|} * (|V_0| - db)\, K_{iq}; & if \quad |V_0| > db \\ 0; & otherwise \end{cases} \tag{6.6}$$

where, V_0 ($V_0 = V_{ac} - V_{ref}$) is the input voltage to the reactive power controller.

The reactive power output values (i.e., Q_1, Q_2, Q_3, and Q_4) are defined as a percentage of available VAr level determined by the present active power output level and the reactive power capability of the PV inverter.

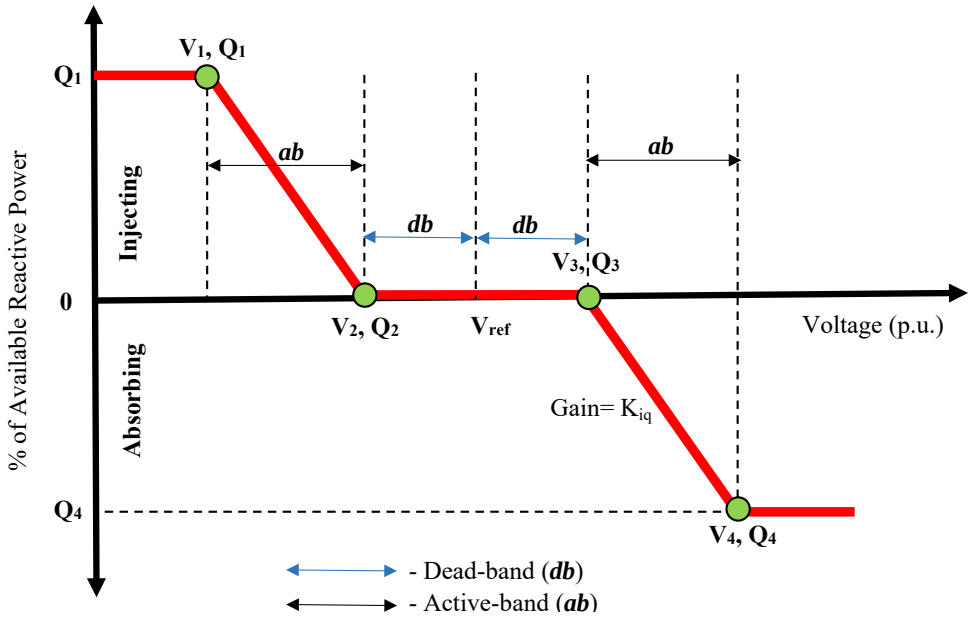

Figure 6.6: Volt-VAr response curve

Active Power Control Scheme

The new active power control scheme was designed in accordance with the Volt-Watt response curve shown in Fig. 6.7. Active power control scheme is activated when the terminal voltage, V_{ac} of the solar PV system exceeds set point, V_2 corresponding to active power curtailment as shown in Fig. 6.7 and generates d-axis current, id in the range of id_min (referred to P_{min}) and id_max (referred to P_{max}) and feeds the current limiter of the controller block.

As per the Volt-VAr characteristic curve shown in Fig. 6.7, a set of points is defined as, (V_1, P_1), (V_2, P_2), (V_3, P_3) and (V_4, P_4) depending on the DNO requirements. In order to design this curve, the statutory voltage limit, 1 p.u. is taken as the reference voltage, V_{ref}. Then, the voltages V_1 and V_2 can be calculated using (6.7) and (6.8), respectively.

$$V_1 = V_{ref} \tag{6.7}$$

$$V_2 = V_1 + ib \tag{6.8}$$

where, ib is the "ideal-band" where PV system is operating at maximum available power (as defined in Fig. 6.7).

Further, V_3 and V_4 can then be calculated using (6.9) and (6.10) respectively.

$$V_3 = V_2 + \left| \frac{P_{max} - P_{min}}{K_{id}} \right| \tag{6.9}$$

$$V_4 = V_3 + db \tag{6.10}$$

where, db is the "dead-band" and K_{id} is the active current droop gain which are defined in Fig. 6.7.

Active power injection, P (referred to id) by the inverter at a measured voltage, V_{ac}, can be computed using the expressions given in (6.11).

$$P = \begin{cases} P_{max}; & if\ V_0 < ib \\ P_{max} + (V_0 - ib) * K_{id}; & if\ ib < V_0 \leq ib + ab \\ P_{min}; & otherwise \end{cases} \tag{6.11}$$

where, V_0 ($V_0 = V_{ac} - V_{ref}$) is the input voltage to the active power controller and P_{max} and P_{min} are the maximum and minimum available real power of the PV system respectively.

The active power output values (i.e., P_1, P_2, P_3, and P_4) are defined as a percentage of the maximum PV power output of the inverter (i.e., P_{max}).

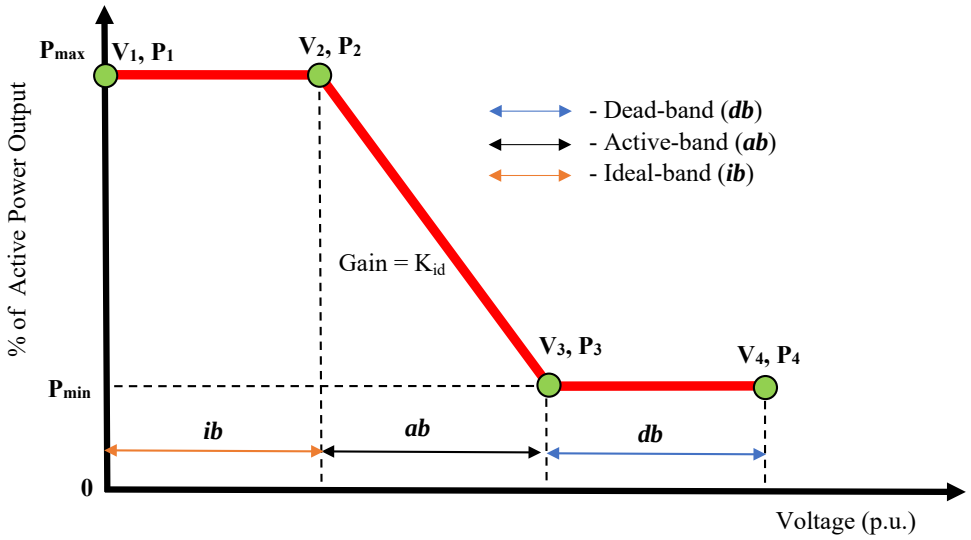

Figure 6.7: Volt-Watt response curve

The reactive current component, iq and the active current component, id which are generated using individual controllers are fed to the current limiter to generate d-axis and q-axis current references, Id_ref and Iq_ref respectively. In Volt-VAr operation (with VAr priority) mode, Id_ref and Iq_ref satisfy the condition given in (6.12) [17].

$$Id\_ref \leq \sqrt{I\_rated^2 - Iq\_ref^2} \tag{6.12}$$

where, I_rated is the rated current of the PV inverter.

Compared with the Volt-VAr control of Watt priority mode, VAr priority Volt-

VAr control mode has the potential to be more effective in reducing over-voltage situations where solar PV inverter output is high and inverters have limited headroom to provide reactive power to regulate the terminal voltage of the inverter [76].

6.2.3 Performance Evaluation of PV Inverter Model

Performance of the modified PV inverter model presented in Section 6.2.2 is used to assess the Volt-VAr and Volt-Watt control strategies focusing on over-voltage curtailment.

A simple LV distribution system serving a 125 kVA lumped load and a 180 kVA PV system at the end of a 100 m long feeder was modelled in DIgSILENT PowerFactory as shown in Fig. 6.8. The PV system of which the detailed specifications are given in Table 6.1, operates at MPP incorporating the appropriate number of series and parallel PV modules relevant to the PV capacity. Current and voltage of the PV module at MPP are given for the irradiance level at 1000 W/m^2. Detailed specifications of the PV system are given in the Appendix C.

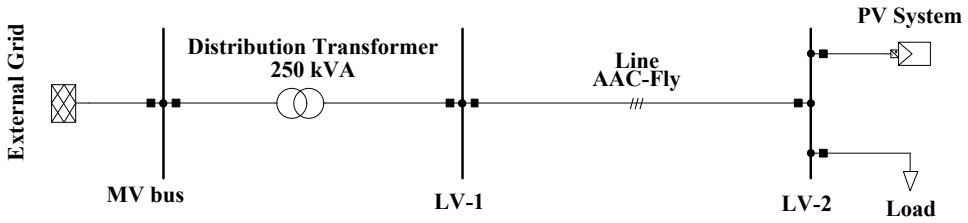

Figure 6.8: Single line diagram of the test system

Table 6.1: Key PV system parameters

Parameters	Value
Module Current at MPP	4.58 A
Module Voltage at MPP	35 V
Irradiance level	1000 W/m^2
Series Modules Number	20
Parallel Modules Number	56

The test network consists of a 250 kVA, 11 kV/0.4 kV transformer connected to a single feeder (Conductor type: $AAC - Fly$, $(R = 0.4505\ \Omega/km, X = 0.292\ \Omega/km)$).

Table 6.2: Volt-VAr and Volt-Watt control settings for the PV inverter model

Volt-VAr controller		Volt-Watt controller	
Voltage (p.u.)	Q/Qrated (%)	Voltage (p.u.)	P/Prated (%)
0.92	+44	0.92	100
0.98	0	1	100
1.02	0	1.04	100
1.08	-44	1.1	0

The lumped three phase, balanced load at the feeder end is 125 kVA operates at 0.8 lagging power factor. 180 kVA PV system and lumped load at the feeder end maintain the initial voltage at the POC (LV-2) at 1 p.u. which is equal to the voltage at secondary of the transformer (LV-1).

Settings of Volt-VAr and Volt-Watt controllers used in the developed smart inverter model are given in Table 6.2 [67]. The test network was simulated for three different operating modes of the smart inverter; Volt-VAr control, Volt-Watt control and combined Volt-VAr and Volt-Watt control[1] which provides a more aggressive mode of control. Inverter performance associated with each scenario was investigated for grid voltage variations; both under-voltage and over-voltage conditions by developing two cases as follows:

- Case 1: LV-1 voltage reduced by 7.5%
- Case 2: LV-1 voltage increased by 7.5%

Effect of Smart Inverter Functions on Under-Voltage Conditions

Case 1: LV-1 voltage reduced by 7.5%

In this case, voltage at the secondary of the transformer was reduced by 7.5% by adjusting the distribution transformer tap position at t=1 s and kept constant to analyse the response of different controllers to under-voltage condition.

Voltage at the POC and the active and reactive power outputs of the inverter system for Volt-VAr, Volt-Watt and combined Volt-VAr and Volt-Watt control modes

[1]Proposed control mode of smart inverters for solar PV hosting capacity enhancement in this thesis.

are shown in Figs. 6.9(a), 6.9(b) and 6.9(c) respectively. According to Fig. 6.9(a), the Volt-VAr controller of the PV system injects a reactive power of 39.564 kVArs at t=1 s in response to the voltage drop of 0.935 p.u. at the POC. In this case, only the reactive power control strategy is effective while active power controller has no control over the under-voltage condition. Further, combined Volt-VAr and Volt-Watt controller mode shows the same response as with the Volt-VAr control mode and hence, the voltage at the POC is improved from 0.935 p.u. to 0.951 p.u. in both Volt-VAr and combined Volt-VAr and Volt-Watt control modes.

Effect of Smart Inverter Functions on Over-voltage Conditions

Case 2: LV-1 voltage increased by 7.5%

In this case, voltage at the secondary of the transformer was increased by 7.5% by adjusting the distribution transformer tap position at t=1 s and kept constant to analyse the voltage at POC and active/reactive power output responses of inverter system. Voltage at the POC and the active and reactive power outputs of the inverter system for Volt-VAr, Volt-Watt and combined Volt-VAr and Volt-Watt control modes are shown in Figs. 6.10(a), 6.10(b) and 6.10(c) respectively.

According to Fig. 6.10(a), the Volt-VAr controller of the PV system absorbs a reactive power of 58.09 kVArs at t=1 s in response to the voltage rise of 1.077 p.u. at the POC and reduces the voltage to 1.057 p.u. Referring Fig. 6.10(b), PV inverter with Volt-Watt control mode curtails the active power output of the PV system to 135.6 kW which leads to a reduction of the voltage at the POC to 1.062 p.u. Hence, both active and reactive power control strategies are effective in responding to over-voltage condition. Fig. 6.10(c) shows results for the combined Volt-VAr and Volt-Watt control mode of the PV inverter where it shows absorption of a reactive power of 52.95 kVArs and curtailment of the active power to 162.4 kW in response to the voltage rise resulting a reduction the voltage to 1.054 p.u. at the POC. Hence, aggressive mode of voltage control avoided over-voltage issue effectively compared to the individual Volt-VAr and Volt-Watt control modes. Even though, the Volt-VAr

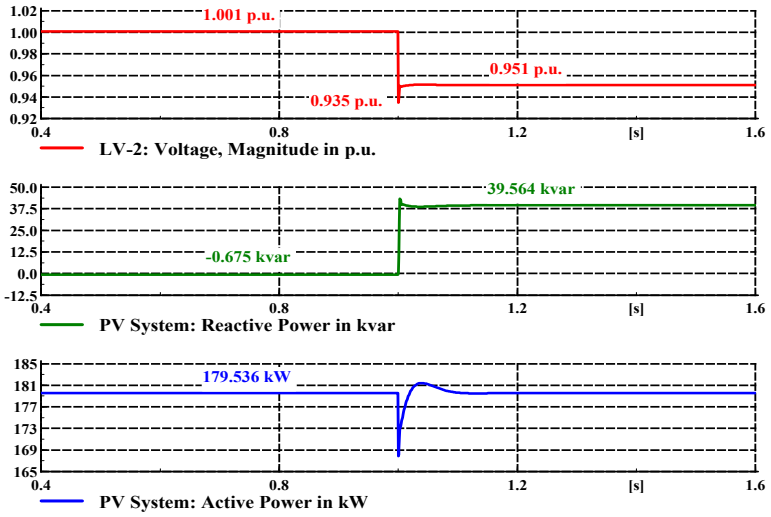

(a)

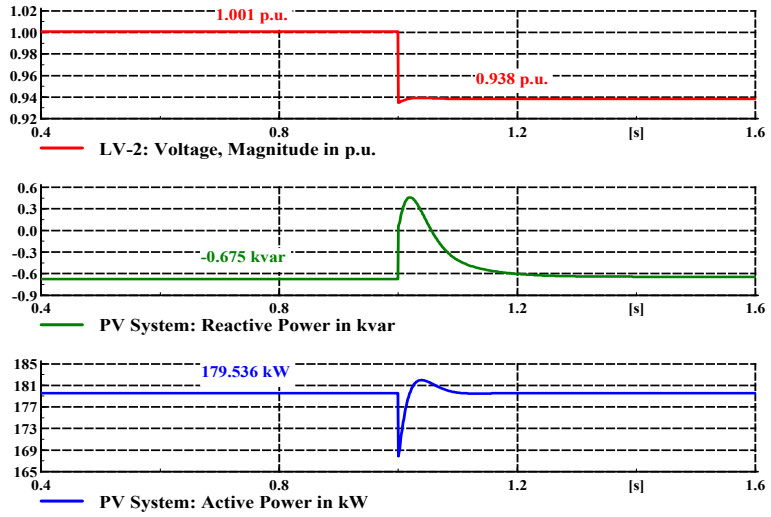

(b)

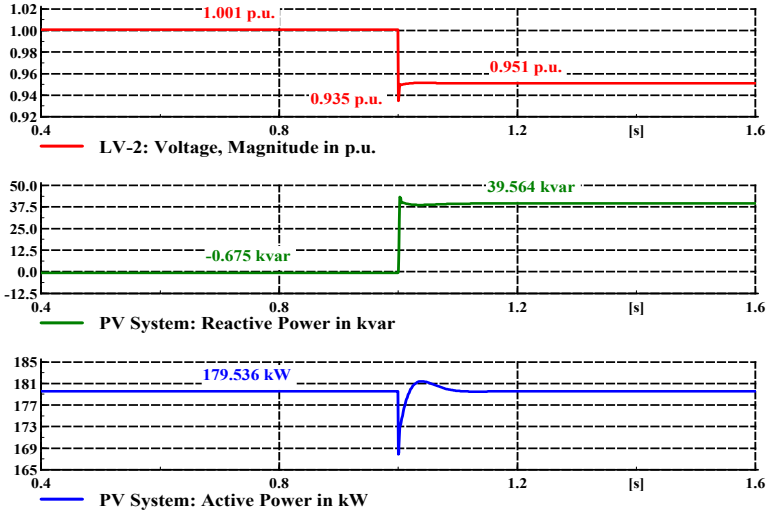

(c)

Figure 6.9: Voltage and power output responses for under-voltage condition: Case 1; (a) With Volt-VAr control (b) With Volt-Watt control and (c) With combined Volt-VAr and Volt-Watt control.

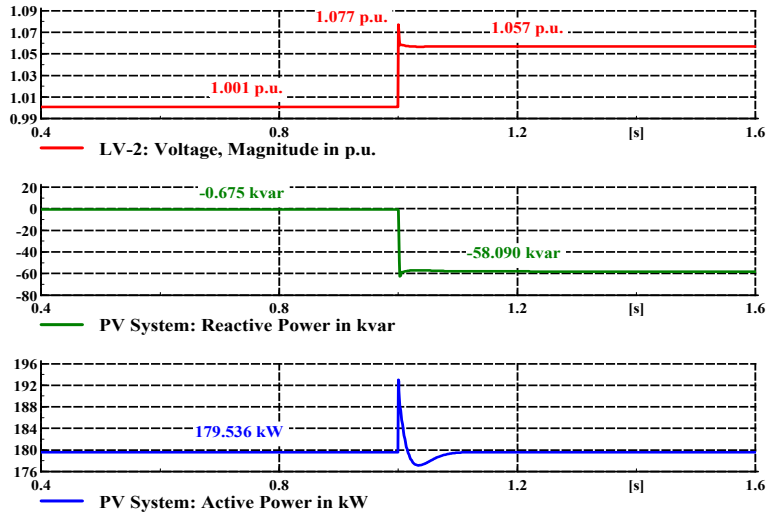

(a)

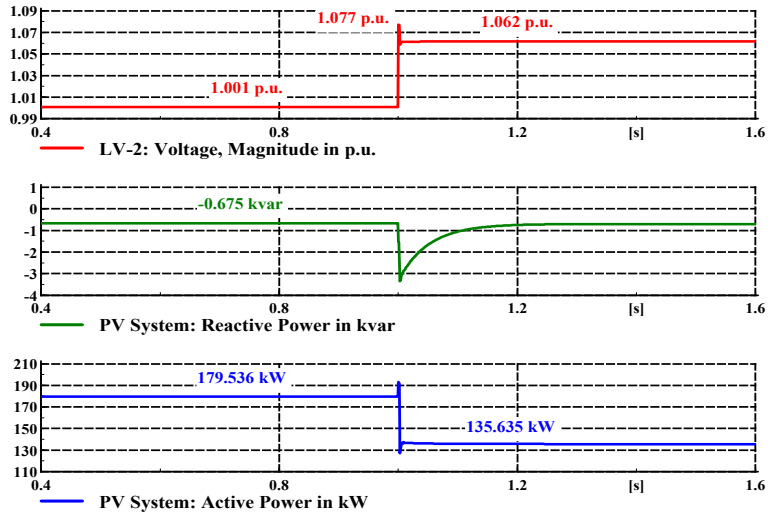

(b)

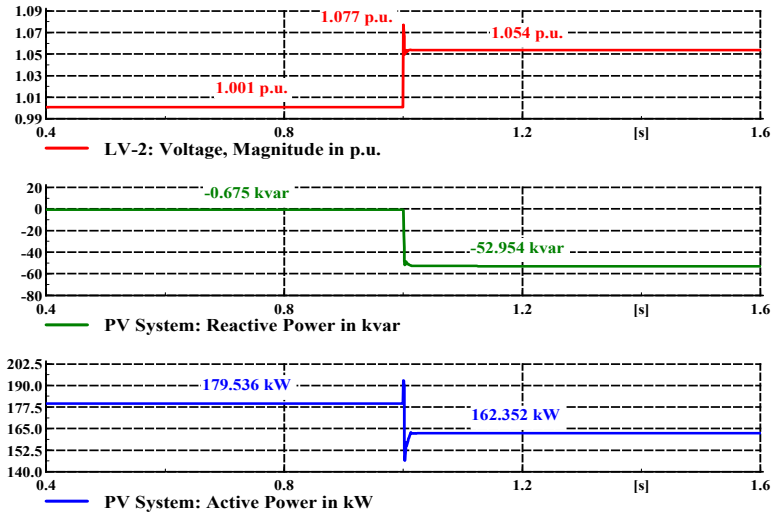

(c)

Figure 6.10: Case 2: Voltage and power output responses for over-voltage condition; (a) With Volt-VAr control (b) With Volt-Watt control and (c) With combined Volt-VAr and Volt-Watt control.

and Volt-Watt control strategies were shown not to be entirely suppressing the over-voltage conditions, the corresponding reductions observed are seen to be generally comparable.

Based on the above results, smart inverters operating at Volt-VAr, Volt-Watt and combined Volt-VAr and Volt-Watt controller modes can be effectively used for grid voltage support and hence the over-voltage curtailment in networks. Thus, maximum connectable solar PV capacity which is primarily limited by over-voltage issues can be increased by choosing a proper control strategy of smart inverters. However, the solar PV HC is influenced by a number of factors such as network characteristics (eg. length of feeders, type of the conductor, no of feeders), loading levels and location of solar PV systems. Further, different recommendations imposed by different standards on smart inverter control strategies may change the level of maximum connectable solar PV capacity. Thus, selection of the optimal control strategy and default settings of smart inverters with regard to HC enhancement referring to various solar connection standards is a challenging task, which requires extensive analysis. Hence, Section 6.3 presents a comparative evaluation of solar PV HC enhancement using smart inverters which can operate at Volt-VAr, Volt-Watt and combined Volt-VAr and Volt-Watt control modes referring to different solar PV connection standards.

In order to effectively evaluate smart inverter functions and their potential impact on grid performance and hosting capacity, simulation models must have the capability to effectively represent the various functions and settings as in a practical inverter. Thus, an inverter test was carried out in a laboratory environment to validate the DIgSILENT PV inverter model.

SMA Sunny Boy 5000TL (1ϕ, 230 V, 50 Hz) 5 kW inverter was used for the validation of DIgSILENT PV inverter model, which is capable of injecting or absorbing reactive power. Inverter was tested for both Volt-VAr and Volt-Watt droop characteristics for two different DNSP settings; a Victorian DNSP and a NSW DNSP. Appendix D provides the details of the laboratory experiment conducted for the

validation of PV inverter model together with relevant results.

6.3 Hosting Capacity Enhancement Using Volt-VAr and Volt-Watt Control Strategies

This section presents investigations in relation to the solar PV HC enhancement provided by smart inverter functions; Volt-VAr, Volt-Watt and combined Volt-VAr and Volt-Watt operation in compliance with the requirements of IEEE 1547-2018 (referred to as Cat.A and Cat.B for settings of Category A and B respectively), AS/NZS 4777 (referred to as AS and NZS for settings used in Australia and New Zealand respectively), California Rule 21 (referred to as CR21) and Hawaii Rule 14 (referred to as HR14). At present, combined Volt-VAr and Volt-Watt control mode is not included in any of these standards, however, the outcome presented in this chapter will pave a path for further contribution to improve the guidelines/standards on solar PV connections.

A feeder based solar PV HC approach, presented in this thesis reduces the complexity of evaluation process and improves the applicability in practical networks. Thus, the solar PV HC enhancement with Volt-VAr and Volt-Watt control strategies of smart PV inverters is investigated in this section based on the feeder level HC approach. Hence, a single feeder radial distribution network is considered for comparative evaluation of solar PV HC enhancement assessment as radial networks are predominantly used in practice.

6.3.1 Modelling Regimes

A simple distribution network which consists of a 250 kVA, 11kV/400V transformer connected to a 1 km long feeder (three different conductor types: $AAC - Fly$, $ABC - 70mm^2$ and $ABC - 50mm^2$ were considered separately) was modelled in DIgSILENT PowerFactory simulation software.

The total three phase load was assumed to be balanced and uniformly dis-

tributed at 10 nodes along the feeder. The individual loads were maintained at 5 kW/customer (operating at 0.8 lagging power factor) assuming an overall 25% transformer loading level (minimum) in all simulation scenarios. It was assumed that 1 p.u. constant supply voltage is maintained at the secondary of the distribution transformer.

Maximum connectable solar PV capacity in this network subjected to over-voltage curtailment and thermal loading limit of the feeder is investigated considering extreme operating conditions: minimum load and maximum PV generation. In addition, HC analysis is conducted based on a set of features: conductor type, upper voltage level and thermal loading level. Two levels of upper voltage limits are considered for HC assessment; 1.06 p.u. and 1.1 p.u. as over-voltage upper limit is not the same for all utilities while the acceptable line loading limit is considered to be 100% of the thermal loading of the conductor. In this analysis, both bare conductors ($AAC - Fly$) and bundled conductors ($ABC - 70mm^2$ and $ABC - 50mm^2$) were selected.

Since, solar PV location is an influential factor on the solar PV HC, the feeder segmentwise HC levels are examined. The modelled feeder is analysed by dividing it into three equal segments; feeder front, feeder middle and feeder end in order to account for randomness of solar PV system locations under four different scenarios listed below with Volt-VAr and Volt-Watt control functions of aforementioned standards (Settings of those control functions associated with different standards are given in Appendix E).

- Scenario 1: Examination of maximum connectable solar PV capacity at the feeder end, feeder middle and feeder front segments as per the Volt-VAr control strategy in different standards (referred to as "VVC")

- Scenario 2: Examination of maximum connectable solar PV capacity at the feeder end, feeder middle and feeder front segments as per the Volt-Watt control strategy in different standards (referred to as "VWC")

- Scenario 3: Examination of maximum connectable solar PV capacity at the feeder end, feeder middle and feeder front segments as per the combined Volt-VAr and Volt-Watt control strategy in different standards (referred to as "Comb. VVC&VWC")

- Scenario 4: Use of two solar PV units of same rating (one unit has Volt-VAr mode and other with Volt-Watt mode) in lieu for combined Volt-VAr and Volt-Watt controller unit and examination of maximum connectable solar PV capacity at the feeder end, middle and front segments for different standards (referred to as "VVC+VWC")

6.3.2 Comparative Evaluation of Solar PV Hosting Capacity Employing Smart Inverter Control Strategies

The effect of smart inverter local control strategies on feeder segmentwise HC levels are shown in Figs. 6.11, 6.12 and 6.13 for the three different conductor types: $AAC - Fly$, $ABC - 70mm^2$ and $ABC - 50mm^2$ respectively. HC enhancement provided by different control strategies was evaluated by comparing with the base HC value established using the conventional inverters (without any control modes activated and referred to as "W/Control"). Furthermore, Figs. 6.11, 6.12 and 6.13 illustrate solar PV hosting capacities corresponding to the considered voltage upper limits (VUL): 1.06 p.u. and 1.1 p.u.

From Figs. 6.11, 6.12 and 6.13, it is evident that the HC can be increased utilising the settings of all considered connection standards except those of AS 4777 when the HC constraint voltage limit is set to be 1.06 p.u. At the upper voltage limit of 1.06 p.u., only NZS 4777 standard shows HC increment with Volt-Watt controller for all selected conductor types. Therefore, it should be highlighted that the Volt-Watt control enables HC enhancement only when the voltage set point is lower than the upper voltage limit. With the increase of the upper voltage limit to 1.1 p.u., HC is

significantly increased by utilising Volt-Watt control, however, exceeded the thermal capacity of the feeder thus limiting the HC to thermal capacity of the feeder.

According to Figs. 6.11(a), 6.11(b), 6.12(a), 6.12(b), 6.13(a) and 6.13(b), the Hawaii Rule 14 and IEEE 1547-Cat.B Volt-VAr function settings were found to be very effective in mitigating/avoiding over-voltages at the feeder end and the feeder middle. HC enhancement[2] as per these two standards at the feeder end and feeder middle were 91%, 50.3% and 62.4%, 53.8% respectively for the $AAC - Fly$ type conductor. For a $ABC - 70\ mm^2$ type feeder, improvement of HC with Hawaii Rule 14 were 33.3% and 31.3% at feeder end and middle respectively and the corresponding figures were 18.2%, 19% respectively for the IEEE 1547-Cat.B. Similarly, with $ABC - 50\ mm^2$ cable, the corresponding figures were observed to be 28.5%, 29.5% and 15.6%, 12.3% for Hawaii Rule 14 and IEEE 1547-Cat.B respectively. Thus, it implies that the Volt-VAr control is more effective with regard to bare conductor type feeders where X/R ratio is comparatively high compared to bundled conductors. On the other hand, Volt-Watt control mode is more effective for the bundled cable type feeders where X/R ratio is low. The HC enhancements at the feeder end with Volt-Watt as per control settings in NZS 4777 standard were 8.6%, 10.2% and 9.8% for $AAC - Fly$, $ABC - 70\ mm^2$ and $ABC - 50\ mm^2$ feeders respectively. The influence of Volt-VAr and Volt-Watt control functions relevant to HC enhancement based on the locational aspects and different conductor types (bare and bundled) are summarised in Fig. 6.14. Furthermore, solar PV HC enhancement at feeder end and feeder middle for all scenarios considered are summarised in Table 6.3 while maximum HC enhancement levels at the feeder end for considered feeder types are listed in Table 6.4.

In general, the increase of voltage constraint limit from 1.06 p.u. to 1.1 p.u., facilitates significant enhancement of HC for both control strategies. However, Figs. 6.11(c), 6.12(c) and 6.13(c), show that distribution of solar PV towards the distribution transformer (feeder front) suppresses the effect of power control functions over

[2]HC enhancement, $\% = \frac{HC_{W/C} - HC_{N/C}}{HC_{N/C}} * 100$, where, $HC_{W/C}$ - HC with power control functions and $HC_{N/C}$ - HC without any power control function

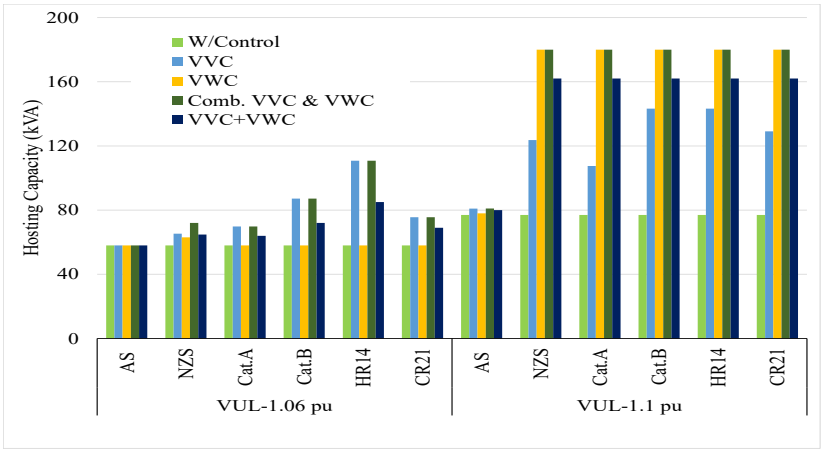

(a)

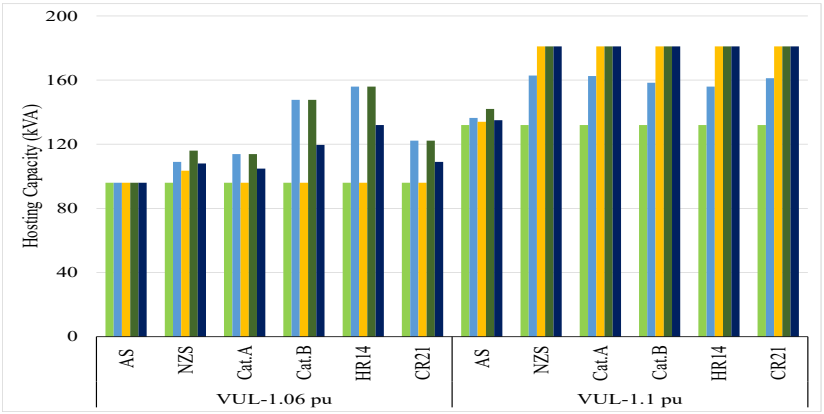

(b)

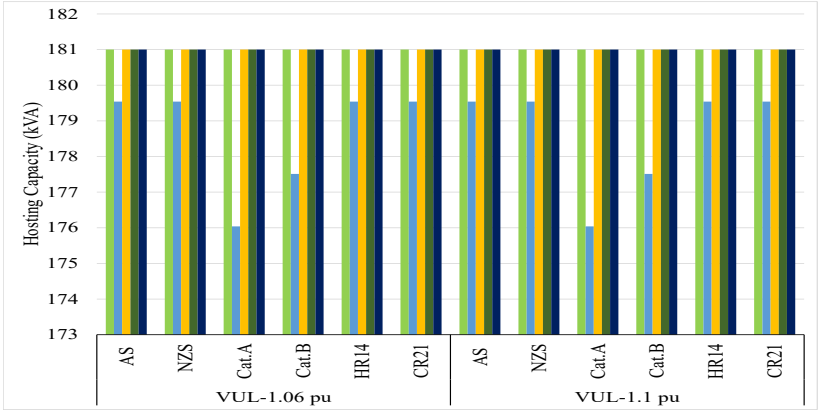

(c)

Figure 6.11: Solar PV HC with Volt-VAr and Volt-Watt control strategies in different standards with 1.06 p.u. and 1.1 p.u. upper voltage levels (Feeder type: AAC-Fly); (a) At feeder end; (b) At feeder middle; (c) At feeder front

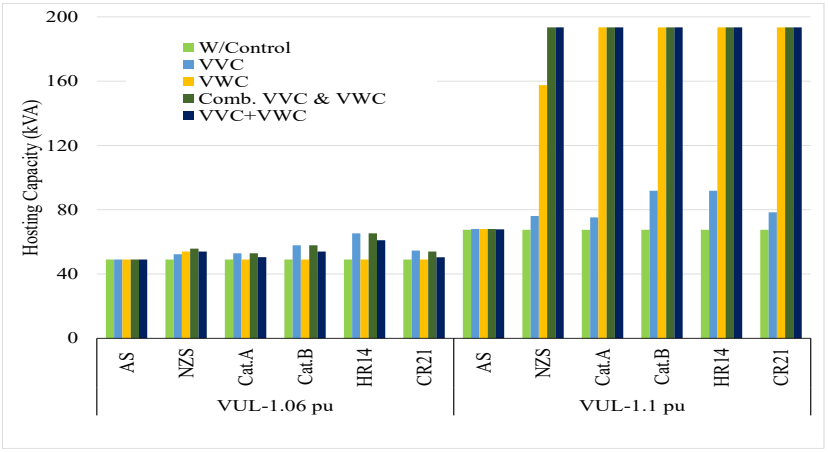

(a)

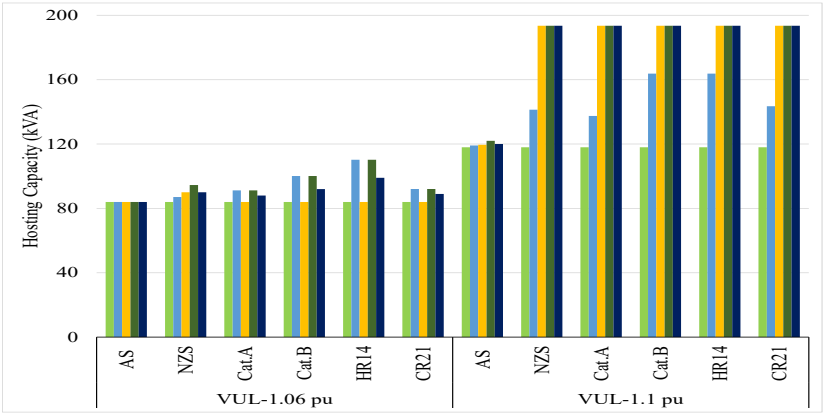

(b)

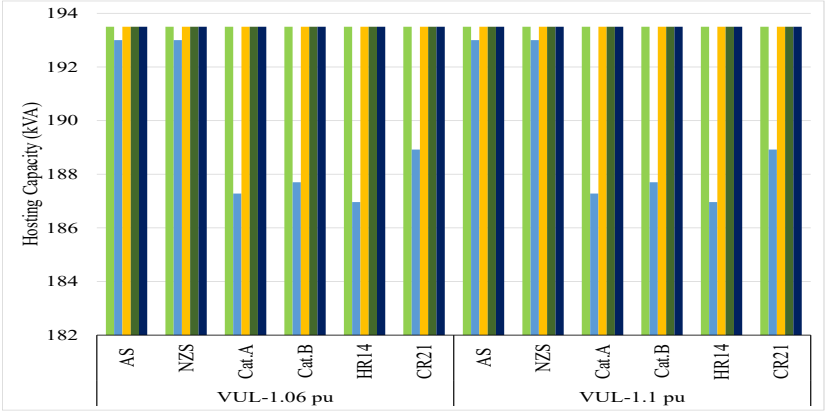

(c)

Figure 6.12: Solar PV HC with Volt-VAr and Volt-Watt control strategies in different standards with 1.06 p.u. and 1.1 p.u. upper voltage levels (Feeder type: $ABC - 70\ mm^2$); (a) At feeder end; (b) At feeder middle; (c) At feeder front

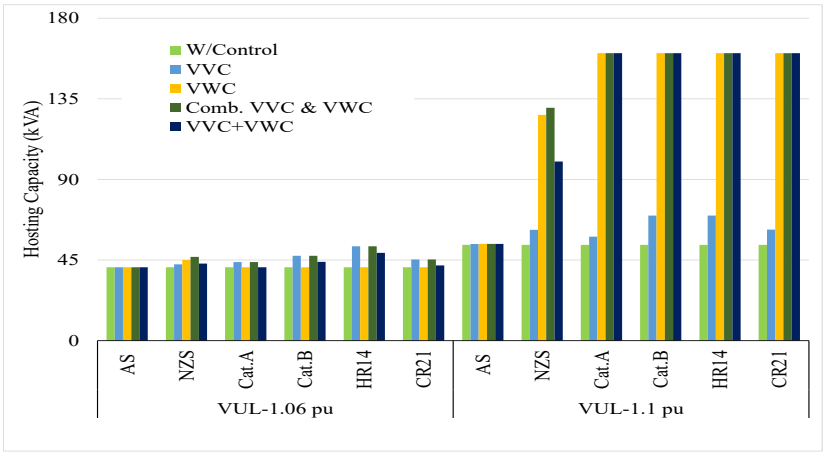

(a)

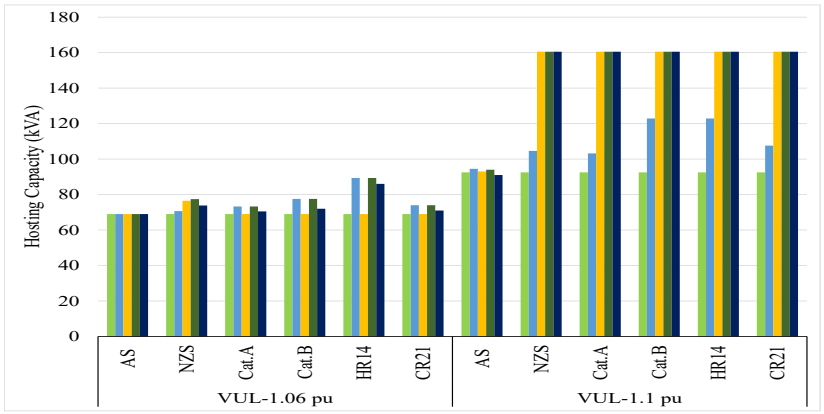

(b)

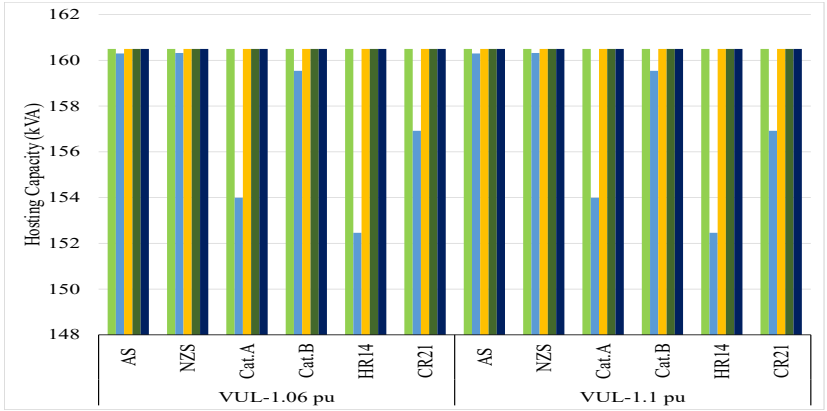

(c)

Figure 6.13: Solar PV HC with Volt-VAr and Volt-Watt control strategies in different standards with 1.06 p.u. and 1.1 p.u. upper voltage levels (Feeder type: $ABC - 50\ mm^2$); (a) At feeder end; (b) At feeder middle; (c) At feeder front

Table 6.3: Solar PV HC enhancement with different power control functions in standards at feeder end and feeder middle

	Upper voltage limit- 1.06 p.u.								Upper voltage limit- 1.1 p.u.							
	VWC		VVC		Comb. VVC&VWC		VVC+VWC		VWC		VVC		Comb. VVC&VWC		VVC+VWC	
	End	Middle	End	Middle	End	Middle	End	Middle	End	Middle	End	Middle	End	Middle	End	Middle
Feeder type: $AAC - Fly$																
AS 4777	0%	0%	0%	0%	0%	0%	0%	0%	1.3%	1.5%	5.1%	3.3%	5.2%	7.6%	3.9%	2.3%
NZS 4777	8.6%	7.8%	12.6%	13.5%	24.1%	20.8%	11.7%	12.5%	-	-	60.6%	23.4%	-	-	-	-
IEEE-1547 Cat.A	0%	0%	20.3%	18.6%	20.3%	18.6%	10.3%	9.2%	-	-	39.6%	23.1%	-	-	-	-
IEEE-1547 Cat.B	0%	0%	50.3%	53.8%	50.3%	53.8%	24.1%	24.6%	-	-	86%	20%	-	-	-	-
Hawaii	0%	0%	91%	62.4%	91%	62.4%	46.6%	37.5%	-	-	86%	18.1%	-	-	-	-
California	0%	0%	30.3%	27.4%	30.3%	27.4%	19%	13.5%	-	-	67.7%	22.1%	-	-	-	-
Feeder type: $ABC - 70\ mm^2$																
AS 4777	0%	0%	0%	0%	0%	0%	0%	0%	0.7%	1.3%	0.7%	0.9%	0.7%	3.4%	0.4%	1.7%
NZS 4777	10.2%	7.1%	6.7%	3.7%	13.9%	12.5%	10.2%	7.1%	133.8%	-	12.8%	19.8%	-	-	-	-
IEEE-1547 Cat.A	0%	0%	8%	8.6%	8%	8.6%	3.1%	4.8%	-	-	11.5%	16.5%	-	-	-	-
IEEE-1547 Cat.B	0%	0%	18.2%	19.2%	18.2%	19.2%	10.2%	9.5%	-	-	36%	38.8%	-	-	-	-
Hawaii	0%	0%	33.3%	31.3%	33.3%	31.3%	24.5%	17.9%	-	-	36%	38.8%	-	-	-	-
California	0%	0%	11.4%	9.6%	10.2%	9.6%	2.9%	6%	-	-	16.1%	21.6%	-	-	-	-
Feeder type: $ABC - 50\ mm^2$																
AS 4777	0%	0%	0%	0%	0%	0%	0%	0%	0.9%	0.5%	0.8%	2.1%	0.9%	1.6%	0.9%	1.6%
NZS 4777	9.8%	10.9%	3.9%	2.4%	14.1%	12.2%	4.9%	7%	135.5%	-	15.6%	13%	143%	-	86.9%	-
IEEE-1547 Cat.A	0%	0%	7.1%	6.2%	7.1%	6.2%	3%	2.2%	-	-	8.5%	11.5%	-	-	-	-
IEEE-1547 Cat.B	0%	0%	15.6%	12.3%	15.6%	12.3%	7.3%	4.3%	-	-	30.3%	32.8%	-	-	-	-
Hawaii	0%	0%	28.5%	29.5%	28.5%	29.5%	19.5%	24.6%	-	-	30.5%	32.8%	-	-	-	-
California	0%	0%	10.3%	7.2%	10.5%	7.2%	2.4%	2.9%	-	-	15.9%	16.3%	-	-	-	-

Table 6.4: Maximum solar PV hosting capacity enhancement at feeder end

Conductor type	With Volt-VAr	With Volt-Watt	With combined Volt-VAr & Volt-Watt
$AAC - Fly$	91% - Hawaii Rule 14	8.6% - NZS 4777	91% - Hawaii Rule 14
$ABC - 70\ mm^2$	33.3% - Hawaii Rule 14	10.2% - NZS 4777	33.3% - Hawaii Rule 14
$ABC - 50\ mm^2$	28.5% - Hawaii Rule 14	9.8% - NZS 4777	28.5% - Hawaii Rule 14

the conductor thermal capacity.

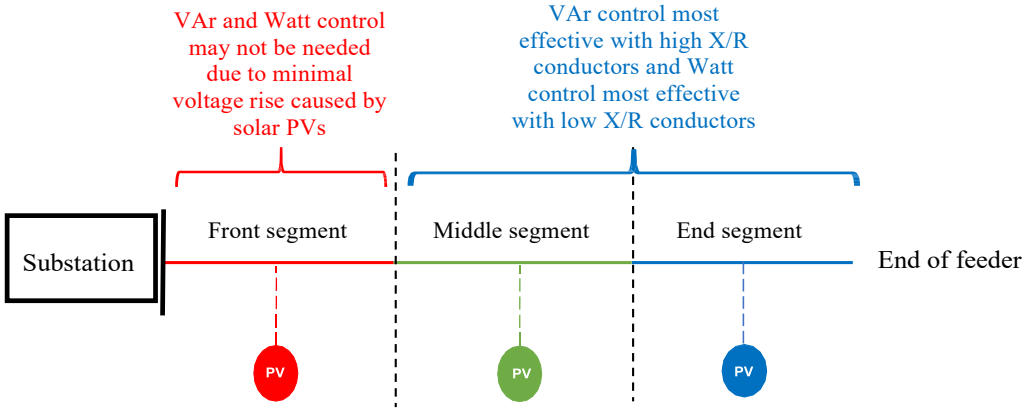

Figure 6.14: Feeder segments where Volt-VAr and Volt-Watt control modes are effective

Compared with individual Volt-VAr and Volt-Watt control, combined Volt-VAr and Volt-Watt control strategy is seen to give higher hosting capacity levels. Furthermore, it should be noted that greater HC enhancement can be achieved by having a single PV inverter with combined control functions (Scenario 3) compared to installing two PV units with individual controls (Scenario 4) due to the capacity for Volt-VAr control in Scenario 3 being larger than that in Scenario 4. Moreover, HC enhancement difference between Scenario 3 and Scenario 4 is larger in the case of $AAC-Fly$ type bare conductor compared to the $ABC-70mm^2$ and $ABC-50mm^2$ types bundled conductors due to the fact that Volt-VAr control in bare conductor works better than that in bundled conductors. Overall, findings of this analysis reveal that combined Volt-VAr and Volt-Watt control strategy is the most effective

method to enhance HC based on all PV interconnection standards. Further, results show that the Volt-Watt control function curtails active power to help over-voltage situation and allow more PV systems. However, feasibility of deploying Volt-Watt control should be evaluated while considering economical aspects as the active power output of the PV inverters are under utilised during over-voltage conditions.

In practice, however, it is important to note that the utility is responsible for addressing high voltage situations with appropriate provision of smart inverters and distribution system planning which may limit the number of over-voltage instances.

6.3.3 Hosting Capacity Enhancement of a Practical LV Distribution Network

A solar PV rich urban LV distribution network in Sri Lanka was studied focusing on potential power quality impact and operational performance considering future expected solar penetration levels described in Chapter 3. The same network was analysed for solar PV HC evaluation using feeder based HC approach in Chapter 5 (see Section 5.3.4). This network is further analysed in this section for solar PV HC enhancement based on the feeder level approach assuming the solar inverters to be smart inverters.

Safe limit of solar PV HC is defined in Chapter 4 as the maximum connectable solar PV capacity in a network which can be connected without any locational influence. The numerous analysis based on the Monte Carlo simulations and sensitivity analysis of influensive factors of solar PV HC reveal that the safe limit of solar PV HC is the maximum solar penetration level at the feeder end. Accordingly, the urban LV distribution network was analysed in Chapter 5 in order to find the safe level of solar PV HC as shown in Table 6.5. Thus, the LV network was analysed for the HC enhancement by modifying the simulation model incorporating smart inverters, i.e. maximum connectable solar PV capacity at the feeder end such that the upper voltage limit of 1.06 p.u. is not violated with Volt-VAr and Volt-Watt and combined Volt-VAr and Volt-Watt control regimes. IEEE 1547-Cat.B settings

were used for the evaluation which is the current practice for solar PV installations in Sri Lanka.

Table 6.5: Solar PV hosting capacity enhancement for the urban LV network

	Safe limit of solar PV HC (kVA)	New solar PV HC as per IEEE 1547-Cat B (kVA)		
		Volt-VAr control	Volt-Watt control	Combined Volt-VAr & Volt-Watt control
Feeder 1	30	35	30	35
Feeder 2	41	52	41	52
Feeder 3	40	50	40	50

Table 6.5 gives enhanced solar PV HC levels in kVA ratings. Results of the simulations show that Volt-Watt control mode has not enhanced solar PV HC compared to that of the traditional solar PV inverters due to its high voltage setting for active power curtailment in IEEE 1547-Cat B standard. Solar PV HC enhancement with Volt-VAr control mode gives a considerable HC enhancement and is the same with the combined Volt-VAr and Volt-Watt control mode.

6.4 Chapter Summary

The study presented in this chapter explored smart PV inverter capabilities of Volt-VAr and Volt-Watt control strategies for solar PV HC enhancement by mitigating over-voltage issues. Accordingly, an aggregated model consisting smart PV inverter with Volt-VAr and Volt-Watt control strategies was developed using DIgSILENT PowerFactory simulation platform. Further, PV inverter model was verified with a laboratory experiment conducted using an SMA Sunny Boy 5000TL single phase PV inverter. This model was used to investigate the influence of different solar PV connection standards on solar PV HC and its enhancement and to investigate the most beneficial approach to address the issue of voltage violations in LV distribution networks. The outcomes of the work include the impact of smart inverter functions defined in IEEE 1547-2018, AS/NZS 4777, California Electric Rule 21 and Hawaiian Electric Rule 14 with a view to understand the successful utilisation and configuration of smart PV inverters to mitigate over-voltage violations.

The investigated Volt-VAr and Volt-Watt control strategies possess differing potentials to enhance the solar PV HC of low-voltage distribution feeders based on outcomes associated with different standards. Furthermore, locational aspects of solar PV systems in distribution feeders also have a greater impact on solar PV HC. A good balance between hosting capacity increase and feeder reactive power consumption was achieved by the default Hawaii Rule 14 and IEEE 1547-Cat.B settings. Hence, smart inverter functions with higher reactive power consumption were observed to be capable of increasing the HC significantly. However, HC is primarily limited by thermal capacity of conductors as solar PV systems connected closer to the distribution transformer end (feeder front) where no voltage control may be needed due to minimal voltage rise.

Overall, increase in the voltage upper limit (HC constraint limit) gives rise to significant HC enhancement, which encourage utilities to increase the voltage upper limits. In addition, compared with Volt-VAr and Volt-Watt controls, combined Volt-VAr and Volt-Watt control capability is the most effective in enhancing solar PV HC. Therefore, practical implementation of the combined Volt-VAr and Volt-Watt control strategy in smart inverters will be essential to accommodate higher levels of PV systems and would help validate the relevance of the outcomes in this chapter.

The outcomes of this chapter will make a significant impact on utility guidelines where the connection of a new solar PV system seeks approval associated with penetration levels exceeding the maximum solar PV limits.

A nomogram based novel PV connection criteria which is presented in Chapter 7 will make use of the high level outcomes associated with stage 3 analysis as presented in Section 7.3.2.

Chapter 7

Nomogram Based Solar PV Hosting Capacity Assessment and Solar PV Connection Criteria in LV Distribution Networks

7.1 Introduction

This chapter presents a systematic approach to evaluate the solar PV HC in LV distribution networks for curtailment of over-voltage conditions, extending the deterministic outcomes presented in Chapter 5. The mathematical formulation presented in Chapter 5 established the solar PV HC in a feeder and reflected on the influential factors, i.e. feeder loading level, location, feeder length and conductor type on the HC level. However, the computational method is seen to be not attractive for new users as specific details are required for HC evaluation. Thus, the main focus of the work presented in this chapter is to introduce a novel computational technique based on a nomogram making the approach highly suitable for novices.

The nomogram developed is specific to all locations of a given feeder and its influential factors are discussed in Chapter 4 (Section 4.3). This chapter further

proposes solar PV connection criteria which permits electricity utilities to approve new solar PV connections which facilitate reasonable modeling insights for HC assessment in LV networks. The proposed solar PV HC assessment and solar PV connection criteria cover technical and regulatory aspects to tackle PV integration in LV distribution networks providing further contributions to the development of solar PV integration guidelines/standards.

As discussed in the Section 2.5, methods widely used by most of electricity distribution companies for preliminary HC assessment and their rules of thumb for solar PV connections are presented in [4, 7] which are mainly based on the percentage of the peak load of the feeder, percentage of transformer rating and thermal limits of the affected feeders. However, adopting a fixed HC value based on a percentage of a load/transformer/feeder rating for networks or feeders is ineffective as the approach does not address the locational impact of solar PV systems or individual feeder characteristics.

Furthermore, electricity utilities around the world seek to develop strategies to increase solar PV integration while maintaining acceptable network performance. Hence, generalised and straightforward methodologies need to be developed to assess the solar PV HC without complex and extensive network modelling and simulations. Thus, the approach proposed in this chapter will be a harmonised solar PV HC assessment method for LV networks which helps PV technologies to become unified and promoted.

The major objectives of the work presented in this chapter are as follows:

- Development of a solar PV HC nomogram which is the graphical representation of HC levels and associated voltage distribution levels specific to a given feeder.
- Development of a simplified solar PV connection criteria in LV distribution feeders which maximises the share of solar PV capacity.

This chapter is organised as follows: Section 7.2 discusses the theoretical basis of developing HC nomograms and Section 7.3 provides a detailed discussion on the

proposed methodology to evaluate solar PV HC and solar PV connection criteria in LV distribution networks.

7.2 Solar PV Hosting Capacity Assessment Based on Nomogram Approach

A nomogram is a diagrammatic illustration representing the relationships between an objective function and variables [77]. Nomograms, consisting of different graduated lines or curves representing given variables, are versatile tools for representing solutions for complicated formulae thus providing several advantages. In addition to being a graphical tool, it helps one to visuliase the outcomes of the formulation in the entire solution space impacted by all associated variables. Specific theoretical aspects of general nomogram development are given in Appendix F.

Furthermore, a formula that does not conform with the standard forms must be transformed into a form of the appropriate type before the corresponding nomogram can be designed and constructed.

The deterministic method of solar PV HC assessment which was presented in Section 5.3 is formulated as the objective function of the problem, aiming at calculation of maximum solar PV capacity that can be connected to an LV network, subjected to over-voltage constraint. Mathematical formulation of the problem is presented in the following section.

7.2.1 Formulation of the Nomogram for Hosting Capacity Assessment

For the case of unity power factor operation of solar PV inverters which represent majority of the solar PV systems in LV networks, the solar PV HC in the three phases at d distance away from the transformer, with a total feeder length l is given

by (5.12) and reproduced as (7.1):

$$P_{PV} = \frac{V_b^2}{Rd}\left\{(V_{PV} - V_S) + \left(2\lambda - \lambda^2\right)\Delta V\right\} \tag{7.1}$$

where λ is the d/l, V_b is the nominal line-line voltage, R is the line resistance in Ohm per unit length, V_S is the supply voltage at the secondary of the transformer, V_{PV} is the voltage at the POC and ΔV is the total voltage drop caused by the customer load along the feeder.

In order to develop the objective function for nomogram representation, (7.1) is rearranged as given in (7.2) defining three dependent variables; P_{PV}, ΔV and d. Hence, (7.2) represents a formula of a Class-III (see Appendix F for the Class definition of a formula in relation to nomogram approach) comprising the three variables.

$$P_{PV} - (K_1 - K_2 d)\Delta V - \frac{K_3}{d} = 0 \tag{7.2}$$

where $K_1 = \frac{2V_b^2}{Rl*10^3}$, $K_2 = \frac{V_b^2}{Rl^2*10^3}$ and $K_3 = \frac{V_b^2(V_{PV}-V_S)}{R*10^3}$. Here, solar PV capacity is stated in kW while K_1, K_2 and K_3 are constants for a given feeder.

To form the basic determinant for the nomogram, applying the substitutions $x = -P_{PV}$ and $y = -\Delta V$ equations, (7.3), (7.4) and (7.5) can be established:

$$x + P_{PV} = 0 \tag{7.3}$$

$$y + \Delta V = 0 \tag{7.4}$$

$$-x + (K_1 - K_2 d) * y - \frac{K_3}{d} = 0 \tag{7.5}$$

Since, (7.3), (7.4) and (7.5) are simultaneously true, the absolute value of the following determinant is zero.

$$\begin{vmatrix} 1 & 0 & P_{PV} \\ 0 & 1 & \Delta V \\ -1 & (K_1 - K_2 d) & -\frac{K_3}{d} \end{vmatrix} = 0 \tag{7.6}$$

Equation (7.6) can be transformed into the basic determinant form of a nomogram by performing row operations as follows;

$R_1 \leftarrow R_1/P_{PV}$, $R_2 \leftarrow R_2/\Delta V$ and $R_3 \leftarrow R_3 * (-d/K_3)$,

$$\begin{vmatrix} 1/P_{PV} & 0 & 1 \\ 0 & 1/\Delta V & 1 \\ d/K_3 & -(K_1 - K_2 d) * d/K_3 & 1 \end{vmatrix} = 0 \tag{7.7}$$

where, K_1 and K_2 depend on the feeder length, l for a given conductor type. Loci of the variables, P_{PV} and ΔV are two straight lines which are coincident with x-axis and y-axis respectively ($(1/P_{PV}, 0)$ and $(0, 1/\Delta V)$). Locus of the variable, d is a parabola represented in (7.8), which is developed using the $(d/K_3, -(K_1 - K_2 d) * d/K_3)$ co-ordinates.

$$y = K_2 K_3 x^2 - K_1 x \tag{7.8}$$

As K_1 and K_2 depend only on the feeder length for a given conductor (constant R and V_b for a given conductor), a set of curves can be obtained for different feeder lengths as illustrated in Fig. 7.1.

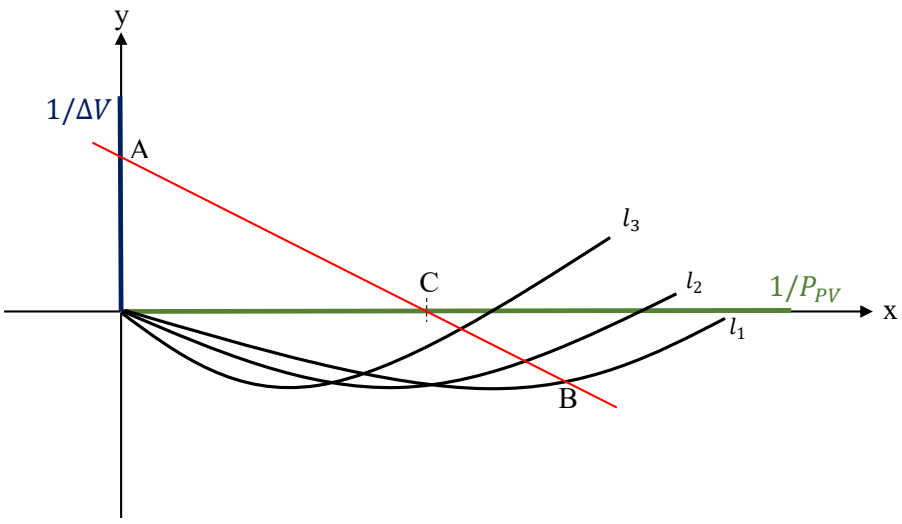

Figure 7.1: Nomogram representation of solar PV HC

When ΔV, l and d are known for a given feeder, solar PV HC, P_{PV} at the

distance of d can be obtained by drawing a straight line connecting the known points; A $(0, 1/\Delta V)$ and B $(d/K_3, -(K_1 - K_2 d) * d/K_3)$ as shown in Fig. 7.1 for a feeder specific length l_1. The intersection of line AB and x-axis; i.e. point C (given in Fig. 7.1) represents the reciprocal of solar PV HC at a distance d from the distribution transformer, $1/P_{PV}$. Thus, Fig. 7.1 can be treated as the complete nomogram for solar PV HC evaluation of a single feeder.

Nomogram gives solutions that are valid for a set of conditions or variables and thus, one can easily visualise the impact of change in one variable or condition on another variable. With regard to the new nomographic tool developed, the loading level, feeder length and the location of the solar PV system are the set of variables applicable to solar PV HC evaluation. Accordingly, Fig. 7.1 can be used to evaluate the solar PV HC for different conditions such as; (a) change of the PV location towards the feeder end, making point C to move to the right along the x-axis resulting lower solar PV HC, (b) increase of the loading level (increase the ΔV) results in movement of point C towards left along x-axis giving higher solar PV HC and (c) change the feeder length makes point C to move depending on the distance to POC resulting higher or lower solar PV HC.

Furthermore, it should be noted that a given nomogram is developed for a specific type of conductor. Types of conductor used in LV distribution networks are limited. A utility needs to have one nomogram for each type of conductor. Therefore, proposed nomogram approach provides a practical tool to meet day-to-day utility requirements.

7.2.2 Solar PV Hosting Capacity Assessment in an LV Distribution Feeder

The proposed nomogram approach for HC assessment was verified using simulations developed in DIgSILENT PowerFactory software for a single feeder distribution test network. The test network consists a 100 kVA, 11kV/0.4kV three phase transformer connected to a 1 km long feeder, as shown in Fig. 7.2 (same model used in Chapter

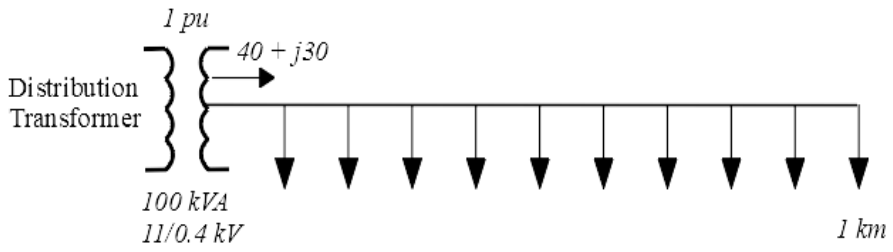

Figure 7.2: Test network for a single distribution feeder

5 (Section 5.3.4) for the validation of deterministic models). The total midday peak demand on the feeder was assumed to be 40 kW and 30 kVAr (P_S and Q_S) (50% of the transformer capacity). The load was assumed to be balanced and uniformly distributed between the 10 nodes along the feeder. Further, the secondary voltage of the transformer, V_S was assumed to be constant at 1 p.u. Three different conductor types; $AAC - Fly$, $ABC - 70\ mm^2$ and $ABC - 50\ mm^2$ were selected for the evaluation of maximum connectable solar PV capacity constrained by the stipulated upper voltage limit of 1.06 p.u. at two different locations; feeder end and middle of the feeder.

Nomograms for HC assessment developed for three types of conductor; $AAC - Fly$, $ABC - 70\ mm^2$ and $ABC - 50\ mm^2$ and shown in Figs. 7.3, 7.4 and 7.5 respectively.

Nomogram-based solar PV HC evaluation procedure at the feeder end and middle for the test network can be described using following steps. The evaluation procedure is explained referring to Fig. 7.3 - $AAC - Fly$ type conductor, as an example.

- **Step 1:** determine K_1, K_2 and K_3 for a given conductor and a given feeder length
- **Step 2:** - determine points A and B for HC calculation at feeder end of the feeder from known system parameters; ΔV, d and l

  - determine points A and D for HC calculation at feeder middle of the feeder from known system parameters; ΔV, d and l
- **Step 3:** - draw a straight line through the points A and B which locates point

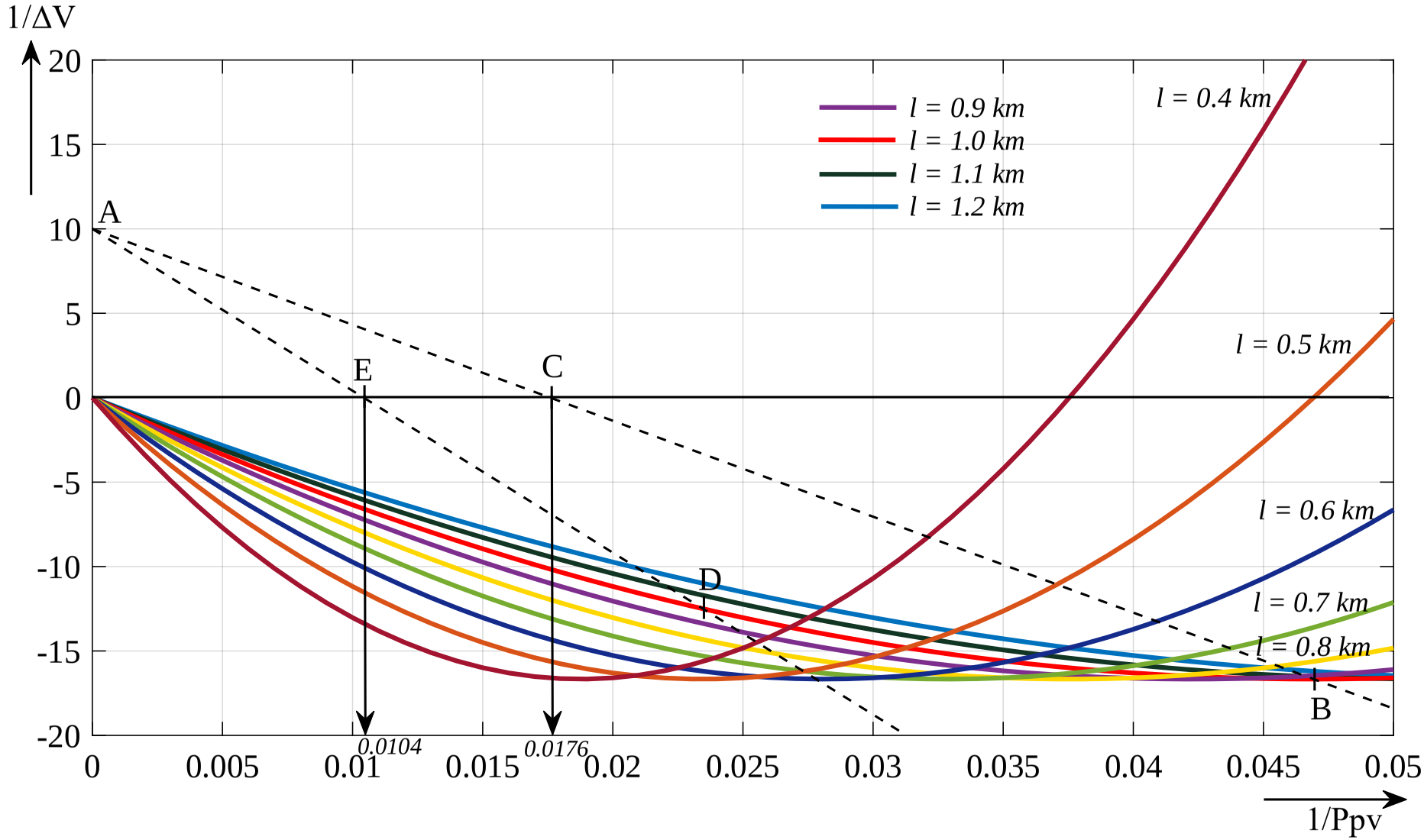

Figure 7.3: Solar PV hosting capacity nomogram for AAC-Fly type feeder

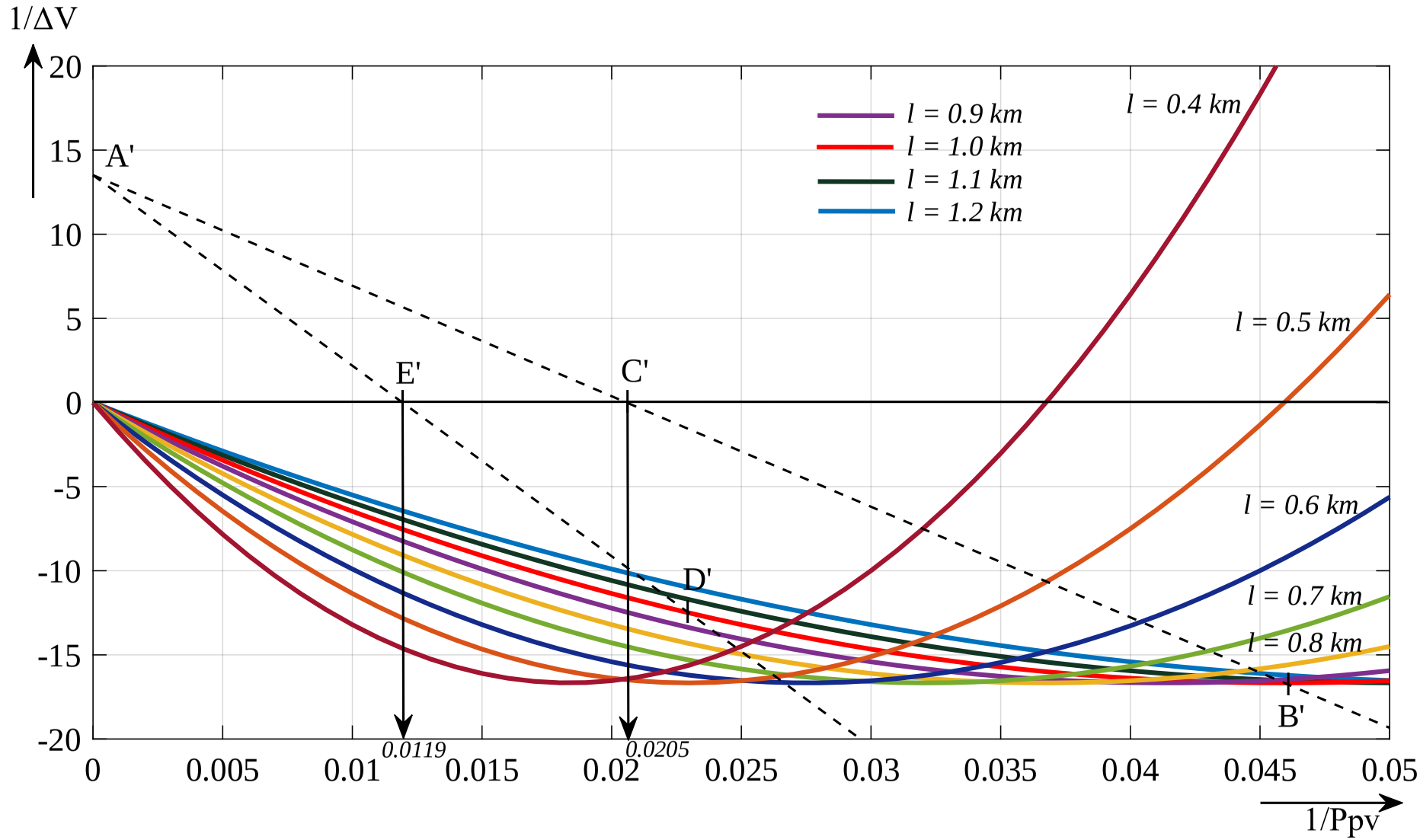

Figure 7.4: Solar PV hosting capacity nomogram for ABC-70 mm^2 type feeder

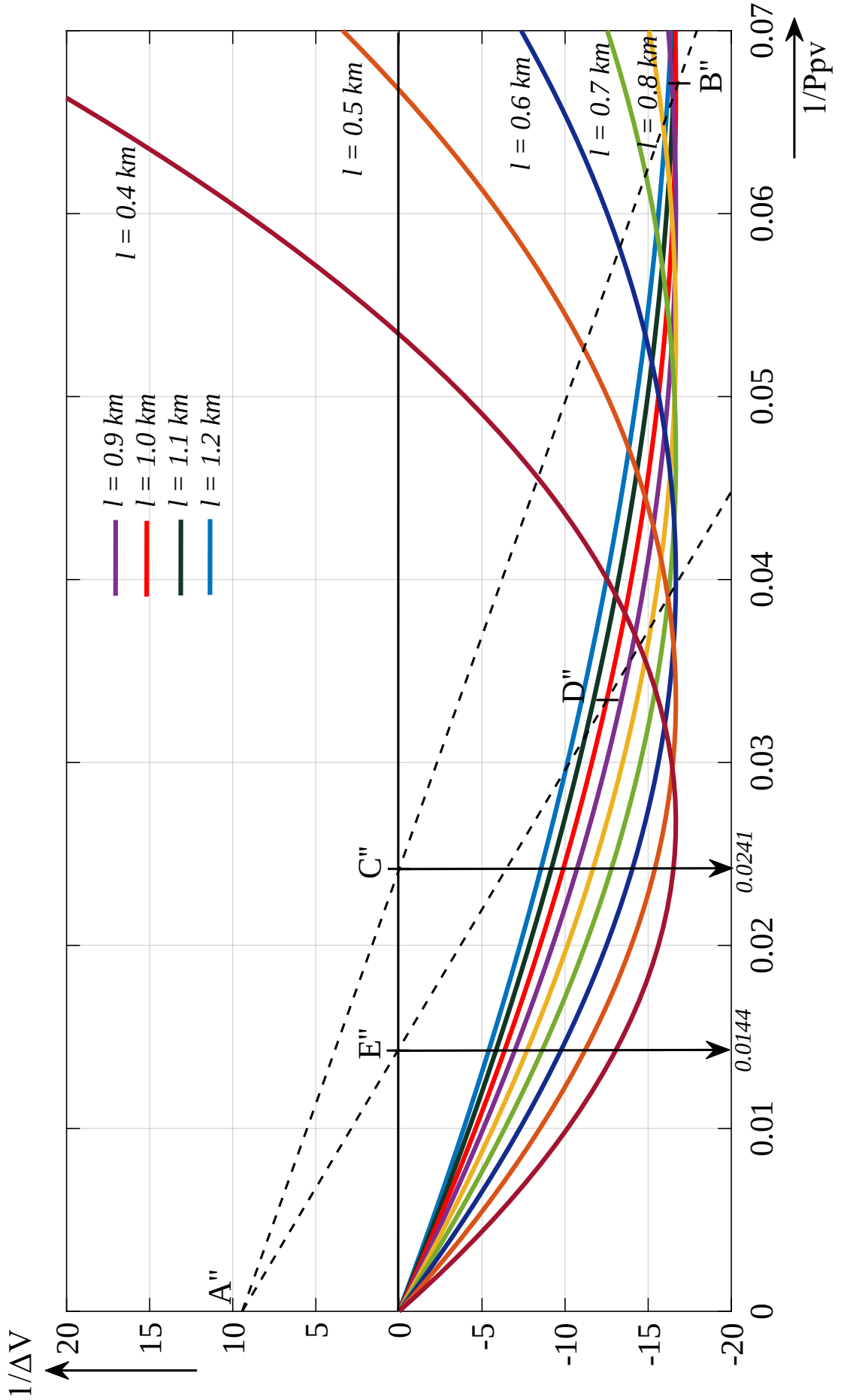

Figure 7.5: Solar PV hosting capacity nomogram for ABC-50 mm^2 type feeder

C, corresponding to the reciprocal of solar PV HC at the feeder end

- draw a line through the points A and D which locates point E, corresponding to the reciprocal of solar PV HC at the feeder middle

Solar PV HC levels obtained from spot simulations in DIgSILENT PowerFactory simulation platform (presented in Section 5.3.4), mathematical model (presented in Section 5.3.4) and nomograms are compared in Tables 7.1 and 7.2 for the three types of conductors. For each feeder, hosting capacity levels relevant to two distinct locations; feeder end and middle of the feeder are evaluated and compared against the mathematical model and the simulations. As shown in the Tables 7.1 and 7.2, solar PV hosting capacities obtained from the simulations and the proposed nomogram method are in close agreement, confirming the validity of the nomogram approach.

Table 7.1: Maximum connectable solar PV capacity at the feeder end

	Simulated (kW)	Deterministic (kW)	Nomogram (kW)
AAC - Fly	58	57	56.8
ABC - 70 mm^2	49	49	48.8
ABC - 50 mm^2	41	41	41.5

Table 7.2: Maximum connectable solar PV capacity at the feeder middle

	Simulated (kW)	Deterministic (kW)	Nomogram (kW)
AAC - Fly	96	96	96.2
ABC - 70 mm^2	84	84	84
ABC - 50 mm^2	69	69	69.4

7.3 A Simplified Solar PV Connection Criteria to Maximise Solar PV Capacity at Feeder Level

The proposed nomogram based HC assessment approach can be utilised effectively to improve the existing solar PV connection guidelines. This approach makes new

solar PV connections in a systematic and versatile manner compared with present utility practices based on rules of thumb. From the perspective of rooftop PV deployment in LV distribution networks, it is quite important to have good integration practices upfront to assure that PV is deployed with the maximum benefit to the community, while maintaining network voltage within stipulated limits. Therefore, the approach proposed in this section provides a straightforward method for new solar PV connections.

7.3.1 Solar PV Hosting Capacity Limits as Defined in Chapter 4

Considering the locational variation of the solar PV systems, two levels of solar PV HC compliant with over-voltage criterion can be identified as the minimum hosting capacity (HC_{min}) and the maximum hosting capacity (HC_{max}), as illustrated in Fig. 7.6 (reproduction of Fig. 4.2(a)).

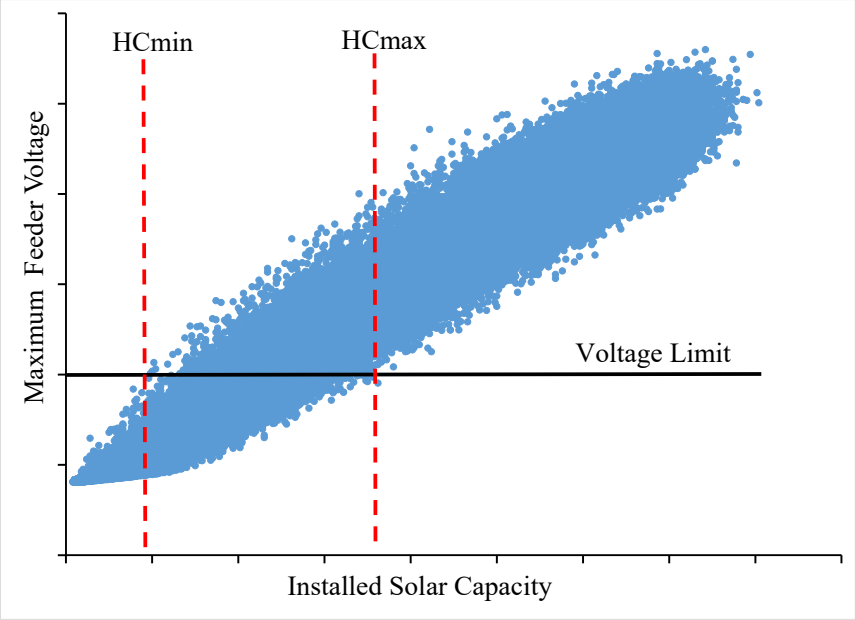

Figure 7.6: Two levels of hosting capacity

With the minimum hosting capacity level, none of the solar penetration levels violate the voltage criterion and solar PV systems can be integrated with the network without any concern on the PV location. Between minimum and maximum hosting

capacity levels, certain solar PV penetration levels arising from random PV locations may violate the network constraints (i.e. over-voltage limit in this context). Therefore, detailed studies are necessary with precise solar PV locations to verify that a given level of penetration is safe. Moreover, solar penetration levels in excess of the maximum hosting capacity limit, independent of the location of the solar installation will violate the relevant operational limits. These minimum and maximum hosting capacity levels can be further defined based on a single distribution feeder or multi-feeder distribution network configurations.

Referring to Section 4.4, for a given feeder, the minimum and maximum solar PV hosting capacities are defined as follows;

- Minimum hosting capacity of a given feeder is the connectable maximum PV capacity at the feeder end and known as the safe limit of hosting capacity (referred to as $HC_{Feeder,Min}$)

- Maximum hosting capacity of a given feeder is the connectable maximum PV capacity at the feeder front (to the transformer) and primarily limited by the thermal over-loading limits of components: eg. feeders and transformer (referred to as $HC_{Feeder,Max}$)

Furthermore, the minimum solar PV HC of a given LV distribution network, HC_{min_LV} is the minimum of the safe limits of each feeder and can be formulated as given in (7.9) - reproduction of (4.1);

$$HC_{min\_LV} = min\left\{HC_{F1\_End}, HC_{F2\_End}, ..., HC_{Fn\_End}\right\} \tag{7.9}$$

where, HC_{Fn_End} is the maximum connectable solar PV capacity at the feeder end of n^{th} feeder (n = 1, 2, 3,. . . . .).

Further, maximum solar PV HC of a given LV distribution network, HC_{max_LV} is the summation of the hosting capacities at the nearest end to the transformer of each feeder and can be formulated as given in the (7.10);

$$HC_{max\_LV} = HC_{F1\_Front} + HC_{F2\_Front} + ... + HC_{Fn\_Front} \tag{7.10}$$

where, HC_{Fn_Front} is the maximum connectable solar PV capacity at the feeder front of n^{th} feeder (n = 1, 2, 3,. . . . .).

Accordingly, solar PV connection criteria for new solar PV systems are developed in the following section, based on a feeder-level HC definition.

7.3.2 Feeder Based Solar PV Connection Criteria for LV Distribution Networks

Proposed solar PV connection criteria comprise of three connection stages where the solar PV HC levels are based on different actions and accordingly classified as Range 1 HC and Range 2 HC. Solar PV HC in Range 1 is evaluated under the conditions of; (a) no operational changes in voltage regulation equipment such as OLTC transformers and capacitor banks, (b) no upgrade of infrastructure/assets such as smart inverters or BESS and (c) no network reinforcements such as upgrade of transformers and feeders. Note that maintaining Range 1 solar PV capacity does not incur any additional cost to network operators. However, network reinforcements, infrastructure/asset upgrades and operational changes in voltage regulation equipment can improve the level of solar PV penetration and the corresponding hosting capacity is referred to as the Range 2 hosting capacity. The extent to which each upgrade could improve the amount of solar PV that can be accommodated in networks varies depending on the network characteristics. However, reaching Range 2 hosting capacity incurs costs for each upgrade. Range 1 hosting capacity is examined in two stages; stage 1 and stage 2 while in stage 3 connection is applicable in Range 2 hosting capacity.

Fig. 7.7 shows an illustrative flowchart for the generalised solar PV connection approval criteria, based on the HC assessment using the nomogram described in Section 7.2. Three stages of solar PV connection criteria are summarised in the

following subsections:

Range 1, Stage 1 Connection Criterion

In stage 1, cumulative solar PV capacity including the new connection is compared with the maximum connectable solar PV capacity at the feeder end which is defined as the safe limit of HC or minimum hosting capacity ($HC_{Feeder,Min}$). Thus, a new solar PV system can be connected anywhere along the feeder without detailed analysis, until the cumulative solar PV capacity (including proposed PV capacity) is equal to the $HC_{Feeder,Min}$ value. If the total solar PV capacity (cumulative solar capacity + proposed solar PV capacity) exceeds the level of $HC_{Feeder,Min}$, new proposed solar PV connection approvals should be evaluated under stage 2.

Stage 1 connection falls into Range 1 hosting capacity where the new solar PV connection does not require any asset upgrades such as smart inverter and BESS.

Range 1, Stage 2 Connection Criterion

In stage 2, the cumulative solar PV capacity including the new solar PV system is compared with the maximum hosting capacity limit ($HC_{Feeder,Max}$) which is defined as the maximum connectable solar capacity at the front of the feeder. The location of the proposed solar PV system and the feeder characteristics including loading level need to be considered in evaluating stage 2 connection.

If, total solar capacity is within $HC_{Feeder,Min}$ and $HC_{Feeder,Max}$, a detailed analysis is required to assess the acceptability of connection of solar PVs based on the nomogram approach proposed in the Section 3 for the given location. If the total solar PV capacity including the new requested value is below the HC level established using the nomogram, the new solar PV connection is approved, otherwise it needs to proceed to stage 3.

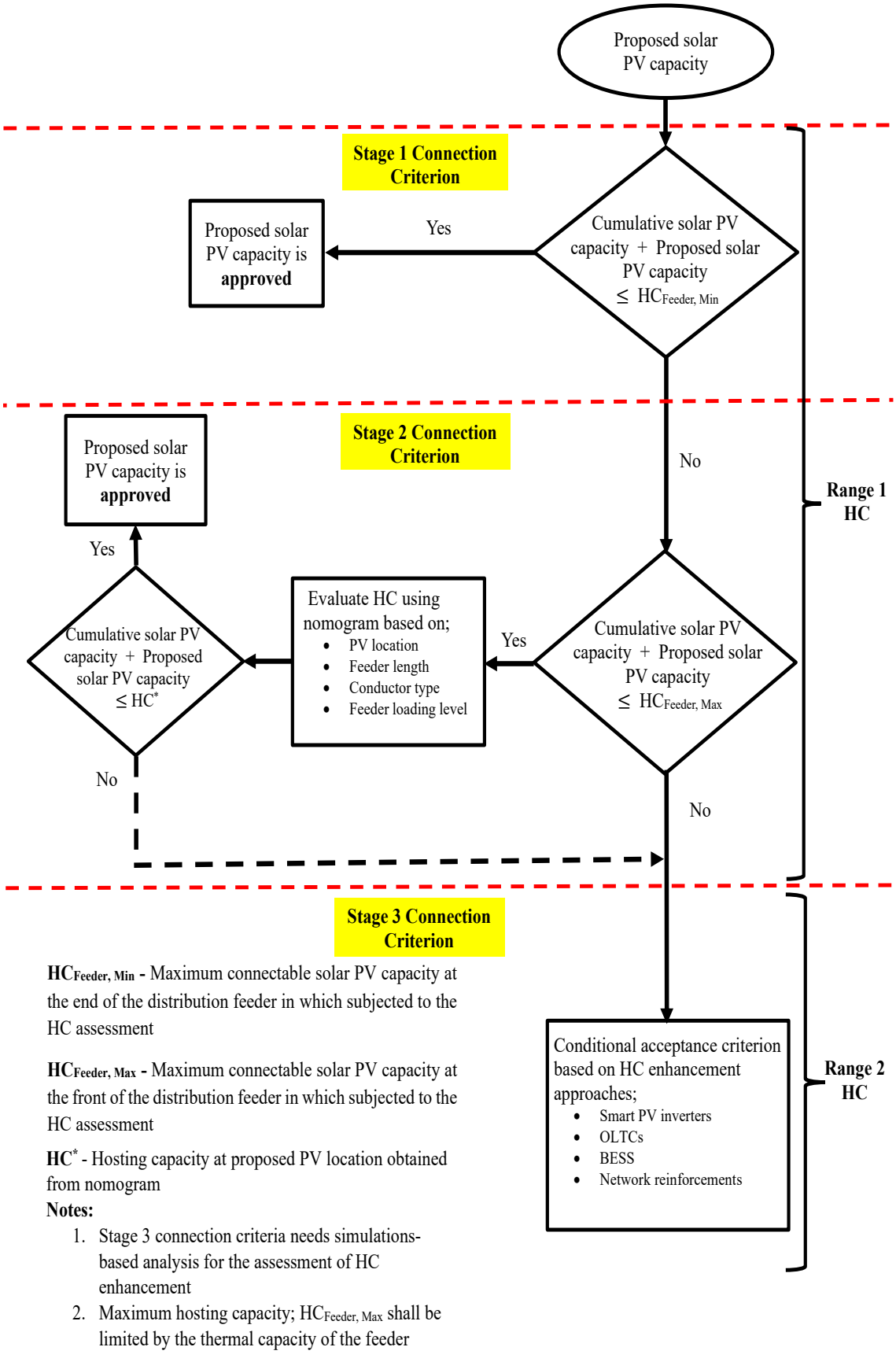

Figure 7.7: Generalised solar PV approval criteria.

Range 2, Stage 3 Connection Criterion

If the total solar PV capacity with new proposal is larger than the $HC_{Feeder,Max}$ value for a given feeder, no further solar PV systems can be connected to the network without taking remedial actions to overcome voltage issues, such as network reinforcements (larger conductors and transformers), smart solar PV inverter technologies for voltage and power control and integration of BESS. In this stage, enhanced solar PV HC can be analysed based on detailed system studies on appropriate simulation platforms with the particular HC enhancement technique proposed.

Range 2 HC can be further divided into two sub stages as Stage 3a and Stage 3b where Stage 3a consists of infrastructure/assets upgrades such as smart inverter or BESS, voltage regulation equipment such as OLTC transformers and capacitor banks. Stage 3b option includes network reinforcements such as upgrade of feeders and transformers. In this regard, cost opptimisation techniques need to be adopted in order to decide on the feasible levels of upgrades together with solar PV HC enhancements.

7.4 Chapter Summary

A nomogram based generalised solar PV HC assessment approach and solar PV connection criteria for LV distribution networks were presented in this chapter. At present, network operators find difficulties in determining the optimum use of existing network assets to maximise the absorption of solar PV generation with existing rules of thumb practices. The nomogram based HC assessment method can be introduced as a versatile decision making tool for distribution network operators and planners to investigate the capability and limitations of solar PV deployment by evaluating the maximum allowable solar PV capacity at a given point along a distribution feeder, constrained by over-voltage limits.

The proposed feeder based solar PV HC evaluation through the nomogram approach can be seen to capture all influential factors on solar PV HC. Thus, the

nomogram can be used as a guide to evaluate solar PV HC at a given point of LV feeders without using complex stochastic techniques and/or deterministic load flow models.

Based on the findings of feeder level solar PV HC analysis, the minimum level of PV hosting capacity (safe limit of the solar PV hosting capacity) and maximum level of PV hosting capacity have been taken as the baseline for connection criteria for new solar PV connections. The proposed criteria equipped with Ranges 1 and 2 hosting capacity limits with/without operational changes/network upgrades of the LV system respectively. From a distribution system planning perspective, the use of a generalised selection approach by means of a nomogram is simple and adoptable in a real-world scenario compared with use of extensive simulations. Furthermore, the proposed systematic approach for HC assessment and PV connection approval contributes to further improvement to guidelines on solar PV installation in LV networks.

Chapter 8

Conclusions and Recommendations for Future Work

8.1 Conclusions

The main thrust of this thesis was to develop significant insights in to the management of solar PV integration in LV distribution networks while enhancing the quality of electric power. Conceptually, this endeavor essentially requires detailed assessment of solar PV HC considering all limiting factors on connectable solar PV capacity. In this regard, the primary focus has been given to the development of a novel feeder based deterministic approach for solar PV HC assessment subjected to over-voltage curtailment. The deterministic methodology can be explicitly used to evaluate the maximum solar PV capacity at a given location of a feeder and accommodates feeder loading conditions and feeder characteristics (conductor types, length of the feeder) as well. Further,the proposed approach can be used as an approximate guide or a rule of thumb to evaluate solar PV HC and provide contributions to further improve the solar PV connection standards/guidelines.

The generalised outcomes and findings of the deterministic approach are used to enhance the understanding of some of the key aspects in solar PV HC enhancement

and solar PV connection criteria. Accordingly, enhancement of solar PV HC is analysed by exploring the potential use of smart PV inverter functions; Volt-VAr and Volt-Watt control strategies in order to mitigate the over-voltage issue. The existing solar connection standards and guidelines were reviewed in order to investigate the level of HC enhancement through different active and reactive power control strategies in mitigating voltage related issues. Further, a nomographic tool for solar PV HC assessment was developed by extending the proposed deterministic approach for unity power factor operating inverters which represent a realistic operating condition applicable to majority of solar PV systems in LV networks. The nomographic tool provides a graphical representation of solar PV HC specific to all locations of a given conductor. Accordingly, solar PV connection criteria are established for the consideration of new solar PV connections in LV networks utilising the nomogram based tool.

The preliminary investigation on solar PV HC assessment was carried out by considering a practical LV distribution network in Sri Lanka which has a 40% solar penetration level based on the distribution transformer capacity. Critical factors affecting on the solar PV HC were investigated with increasing solar penetration levels and local voltage rise (over-voltage situations) was identified as the limiting factor which curtailed solar PV proliferation. Subsequently, well defined stochastic HC assessment approach was used to evaluate solar PV HC of practical LV distribution network following the MCS method. Based on the MCS results, two levels of solar PV hosting capacity; minimum hosting capacity (HC_{min}) and maximum hosting capacity (HC_{max}) compliant with the given performance index, were identified. For the network in consideration, solar PV HC was evaluated considering two performance indices; maximum feeder voltage violations and thermal over-loading the feeder and transformer. MCS results for the practical LV network illustrated that the over-voltage is the most prominent performance index limiting factor.

One of the main objectives of this thesis was to propose a systematic approach to assess solar PV HC of LV distribution networks considering over-voltage curtailment.

This objective was accomplished by developing a novel feeder based solar PV HC assessment approach, giving emphasis to the drawbacks of stochastic approach for HC evaluation. Further, the proposed feeder based solar PV HC assessment approach was developed employing a number of sensitivity analysis; locational variation of PV systems, feeder loading level and feeder characteristics (type of the conductor, feeder length). The proposed approach presented a broader classification on the level of solar PV hosting capacities under the umbrella of HC assessment in single feeder or multi-feeder distribution network levels. Accordingly, the minimum (safe limit of solar PV HC; HC_{min}) and maximum solar PV HC levels (HC_{max}) of a given LV distribution feeder were established as;

- Minimum hosting capacity of a given feeder is the connectable maximum PV capacity at the feeder end and known as safe limit of hosting capacity
- Maximum hosting capacity of a given feeder is the connectable maximum PV capacity at the feeder front (to the transformer) and primarily limited by the thermal over-loading limits of components: eg. feeders and transformer

Further, multi-feeder networks will exhibit different solar PV HC values in individual feeders. Hence, the minimum and maximum solar PV HC of a given LV distribution network were established as;

- Minimum hosting capacity of a given LV distribution network is the minimum of the safe limits of each feeder
- Maximum hosting capacity of a given LV distribution network is the summation of the hosting capacities at the nearest end to the transformer of each feeder and primarily limited by the thermal over-loading limits of components: eg. feeders and transformer

Based on the outcomes of feeder based HC classification, a mathematical formulation on solar PV HC assessment at a given location for over-voltage curtailment was developed. The proposed deterministic approach was developed to evaluate

the solar PV HC under different operating conditions of solar PV inverter; unity power factor and fixed power factor (leading or lagging) operation. Furthermore, the proposed deterministic method for solar PV HC assessment was developed accommodating following uncertainties; PV location and size of PV system, feeder characteristics, demand on the feeder, voltage at the distribution transformer and stipulated voltage limits on the feeder in the distribution network. The accuracy of the proposed deterministic approach was evaluated employing two case studies; the practical LV distribution network (of Sri Lanka) and a simple distribution feeder with the aid of DIgSILENT PowerFactory simulations.

Solar PV HC enhancement techniques were investigated with the use of smart inverter technology which comprises active and reactive power control functions in order to mitigate over-voltage issues. The specific voltage support functions mainly Volt-VAr and Volt-Watt control strategies were investigated in order to address over-voltage violation issue and their impact on HC enhancement. Thus, an aggregated smart PV inverter model with Volt-VAr and Volt-Watt control strategies was developed in DIgSILENT PowerFactory simulation platform. Performance of the novel PV inverter model was investigated to assess the Volt-VAr and Volt-Watt control strategies for grid voltage variations; under-voltage and over-voltage conditions. Further, smart inverter functions and their potential impact on grid performance were tested in a laboratory environment to validate the accuracy of the DIgSILENT based PV inverter model.

Solar connection standards provide a set of guideline and practices associated with smart inverter functions, mainly on Volt-VAr and Volt-Watt control, to mitigate voltage related issues in networks while, power control functions provide different settings as in covered in different standards. Thus, a comparative evaluation of solar PV HC enhancement facilitated by different connection standards was conducted to investigate most appropriate functions and settings to enhance solar PV HC and the favorable approaches to address the issue of voltage violations.

Based on the deterministic approach for solar PV HC assessment of distribution

feeders, a nomogram based solar PV HC assessment method was further developed for PV inverters operating at unity power factor. Further, three stage solar PV connection criteria were developed for consideration of new solar PV connections. In this regard, the proposed nomogram based approach for solar PV HC assessment in LV distribution networks and suggestions for solar PV HC enhancement with smart inverter technology were reviewed. Accordingly, a nomogram based simplified solar PV connection criteria was developed to maximise the grid connected solar PV capacity at distribution feeder level, specifying the selection criteria for different network configurations. The solar PV connection criteria and the nomographic tool developed in this thesis will be beneficial to electricity distribution utilities who at present, have to deal with voltage uncertainties related to the impact of high penetration levels of PV systems. Furthermore, the proposed generalised HC assessment and solar PV connection criteria enable hosting capacity studies to capture and cope with the complexity of network modelling. From a distribution system planning perspective, the use of a generalised selection approach by means of a nomogram is simple and adoptable in real world scenarios compared to the use of extensive simulations. Therefore, distribution network planners can make use of the proposed nomographic tool and connection criteria to maximise connectable solar PV capacity of a given distribution feeder or network. Further, this approach provides a more generalised and straightforward method to assess solar PV HC in LV networks and hence will contribute to further improvements of the available guidelines on solar PV installation in LV networks.

8.2 Recommendations for Future work

Main research outcomes of the thesis include development of a systematic approach to assess solar PV HC in LV distribution networks emphasising on over-voltage curtailment and a three stage solar PV connection criteria. All recommendations provide further improvements to the solar PV connection guidelines and practices. However, further investigations can be carried out to confirm the applicability of the

developed approach in realistic network environments. In particular, influence of other network performance indices such as voltage unbalance, thermal over-loading on solar PV hosting was not considered in the present work and it is worth while to carry out detailed investigations on such aspects.

Further, diverse behavior of the power system; load and PV output (uncertainty in load and solar power generation) for the application of proposed methodologies can be accommodated rather than with snap-shot based evaluations (minimum demand and maximum power generation). Therefore, varying load profiles and solar PV output profiles for data analysis techniques can be adopted to account for the variable nature of the power system. It should be relatively straightforward to incorporate varying loads, such as if all residential customers are following the same profile.

Furthermore, the deterministic approach (work presented in Chapter 4) can be extended to ring type network configurations in order to improve the applicability to all network configurations in practical environments although radial distribution networks are dominant in practice in LV distribution.

The proposed solar PV HC assessment based on nomogram was developed only for the unity power factor operating conditions and can be modified further for leading and lagging operation of solar PV inverters by developing a four variable formulae. It will be one of the most complicated future work which would investigate how to aggregate distributed PV systems with inverter operating power factor. Furthermore, present nomogram tool can be investigated in order to comply with different grid codes introduced by various countries.

The three stage solar PV connection criteria was proposed to approve new solar PV connections considering over-voltage curtailment in LV distribution feeders and further investigation can be carried out to enhance the usability of the connection criteria which can be utilised considering power quality market aspects to revise guidelines and make precise PV connections. Further, similar approaches can be developed in order to accommodate other network performance indices such

as over-loading (feeders and transformers) and voltage unbalance criteria extending the present work which may require extensive investigations to decide under which conditions such parameters become dominant or not. Furthermore, Range 2 HC enhancement options in the three stage solar PV connection criteria can be expanded by considering network reinforcement upgrades with in-depth cost optimisation techniques.

References

[1] Renewables 2021 Global States Report. Technical report, REN21, 2021.

[2] Small Scale Domestic Rooftop Solar Photovoltaic Systems. Technical report, Endeavour Energy, Power Quality & Reliability Centre, University of Wollongong, Australia, 2011.

[3] V. Kumar, A. S. Pandey, and S. K. Sinha. Grid integration and power quality issues of wind and solar energy system: A review. In *2016 International Conference on Emerging Trends in Electrical Electronics Sustainable Energy Systems (ICETEESES)*, pages 71–80, 2016.

[4] Sherif M. Ismael, Shady H.E. [Abdel Aleem], Almoataz Y. Abdelaziz, and Ahmed F. Zobaa. State-of-the-art of hosting capacity in modern power systems with distributed generation. *Renewable Energy*, 130:1002 – 1020, January 2019.

[5] Maryam Hasheminamin, Vassilios Agelidis, Vahid Salehi, Remus Teodorescu, and Branislav Hredzak. Index-based assessment of voltage rise and reverse power flow phenomena in a distribution feeder under high pv penetration. *IEEE Journal of Photovoltaics*, 5:1–11, 07 2015.

[6] Power quality aspects of solar power - JWG C4/C6.29. Technical report, CIGRE, December 2016.

[7] Capacity of Distribution Feeders for Hosting DER - JWG C6.24. Technical report, CIGRE, June 2014.

[8] Math H. J. Bollen and Sarah K. Rönnberg. Hosting capacity of the power grid for renewable electricity production and new large consumption equipment. *Energies*, 10(9):1996–1073, September 2017.

[9] Enock Mulenga, Math Bollen, and Nicholas Etherden. A review of hosting capacity quantification methods for photovoltaics in low-voltage distribution grids. *International Journal of Electrical Power & Energy Systems*, 115.

[10] Stochastic Analysis to Determine Feeder Hosting Capacity for Distributed Solar PV. Technical report, Electric Power Research Institude, December 2012.

[11] N. C. Tang and G. W. Chang. A stochastic approach for determining pv hosting capacity of a distribution feeder considering voltage quality constraints. In *2018 18th International Conference on Harmonics and Quality of Power (ICHQP)*, pages 1–5, 2018.

[12] D. Schwanz, F. Möller, S. K. Rönnberg, J. Meyer, and M. H. J. Bollen. Stochastic assessment of voltage unbalance due to single-phase-connected solar power. *IEEE Transactions on Power Delivery*, 32(2):852–861, April 2017.

[13] S. Jothibasu, D. Anamika, and S. Santoso. Cost of Integrating Distributed Photovoltaic Generation to the Utility Distribution Circuits,. Technical report, The University of Texas at Austin, January 2016.

[14] Samar Fatima, Verner Püvi, and Matti Lehtonen. Review on the pv hosting capacity in distribution networks. *Energies*, 13(18), 2020.

[15] Common Functions for Smart Inverters. Technical report, Electric Power Research Institude, December 2016.

[16] Kelsey A.W. Horowitz, Akshay Jain, Fei Ding, Barry Mather, and Bryan Palmintier. A techno-economic comparison of traditional upgrades, volt-var controls, and coordinated distributed energy resource management systems for integration of distributed photovoltaic resources. *International Journal of Electrical Power & Energy Systems*, 123:106222, 2020.

[17] Analysis of PV Advanced Inverter Functions and Setpoints under Time Series Simulation. Technical report, Sandia National Laboratories,, May 2016.

[18] Mehmet Yilmaz and Ramadan El-Shatshat. State-based volt/var control strategies for active distribution networks. *International Journal of Electrical Power & Energy Systems*, 100:411 – 421, 2018.

[19] Network integration of distributed power generation. *Journal of Power Sources*, 106(1):1 – 9, 2002. Proceedings of the Seventh Grove Fuel Cell Symposium.

[20] DISTRIBUTION CODE OF SRI LANKA. Technical report, Public Utilities Commission of Sri Lanka, 2012.

[21] AS61000.3.100-2011: Electromagnetic compatibility (EMC) - limits - Steady state voltage limits in public electricity systems, Amendment No. 1. Technical report, Australian Standard, December 2011.

[22] AS60038-2012: Standard Voltages, Ed. 2. Technical report, Australian Standard, December 2012.

[23] Masoud Farhoodnea, Azah Mohamed, Hussain Shareef, and Hadi Zayandehroodi. Power quality analysis of grid-connected photovoltaic systems in distribution networks. *Przeglad Elektrotechniczny*, 89:208–213, 01 2013.

[24] M.A. Mahmud, M.J. Hossain, and H.R. Pota. Analysis of voltage rise effect on distribution network with distributed generation. *IFAC Proceedings Volumes*, 44(1):14796 – 14801, 2011. 18th IFAC World Congress.

[25] Reinaldo Tonkoski, Dave Turcotte, and Tarek EL-Fouly. Impact of high pv penetration on voltage profiles in residential neighborhoods. *IEEE Transactions on Sustainable Energy*, 3:518–527, 07 2012.

[26] Ahmed A. Latheef. *Harmonic Impact of Photovoltaic Inverter Systems on Low and Medium Voltage Distribution Systems*. PhD thesis, School of Electrical, Computer and Telecommunucation Engoneering, University of Wollongong, 2006.

[27] D. Martin, S. Goodwin, O. Krause, and T. Saha. The effect of pv on transformer ageing: University of queensland's experience. In *2014 Australasian Universities Power Engineering Conference (AUPEC)*, pages 1–6, 2014.

[28] Farhad Shahnia, Ritwik Majumder, Abhijit Ghosh, Gerard Ledwich, and Firuz Zare. Sensitivity analysis of voltage imbalance in distribution networks with rooftop pvs. pages 1 – 8, 08 2010.

[29] Farhad Shahnia, Ritwik Majumder, Arindam Ghosh, Gerard Ledwich, and Firuz Zare. Voltage imbalance analysis in residential low voltage distribution networks with rooftop pvs. *Lancet*, 81:1805–1814, 09 2011.

[30] Farhad Shahnia. *Analysis and Correction of Voltage Profile in Low Voltage Distribution Networks Containing Photovoltaic Cells and Electric Vehicals*. PhD thesis, School of Engineering Systems, Queensland University of Technology, Queensland, Australia, August 2011.

[31] Farhad Shahnia, Arindam Ghosh, Gerard Ledwich, and Firuz Zare. Voltage unbalance improvement in low voltage residential feeders with rooftop pvs using custom power devices. *International Journal of Electrical Power & Energy Systems*, 55:362–377, 02 2014.

[32] Md Moktadir Rahman, Ali Arefi, G.M. Shafiullah, and Sujeewa Hettiwatte. A new approach to voltage management in unbalanced low voltage networks using demand response and oltc considering consumer preference. *International Journal of Electrical Power & Energy Systems*, 99:11–27, 2018.

[33] Busra Uzum, Ahmet Onen, Hany M. Hasanien, and S. M. Muyeen. Rooftop solar pv penetration impacts on distribution network and further growth factors—a comprehensive review. *Electronics*, 10(1), 2021.

[34] Elizabeth Begumisa Liwanga Namangolwa. *Impacts of Solar Photovoltaic on the Protection System of Distribution Networks: A case of the CIGRE low voltage network and a typical medium voltage distribution network in Sweden*. PhD

thesis, Department of Energy and Environment, CHALMERS UNIVERSITY OF TECHNOLOGY, Gothenburg, Sweden, 2016.

[35] Martin Lindner Ammar Arshad and Matti Lehtonen. An analysis of photovoltaic hosting capacity in finnish low voltage distribution networks. *Energies, MDPI, Open Access Journal*, 10(11), 2017.

[36] T. Stetz, F. Marten, and M. Braun. Improved low voltage grid-integration of photovoltaic systems in germany. *IEEE Transactions on Sustainable Energy*, 4(2):534–542, 2013.

[37] H. V. Haghi, Z. Pecenak, J. Kleissl, J. Peppanen, M. Rylander, A. Renjit, and S. Coley. Feeder impact assessment of smart inverter settings to support high pv penetration in california. In *2019 IEEE Power Energy Society General Meeting (PESGM)*, pages 1–5, 2019.

[38] M. J. E. Alam, K. M. Muttaqi, and D. Sutanto. Community energy storage for neutral voltage rise mitigation in four-wire multigrounded lv feeders with unbalanced solar pv allocation. *IEEE Transactions on Smart Grid*, 6(6):2845–2855, 2015.

[39] Network Power Quality Limits and Levels, Amendment No. 0. Technical report, Endeavour Energy, 2015.

[40] Kalpesh Joshi and Ramakrishna Gokaraju. An iterative approach to improve pv hosting capacity for a remote community. 08 2018.

[41] Mohammad Zain ul Abideen, Omar Ellabban, and Luluwah Al-Fagih. A review of the tools and methods for distribution networks' hosting capacity calculation. *Energies*, 13(11), 2020.

[42] Jeremy Watson, Neville Watson, David Santos-Martin, Alan Wood, Scott Lemon, and Allan Miller. Impact of solar photovoltaics on the low-voltage

distribution network in new zealand. *IET Generation Transmission & Distribution*, 10, 10 2015.

[43] Y. Liu, Y. Tai, C. Huang, H. Su, P. Lan, and M. Hsieh. Assessment of the pv hosting capacity for the medium-voltage 11.4 kv distribution feeder. In *2018 IEEE International Conference on Applied System Invention (ICASI)*, pages 381–384, 2018.

[44] R. Torquato, D. Salles, C. Oriente Pereira, P. C. M. Meira, and W. Freitas. A comprehensive assessment of pv hosting capacity on low-voltage distribution systems. *IEEE Transactions on Power Delivery*, 33(2):1002–1012, 2018.

[45] M. Rossi, G. Viganò, D. Moneta, and D. Clerici. Stochastic evaluation of distribution network hosting capacity: Evaluation of the benefits introduced by smart grid technology. In *2017 AEIT International Annual Conference*, pages 1–6, 2017.

[46] S. Elsaiah, M. Benidris, and J. Mitra. An analytical method for placement and sizing of distributed generation on distribution systems. In *2014 Clemson University Power Systems Conference*, pages 1–7, 2014.

[47] Shixiong Fan, Chen Li, Zechen Wei, Tianjiao Pu, and Xingwei Liu. Method to determine the maximum generation capacity of distribution generation in low-voltage distribution feeders. *The Journal of Engineering*, 1, 02 2009.

[48] Simon Heslop, Iain MacGill, and John Fletcher. Maximum pv generation estimation method for residential low voltage feeders. *Sustainable Energy, Grids and Networks*, 7:58–69, 2016.

[49] Michael Emmanuel and Ramesh Rayudu. The impact of single-phase grid-connected distributed photovoltaic systems on the distribution network using p-q and p-v models. *International Journal of Electrical Power & Energy Systems*, 91:20–33, 2017.

[50] R. A. Shayani and M. A. G. de Oliveira. Photovoltaic generation penetration limits in radial distribution systems. *IEEE Transactions on Power Systems*, 26(3):1625–1631, 2011.

[51] M. Vandenbergh, R. Hermes, V. Helmbrecht, H. Loew, and D. Craciun. Technical solutions supporting the large scale integration of photovoltaic systems in the future distribution grids. In *22nd International Conference and Exhibition on Electricity Distribution (CIRED 2013)*, pages 1–4, 2013.

[52] F. Ding and B. Mather. On distributed pv hosting capacity estimation, sensitivity study, and improvement. *IEEE Transactions on Sustainable Energy*, 8(3):1010–1020, 2017.

[53] S. M. Ismael, S. H. E. Abdel Aleem, A. Y. Abdelaziz, and A. F. Zobaa. Practical considerations for optimal conductor reinforcement and hosting capacity enhancement in radial distribution systems. *IEEE Access*, 6:27268–27277, 2018.

[54] D. E. Mawarni, M. M. V. M. Ali, P. H. Nguyen, W. L. Kling, and M. Jerele. A case study of using oltc to mitigate overvoltage in a rural european low voltage network. In *2015 50th International Universities Power Engineering Conference (UPEC)*, pages 1–5, 2015.

[55] A. Arshad and M. Lehtonen. A stochastic assessment of pv hosting capacity enhancement in distribution network utilizing voltage support techniques. *IEEE Access*, 7:46461–46471, 2019.

[56] A. T. Procopiou and L. F. Ochoa. Voltage control in pv-rich lv networks without remote monitoring. *IEEE Transactions on Power Systems*, 32(2):1224–1236, 2017.

[57] T. S. Ustun, J. Hashimoto, and K. Otani. Impact of smart inverters on feeder hosting capacity of distribution networks. *IEEE Access*, 7:163526–163536, 2019.

[58] Y. Xue, M. Starke, J. Dong, M. Olama, T. Kuruganti, J. Taft, and M. Shankar. On a future for smart inverters with integrated system functions. In *2018 9th IEEE International Symposium on Power Electronics for Distributed Generation Systems (PEDG)*, pages 1–8, 2018.

[59] Raeey A. Regassa. *IMPACT OF INCREASING AMOUNTS OF DISTRIBUTED GENERATION ON TRANSIENT BEHAVIOR OF THE DISTRIBUTION SYSTEM.* PhD thesis, Electrical and Computer Engineering, Georgia Institute of Technology, May 2017.

[60] Ahmed M.M. Nour, Ahmed A. Helal, Magdi M. El-Saadawi, and Ahmed Y. Hatata. A control scheme for voltage unbalance mitigation in distribution network with rooftop pv systems based on distributed batteries. *International Journal of Electrical Power & Energy Systems*, 124:106375, 2021.

[61] Ahmed Nour, Ahmed Hatata, Ahmed Helal, and Magdi El-Saadawi. A review on voltage violation mitigation techniques of distribution networks with distributed rooftop photovoltaic systems. *IET Generation, Transmission & Distribution*, 14, 11 2019.

[62] B. Wang, C. Zhang, K. Meng, B. Liu, Z. Dong, P. K. C. Wong, T. Ting, and Q. Qi. Improving hosting capacity of unbalanced distribution networks via battery energy storage systems. In *2019 IEEE PES Asia-Pacific Power and Energy Engineering Conference (APPEEC)*, pages 1–5, 2019.

[63] Priyanka Chaudhary and M. Rizwan. Voltage regulation mitigation techniques in distribution system with high pv penetration: A review. *Renewable and Sustainable Energy Reviews*, 82:3279–3287, 2018.

[64] N. Altin. Energy storage systems and power system stability. In *2016 International Smart Grid Workshop and Certificate Program (ISGWCP)*, pages 1–7, 2016.

[65] Fei Ge, Bin Ye, Xuli Wang, Zhuang Cai, Lei Dai, and Bin Hu. Technical and economic feasibility of applying battery energy storage for enabling voltage stability of grid-connected photovoltaic power systems. 01 2018.

[66] IEEE Standard for Interconnection and Interoperability of Distributed Energy Resources with Associated Electric Power Systems Interfaces, Revision of IEEE Std 1547-2003 . Technical report, Institute of Electrical and Electronics Engineers, 2018.

[67] AS/NZS 4777.2.2015 Standard for Grid connection of energy systems via inverters inverter requirements . Technical report, Institute of Electrical and Electronics Engineers, 2015.

[68] IEEE 2030.5 Common California IOU Rule 21 Implementation Guide for Smart Inverters . Technical report, Institute of Electrical and Electronics Engineers, 2016.

[69] Rule No. 14 - Distributed Generating Facility Interconnection Standards Technical Requirements - Revised Sheet No. 34B-1. Technical report, Hawaii Electricity Company, 2011.

[70] IEEE Std 1547-2003 - Standard for Interconnection and Interoperability of Distributed Energy Resources with Associated Electric Power Systems Interfaces. Technical report, Institute of Electrical and Electronics Engineers, 2003.

[71] Solar and Wind Energy Resource Assessment (SWERA) - High Resolution Solar Radiation Assessment for Sri Lanka . Technical report, Deutsches Zentrum für Luft- und Raumfahrt e.V., October 2004.

[72] J. Fiorelli and M.Z. Martinson. How oversizing your array-to-inverter ratio can improve solar-power system performancel. In *Solectria Renewables Contributors*, July 2013.

[73] W. H. Kersting. *Distribution System Modelling and Analysis*. Taylor and Francis Group, third edition, 2012.

[74] J. F. B. Sousa, C. L. T. Borges, and J. Mitra. Pv hosting capacity of lv distribution networks using smart inverters and storage systems: a practical margin. *IET Renewable Power Generation*, 14(8):1332–1339, 2020.

[75] Farhan Mahmood. *Improving the Photovoltaic Model in PowerFactory*. PhD thesis, Electrical Engineering, Royal Institute of Technology, Stockholm, Sweden, March 2012.

[76] Smart Grid Inverters to Support Photovoltaic in New York Distribution Systems. Technical report, Electric Power Research Institude, April 2015.

[77] Reginald J Allcock J and J. G. L. Michel. *The Nomogram: The Theory and Practical Construction of Computation Charts*. Sir Isaac Pitman & Sons Ltd, fifth edition, 1963.

Appendix A

Solar PV Hosting Capacity Analysis Using Monte Carlo Simulation: Case 2 Results (Section 4.3.1)

Results obtained from MCS for Case 2 scenario; 40% of total load allocated to feeder 1 and the remaining (60%) to feeder 2 are given in Fig. A.1 and Fig. A.2 with regard to over-voltage and feeder over-loading criteria respectively.

The limit for over-voltage exceedance is 1.06 p.u. and the acceptable feeder loading limit is considered to be 100% of the thermal loading of the conductor.

To be complied with HC constraints limits; feeder over-voltage and over-loading, minimum (HC_{min}) and maximum (HC_{max}) hosting capacity levels for considered scenarios must not violate HC limits of each constraint as illustrated in Fig. A.3. Here, HC_{min} and HC_{max} are defined as the HC levels where 0% and 100% of violation of penetration limits under the given constraint respectively. Thus, the minimum hosting capacity of a given segment is the maximum connectable solar capacity at 0% of constraint limit violation and the maximum hosting capacity is the maximum connectable solar capacity at 100% of constraint limit violation.

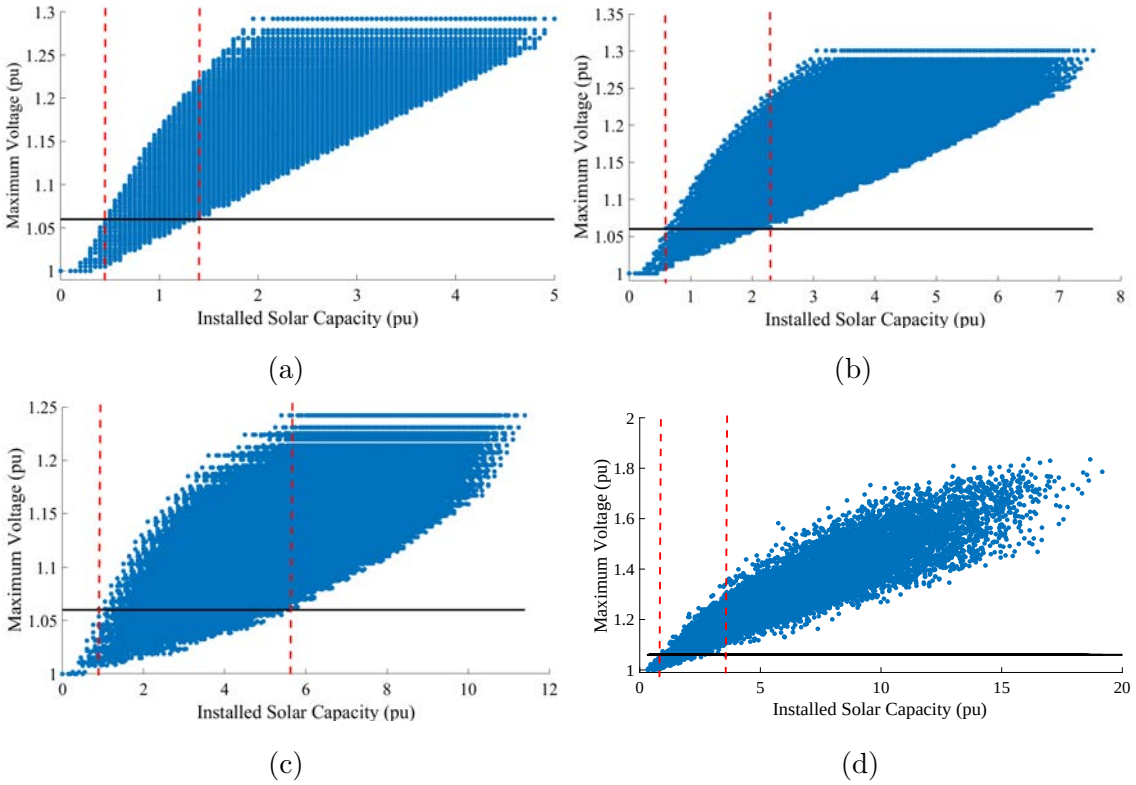

Figure A.1: Variation of segment wise hosting capacity levels for over-voltage criterion; Case 2, Solar PVs are distributed in; (a) Feeder end segment (b) Feeder middle segment (c) Feeder front segment (d) Over all segments of the feeder

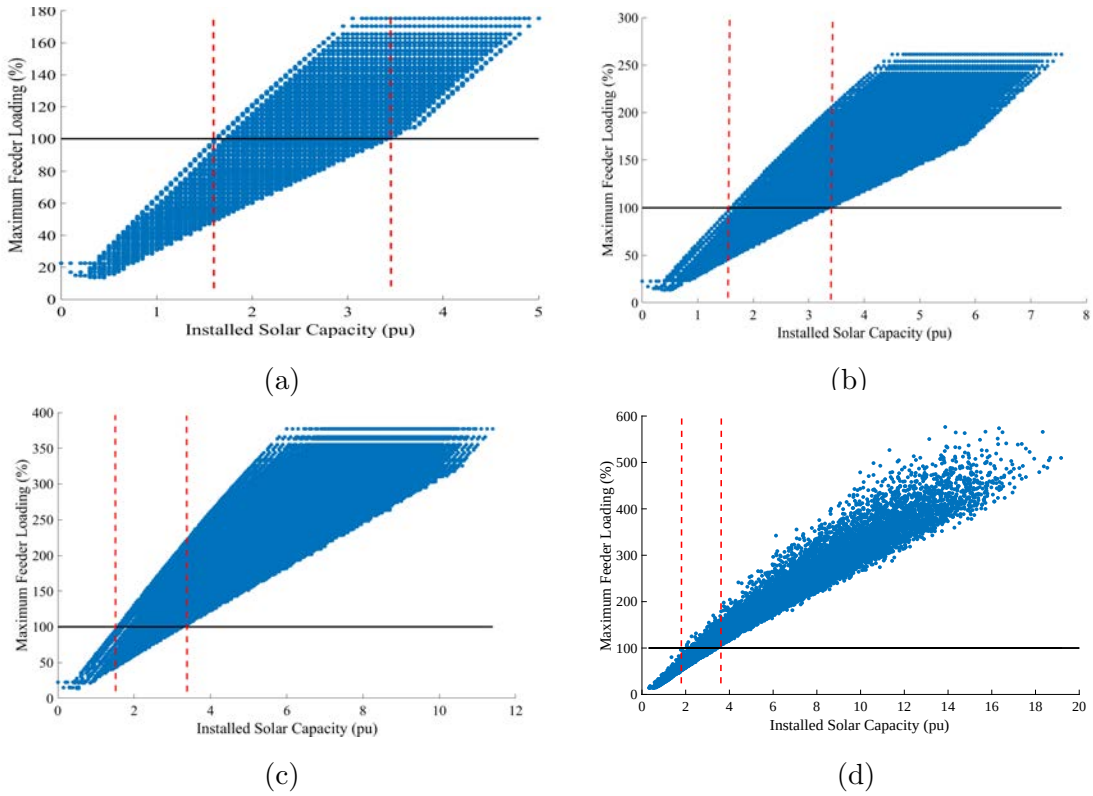

Figure A.2: Variation of segment wise hosting capacity levels for feeder over-loading criterion; Case 2, solar PVs are distributed in; (a) Feeder end segment (b) Feeder middle segment (c) Feeder front segment (d) Over all segments of the feeder

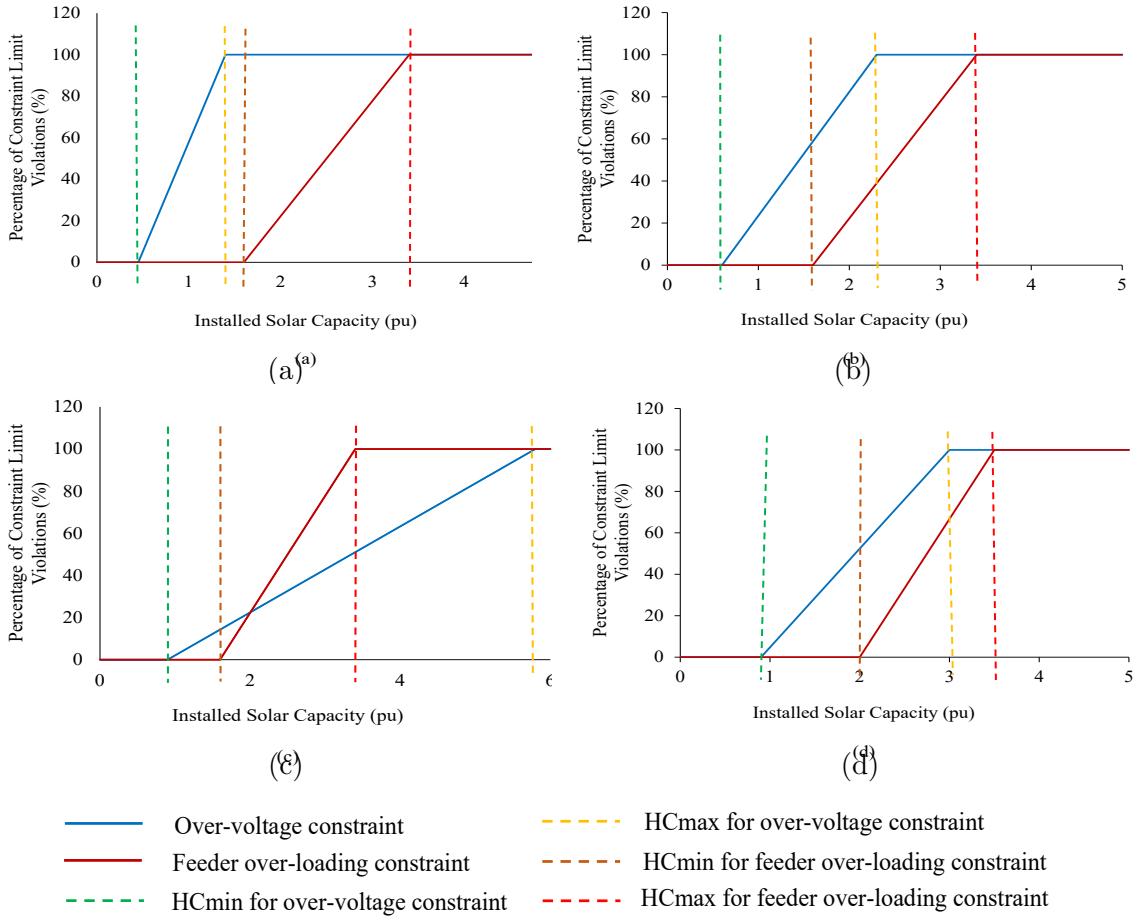

Figure A.3: Segment wise minimum and maximum hosting capacity levels; Case 2, Solar PVs are distributed in; (a) Feeder end segment (b) Feeder middle segment (c) Feeder front segment (d) Over all segments of the feeder

Appendix B

Theoretical Basis for the Characteristic Curve of Voltage Angle Deviation; θ and Solar PV Capacity; P_{PV}

Simplified single distribution feeder network shown in Fig. B.1 (regenerated distribution feeder model using Fig. 5.6) was used to investigate the voltage angle deviation with solar PV connection. In order to the comply with the mathematical model in (5.5) (presented in Section 5.3), uniformly distributed load model can be interpreted in two ways. The first is to recognise that the distributed load of the feeder can be lumped at the midpoint of the feeder and the second interpretation of (5.5) is to lump one-half of the total load at the end of the feeder. In the modelling exercise in this section, one-half of lumped load at feeder end was selected.

P_S and Q_S are real and reactive total power demand of the uniformly distributed load which result a net current I_L flow in the feeder. The resistance and reactance of the feeder are R and X in Ohm per unit length respectively and the shunt capacitance is neglected. V_S is the supply voltage at the secondary of the transformer and l is the total length of the feeder.

Fig. B.2 shows the variation of voltage and current phasors when solar PV system is operating at lagging power factor. If the PV inverter is operating at a lagging power factor of pf_{pv}, reactive power Q_{PV} is absorbed from the upstream grid resulting in a net current I_{PV} from PV system. Here, θ is the angle deviation which arise as a result of the solar PV connection with respect to the supply end voltage. I_p is the active current component and I_q is the reactive current component of the net current flow in the feeder, I_S ($\vec{I_S} = \vec{I_L} + \vec{I_{PV}}$).

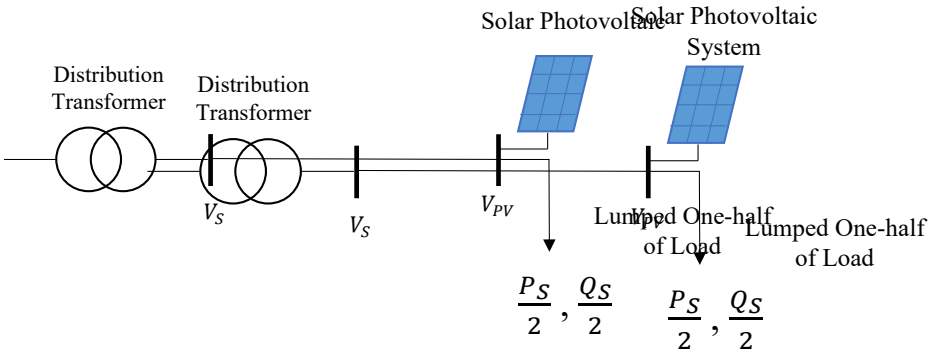

Figure B.1: Simplified distribution feeder model

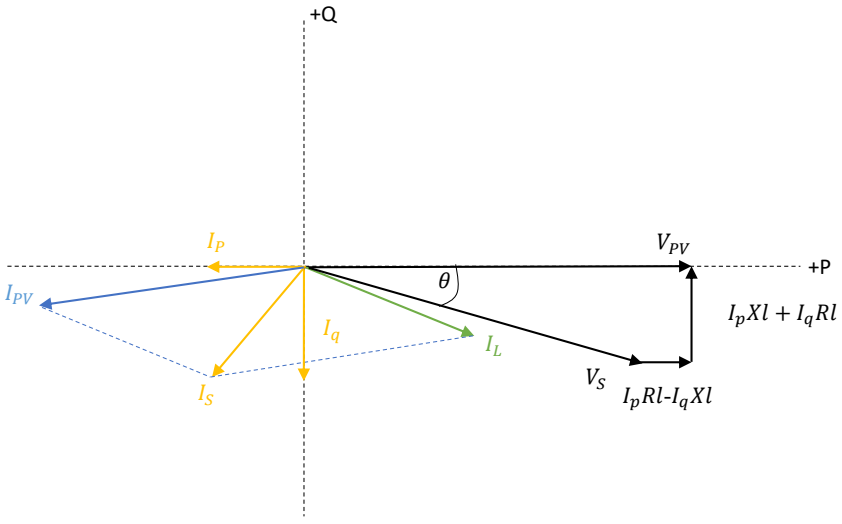

Figure B.2: Current and voltage phasor diagrams for a distribution feeder with solar PVs; Solar PV inverter operating at lagging power factor

Referring to Fig. B.2, (B.1) and (B.2) can be formulated.

$$V_{PV} - V_S con\theta = I_p Rl - I_q Xl \tag{B.1}$$

$$V_S sin\theta = -I_p Xl - I_q Rl \tag{B.2}$$

Real and imaginary current components (I_p and I_q are in p.u.) of the resulting current can be formulated as (B.3):

$$I_p + jI_q = \frac{P_S/2 - jQ_S/2}{V_b^2} + \frac{-P_{PV} - jQ_{PV}}{V_b^2}$$

$$I_p + jI_q = \frac{P_S/2 - P_{PV}}{V_b^2} + j\frac{-Q_S/2 - Q_{PV}}{V_b^2} \tag{B.3}$$

From (B.2) and (B.3), voltage angle deviation can be obtained as in (B.4).

$$sin\theta = \frac{P_{PV}Xl + Q_{PV}Rl}{V_b^2 V_S} - \frac{P_S Xl - Q_S Rl}{2V_b^2 V_S}$$

$$sin\theta = \left(\frac{P_{PV}l(X + Rtan(cos^{-1}pf_{pv}))}{V_b^2 V_S}\right) - \left(\frac{P_S Xl - Q_S Rl}{2V_b^2 V_S}\right) \tag{B.4}$$

where, $Q_{PV} = P_{PV}tan(cos^{-1}pf_{pv})$. The angle deviation which arise as a result of the initial load can be neglected and hence the resultant voltage angle deviation that arise as a result of the solar connection at the feeder end can be simplified as,

$$\theta = sin^{-1}\left(\frac{P_{PV}l(X + Rtan(cos^{-1}pf_{pv}))}{V_b^2 V_S}\right) \tag{B.5}$$

Further, the voltage angle deviation at a given location of POC (at a distance d from the distribution transformer) can be obtained using (B.6)

$$\theta = sin^{-1}\left(\frac{P_{PV}d(X + Rtan(cos^{-1}pf_{pv}))}{V_b^2 V_S}\right) \tag{B.6}$$

Accordingly, the maximum connectable solar PV capacity at a distance d from distribution transformer can be formulated as in (B.7).

$$P_{PV} = \frac{V_b^2}{d\left(R - X\tan\left(\cos^{-1}\left(pf_{pv}\right)\right)\right)}\left\{\left(V_{PV} - V_S cos\theta\right) + \left(2\lambda - \lambda^2\right)\Delta V\right\} \tag{B.7}$$

where, V_{PV} is the voltage at solar PV terminal which will be the magnitude of voltage upper limit for maximum connectable solar PV analysis. λ is the ratio of

location of POC to feeder length, d/l, and ΔV is the approximate voltage drop associated with the initial load. Here, V_{PV}, V_S and ΔV are in p.u.

Appendix C

Parameters Used for the Solar PV Inverter Model

This PV system is designed mainly based on the data given in Tables C.1, C.2 and C.3.

Table C.1: PV system parameters

System components	Value
PV system	
Static generator	0.18 MVA
DC side voltage of PV	0.7 kV
LV terminal AC voltage	0.4 kV
MV bus terminal AC voltage	11 kV
Transformer	
Transformer, Nominal power	0.25 MVA
Transformer, Voltage ratio	0.4 kV/11 kV
Transformer, Vector group	Dyn0
Transformer, Impedance	4%
Distribution network	
Feeder length	100 m
Feeder type	AAC-Fly (All Aluminum Conductor)
Resistance per km	0.4505 Ω
Reactance per km	0.292 Ω

Table C.2: Solar PV module parameters [75]

Parameters	Value
Time constant, T	0.05 s
Short circuit current per module	5 A
Short circuit voltage per module	43.8 V
Current at MPP	4.58 A
Voltage at MPP	35 V
Reference Temperature, T_{ref}	25 C
Irradiance at STC	1000 W/m^2
Number of serial modules	20
Number of parallel modules	56

Table C.3: DC busbar and capacitor parameters [75]

Parameters	Value
Capacitance	0.0172 F
Initial DC voltage	700 V
Nominal DC voltage	1 p.u.
Rated power	0.2 MVA

Appendix D

Smart PV Inverter Model Validation with Laboratory Experiments

SMA Sunny Boy 5000TL (5 kW, single phase) inverter was used to validate the DIgSILENT PowerFactory solar PV inverter model. Inverter was tested for both Volt-VAr and Volt-Watt droop characteristics for two different DNSP settings; Victorian DNSP and NSW DNSP as given in Tables D.1 and D.2 respectively.

Inverter test module was directly connected to a programmable source which can be used as the external grid and has the capability to either absorb or inject active and reactive power as required.

Table D.1: Victorian DNSP: Example settings for Volt-VAr and Volt-Watt characteristics

Volt-VAr controller		Volt-Watt controller	
Voltage (V)	Q/Qrated (%)	Voltage (V)	P/Prated (%)
208	+44	207	100
220	0	220	100
241	0	253	100
253	-44	259	20

Table D.2: NSW DNSP: Example settings for Volt-VAr and Volt-Watt characteristics

Volt-VAr controller		Volt-Watt controller	
Voltage (V)	Q/Qrated (%)	Voltage (V)	P/Prated (%)
207	+60	207	100
220	0	220	100
248	0	255	100
260	-60	265	20

D.0.1 Test Procedure

SMA Sunny Boy inverter could only be operated at 3.25 kW due to practical constraints (although inverter was set to operate at unity power factor, it absorbed considerably lower reactive power, 0.25 kVAr). The inverter test steps are listed as follows;

- Step 1: Volt-VAr and Volt-Watt responses were adjusted using data manager of the inverter applying both Victorian DNSP and NSW DNSP settings
- Step 2: Voltage at the supply end (programmable source) was manually increased by 5 V. Voltage was increased from 205V to 260V and measured the real power (P) and reactive power (Q) of the inverter
- Step 3: Same procedure was repeated with modelled inverter in DIgSILENT PowerFactory Simulation software
- Step 4: Voltage-reactive power and voltage-active power droop characteristics were reproduced using the measured data and simulations

D.0.2 Experimental Results and PV Inverter Model Validation

Fig. D.1 shows the Volt-VAr and Volt-Watt control characteristic curves generated from both experimental and simulation results. Figs. D.1a and D.1c show the comparison of characteristic curves corresponding to Victorian DNSP settings while

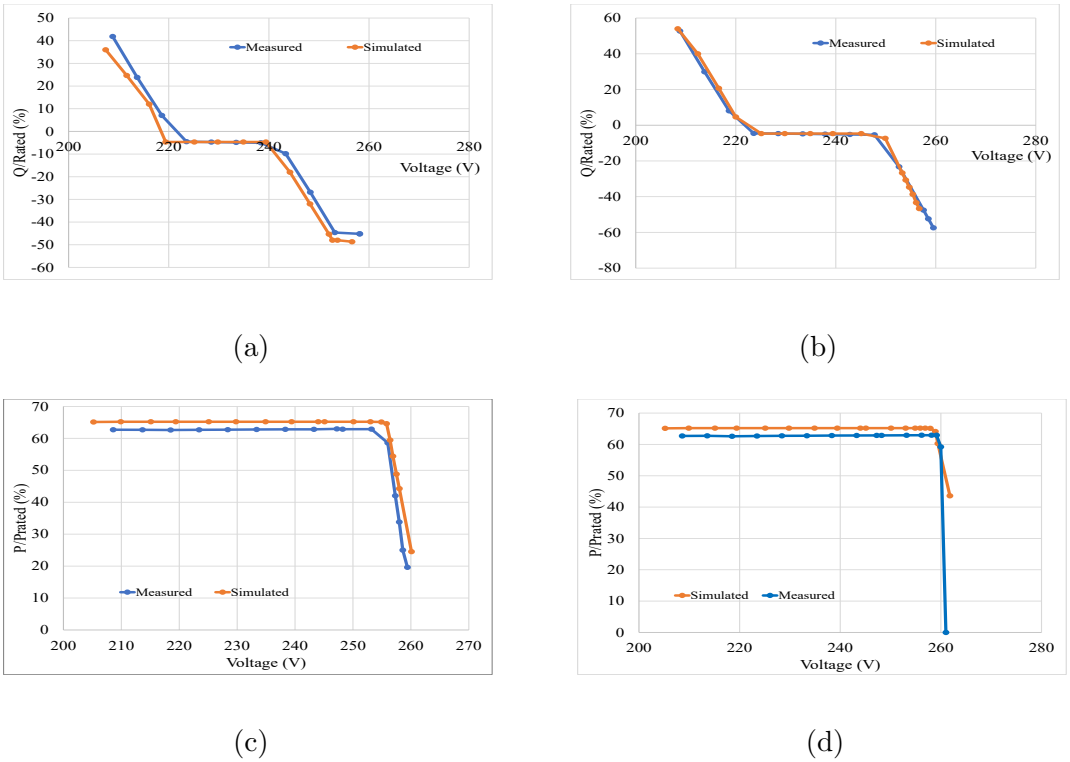

Figure D.1: Comparison of simulated and measured Q(V) and P(V) curves (a) Volt-VAr controller with Victorian DNSP settings (b) Volt-VAr controller with NSW DNSP settings (c) Volt-Watt controller with Victorian DNSP settings (d) Volt-Watt controller with NSW DNSP settings

Figs. D.1b and D.1d illustrate the comparison of characteristic curves corresponding to NSW DNSP settings. A lack of agreement is seen in the case of Victorian settings for Volt-VAr control function. However, with the NSW DNSP setting for the same control characteristic; simulations results were in good agreement with the measurements.

A comparison between simulation results and the experimental results has shown reasonable similarity associated with both control function characteristics. This implies that the PV inverter model developed in DIgSILENT PowerFactory has acceptable accuracy and can be used for further development of tools from a distributed network analysis perspective.

Appendix E

Solar PV Connection Standards: Volt-VAr and Volt-Watt Control Function Settings

Example voltage-reactive power and voltage-active power characteristics are shown in Figs. E.1 and E.2 respectively. The voltage-reactive power and voltage-active power characteristics will be configured in accordance with the default parameter values specified in Tables E.1, E.2, E.3, E.4, E.5, E.6, E.7 and E.7 for IEEE 1547-2018, AS/NZS 4777-2015, California Rule 21 and Hawaii Rule 14 standards respectively.

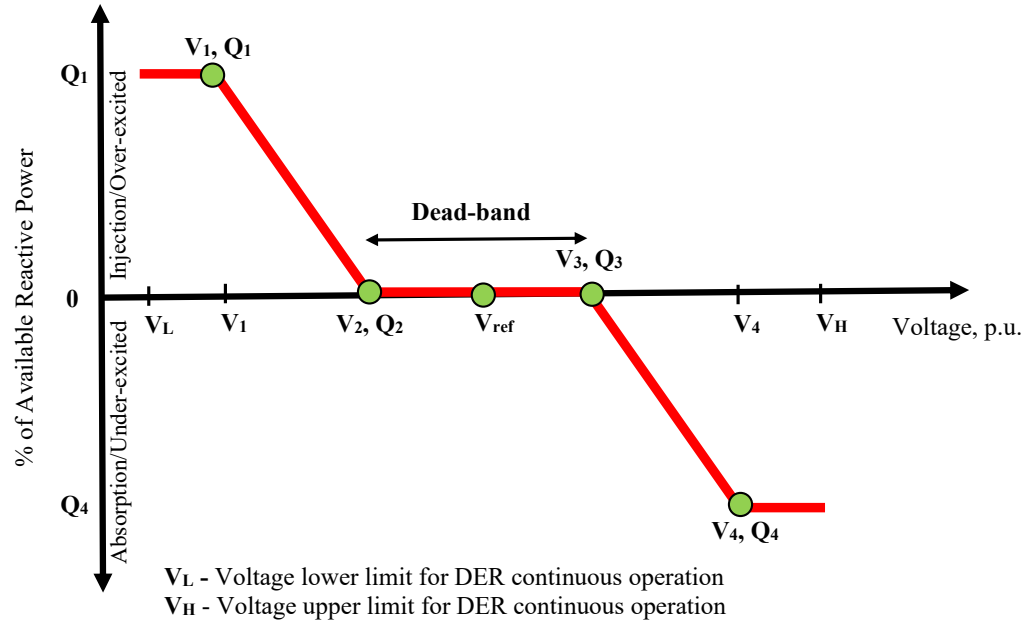

Figure E.1: Example voltage-reactive power characteristic

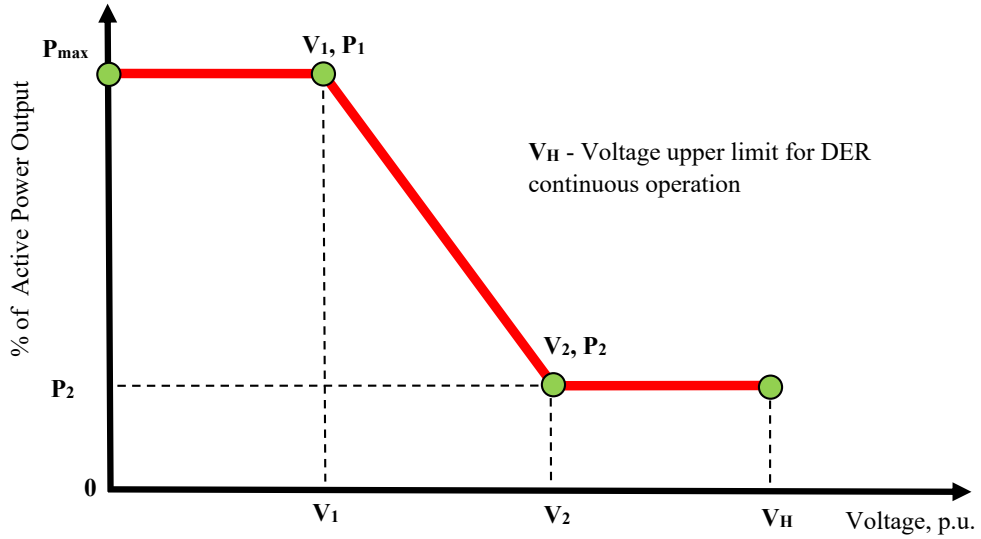

Figure E.2: Example voltage-active power characteristic

Table E.1: Voltage-reactive power settings for IEEE 1547 Category A and Category B

Voltage-reactive power parameters	Default settings	
	Category A	Category B
V_L	0.9	0.9
V_1	0.9	0.92
V_2	1	0.98
V_{ref}	1	1
V_3	1	1.02
V_4	1.1	1.08
V_H	1.1	1.1
Q_1	25% of nameplate apparent power rating, injection	44% of nameplate apparent power rating, injection
Q_2	0	0
Q_3	0	0
Q_4	25% of nameplate apparent power rating, absorption	44% of nameplate apparent power rating, absorption

Note: Voltages are given in p.u.

Table E.2: Voltage-active power settings for IEEE 1547 Category A and Category B

Voltage-active power parameters	Default settings
V_1	1.06
V_2	1.1
V_H	1.1
P_1	100% (P_{rated})
P_2	20% ($0.2P_{rated}$)

Note: P_{rated} is the nameplate active power rating of the PV system. Voltages are given in p.u.

Table E.3: Voltage-reactive power settings for AS/NZS 4777

Voltage-reactive power parameters	Default settings	
	Australia	New Zealand
V_L	0.87	0.87
V_1	0.9	0.9
V_2	0.96	0.96
V_{ref}	1	1
V_3	1.09	1.06
V_4	1.15	1.1
V_H	1.15	1.1
Q_1	30% of nameplate apparent power rating, injection	30% of nameplate apparent power rating, injection
Q_2	0	0
Q_3	0	0
Q_4	30% of nameplate apparent power rating, absorption	30% of nameplate apparent power rating, absorption

Note: Voltages are given in p.u.

Table E.4: Voltage-active power settings for AS/NZS 4777

Voltage-active power parameters	Default settings	
	Australia	New Zealand
V_1	1.09	1.06
V_2	1.15	1.1
V_H	1.15	1.1
P_1	100% (P_{rated})	100% (P_{rated})
P_2	20% ($0.2P_{rated}$)	20% ($0.2P_{rated}$)

Note: P_{rated} is the nameplate active power rating of the PV system.
Voltages are given in p.u.

Table E.5: Voltage-reactive power settings for California Rule 21

Voltage-reactive power parameters	Default settings
V_L	0.9
V_1	0.92
V_2	0.967
V_{ref}	1
V_3	1.033
V_4	1.07
V_H	1.1
Q_1	30% of nameplate apparent power rating, injection
Q_2	0
Q_3	0
Q_4	30% of nameplate apparent power rating, absorption

Voltages are given in p.u.

Table E.6: Voltage-active power settings for California Rule 21

Voltage-reactive power parameters	Default settings
V_1	1.06
V_2	1.1
V_H	1.1
P_1	100% (P_{rated})
P_2	0%

Note: P_{rated} is the nameplate active power rating of the PV system.
Voltages are given in p.u.

Table E.7: Voltage-reactive power settings for Hawaii Rule 14

Voltage-reactive power parameters	Default settings
V_L	0.9
V_1	0.94
V_2	0.97
V_{ref}	1
V_3	1.03
V_4	1.06
V_H	1.1
Q_1	44% of nameplate apparent power rating, injection
Q_2	0
Q_3	0
Q_4	44% of nameplate apparent power rating, absorption

Note: Voltages are given in p.u.

Table E.8: Voltage-active power settings for Hawaii Rule 14

Voltage-reactive power parameters	Default settings
V_1	1.06
V_2	1.1
V_H	1.1
P_1	100% (P_{rated})
P_2	0%

Note: P_{rated} is the nameplate active power rating of the PV system. Voltages are given in p.u.

Appendix F

Theoretical Background for Basic Determinant of a Nomogram: Proof of (7.7)

Nomoogram is a diagram representing a formula in which variables are represented by different graduated lines or curves and the solution for a given set of variables can be read by means of an index line. Nomogram has been developed on the basis of the determinants which is a convenient form of representing a mathematical formula [77].

The basic determinant of a nomogram should satisfy the following conditions if a given formula can be represented in the required form,

- The absolute value of the determinant must be zero
- Each row must contain one variable only
- The last element of each row must be positive and equal to unity

Nomograms can be classified into various groups and the most convenient way of carrying out this is by classification according to the number of variables contained in the formula which is known as "Class". For example, a formula containing three variables is of the Class-III nomogram. Class of the nomogram is equivalent to the

number of different curves or lines to be constructed in the nomogram. However, Class of a formula has no connection with the degree of each variable in the formula.

For a given formula in Class III, which contains variables u, v and w, the basic determinant of the nomogram is formed as given in (F.1).

$$\begin{vmatrix} g_1(u) & f_1(u) & 1 \\ g_2(v) & f_2(v) & 1 \\ g_3(w) & f_3(w) & 1 \end{vmatrix} = 0 \tag{F.1}$$

where $(g_1(u), f_1(u))$, $(g_2(v), f_2(v))$ and $(g_3(w), f_3(w))$ represent the curves of the variable u, v and w in x, y Cartesian plane, respectively. Nomogram can be constructed by plotting the positions of the points $(g_1(u) = x_1, f_1(u) = y_1)$, $(g_2(v) = x_2, f_2(v) = y_2)$ and $(g_3(w) = x_3, f_3(w) = y_3)$ which represent the curves of u, v and w in the Cartesian plane.

In general, if three common points in each locus satisfy (F.1), those three points are co-linear. This implies that respective variables u, v and w satisfy the given formula. Each line or curve in a nomogram may be regarded as a set of points representing successive values of one of the variables in the formula which the nomogram as a whole represents.

However, any formula that met with in practice shall be rearrange to form of basic determinant before the corresponding nomogram can be designed and constructed. For example, consider the formula (F.2):

$$u^2 + uv = w \tag{F.2}$$

(F.2) can be expressed in the form (F.3):

$$u^2 + uv - w = 0 \tag{F.3}$$

Take $x = v$ and $y = w$ and substituting to (F.3), the following set of equations can be obtained:

$$x - v = 0$$

$$y - w = 0$$

$$u^2 + ux - y = 0$$

Since, all three equations are true, the following determinant is zero.

$$\begin{vmatrix} 1 & 0 & -v \\ 0 & 1 & -w \\ u & -1 & u^2 \end{vmatrix} = 0 \tag{F.4}$$

(F.4) can be transformed into the form of (F.1) by applying row and column operations appropriately.